Title
Exit from mitosis and hypoxia in the D.melanogaster embryo

Author
DiGregorio, Paul J.

Publication Date
2001

Peer reviewed|Thesis/dissertation

Exit from mitosis and hypoxia in
the D. melanogaster embryo

by

Paul J. DiGregorio

DISSERTATION

Submitted in partial satisfaction of the requirements for the degree of

DOCTOR OF PHILOSOPHY

in

Biochemistry

in the

GRADUATE DIVISION

of the

UNIVERSITY OF CALIFORNIA SAN FRANCISCO

Date University Librarian

Degree Conferred: .....

This thesis is dedicated to my parents,

Anthony and Maria DiGregorio

Acknowledgements

Science is not done in a vacuum. There are many people that have helped me scientifically and emotionally in the past few years to achieve the success of a completed thesis.

I would like to begin by thanking my advisor, Patrick O'Farrell. Through many long hours of discussion in his office, Pat taught me how to think critically about data and science. Pat has a tremendous ability to make models and conclusions from data. I will take the lessons learned from in into the future. In addition to being a good mentor, Pat cared about my personal well being. This quality is not shared amongst all advisors and I appreciate Pat's sincerity and good will in helping me through the my graduate career.

All of my thesis committee meetings were pure pleasure, resulting in inspirational and positive directions for my thesis research. I would like to thank Andrew Murray and Erin O'Shea for providing insight and direction. Dave Morgan was an especially large influence in my graduate career. Dave was on my orals and thesis committee and a rotation advisor. I consider Dave a second advisor and will always value his succinct and profound advice.

The base from which all of my ideas and work originated is the effervescent O'Farrell lab. Tin Tin Su and Shelagh Campbell were positive influences scientifically when I rotated and initially joined the lab. I am particularly indebted to Peter Follette for his insight as a senior graduate student as I was just beginning my thesis work. Smruti Vidwans on the surface appeared to be my scientific nemesis. In reality, her prowess in asking insightful questions and excitement for other people's research was an essential element to my thesis

work. I consider her an inspiration and a good friend. In addition to providing technical expertise, Antony Shermoen through his upbeat demeanor is responsible for creating the friendly and welcoming work environment of the O'Farrell lab.

There have been three important lab members without them I would have never finished. Devin Parry was my bay-mate, friend, and colleague. I appreciate all of his support and patience and cannot begin to communicate all of the ways he has helped along the way. Jim Wingrove was the single most important lab member in my thesis work. He acted as a collaborator, advisor, big brother, and friend. Finally, I would like to thank Renny Feldman for his friendship and support in the last year of my thesis.

In addition to scientific and work-related support, I have considered myself lucky to have a strong network of friends and family. I would like to thank Julia Owens, Carlos Palomares, Oren Beske, and Arash Komeili for being good friends along the way. The "boys" in SoCal, Nathan Johnson, Corey Senn, Todd Smith, and Jonathan Davies were always there when I needed to escape. I give credit to all of my achievements to Annemieke van Zante. She was the source of influence and support throughout my thesis work. I would like to thank my parents for their emotional (and financial) support. Most of all for believing in me and supporting me throughout my life. My brother, David, was an early influence and guide into the scientific world. Through a common love for basic research, we have a strong bond between us. His guidance and advice throughout my graduate work helped me avoid much pain and suffering.

Chapters 2 and 5 of this dissertation contain results and discussion that have been previously published. The references for these publications are listed below.

Su, T.T., Sprenger, F., DiGregorio, P.J., Campbell, S., and O'Farrell, P.H. (1998). Exit from mitosis in *Drosophila* syncytial embryos requires proteolysis and cyclin degradation, and is associated with localized dephosphorylation. *Genes and Development* 12, 1495-1503.

DiGregorio, P.J., Ubersax, J. A., and O'Farrell, P.H. (2001). Hypoxia and nitric oxide induce a rapid, reversible cell cycle arrest of the *Drosophila* syncytial divisions. *Journal of Biological Chemistry* 276(3), 1930-1937.

Exit from mitosis and Hypoxia in the *D. melanogaster* embryo

Paul DiGregorio

Abstract

To better understand the complex regulation of the cell cycle, I investigated the mechanisms that control the *Drosophila* embryonic cell cycles. The first 13 mitotic divisions of the *Drosophila* embryo are synchronous, syncytial divisions. A pioneering study by Edgar et. al, 1994 provided evidence that the early syncytial divisions occur with continuously high bulk CDK1 activity without fluctuations in mitosis. The authors proposed a model that small, local changes in CDK1 activity drive the exit from mitosis. To test this model, I microinjected an inhibitor to the APC to block targeted degradation of mitotic cyclins and other substrates during mitosis. The APC inhibitor blocked the exit from mitosis beginning in metaphase. Together with other evidence from our lab, the data suggests a requirement for cyclin degradation and CDK1 inactivation, supporting a model for local changes in CDK1 activity.

The APC is a key cell cycle regulator that functions as a critical E3 ubiquitin ligase targeting substrates for degradation by polyubiquitination. I used genetic and *in vitro* studies to better understand the regulation of APC

activity *Drosophila*. To probe the role of CDKs as negative regulators of the APC, CDK activity was abolished by a mutation in cyclin E and overexpression of the mitotic cyclin/CDK inhibitor, *roughex*. When CDK activity is suppressed under these conditions, mitotic cyclins are downregulated suggesting that the APC is ectopically activated. To complement the *in vivo* result, I established an *in vitro* ubiquitination assay to probe APC activity directly. The assay was ATP, ubiquitin, time, and destruction box dependent. The APC assay appears to be *fizzy-related* dependent and not *fizzy* dependent. APC activity is increased in extracts derived from cyclin E mutant embryos, supporting the model that CDKs negatively regulate APC activity.

Cells can respond to reductions in oxygen (hypoxia) by metabolic adaptations, quiescence or cell death. The nuclear division cycles of syncytial stage *Drosophila melanogaster* embryos reversibly arrest upon hypoxia. We examined this rapid arrest in real time using a fusion of green fluorescent protein and histone 2A. In addition to an interphase arrest, mitosis was specifically blocked in metaphase, much like a checkpoint arrest. Nitric oxide, recently proposed as a hypoxia signal in *Drosophila*, induced a reversible arrest of the nuclear divisions comparable to that induced by hypoxia. Syncytial stage embryos die during prolonged hypoxia while post-gastrulation embryos (cellularized) survive. We examined ATP levels and morphology of syncytial and cellularized embryos arrested by hypoxia, nitric oxide, or cyanide. Upon oxygen deprivation, the ATP levels declined only slightly in cellularized embryos and more substantially in syncytial embryos. Reversal of hypoxia restored ATP levels, and relieved the cell cycle and developmental arrests. However, morphological abnormalities suggested that syncytial embryos

suffered irreversible disruption of developmental programs. Our results suggest that nitric oxide plays a role in the response of the syncytial embryo to hypoxia, but that it is not the sole mediator of these responses.

Table of Contents

List of Figures

Chapter 1

Introduction

185,000 strong and still growing

On April 2, 2001, a PubMed search of the keyword "cell cycle" resulted in approximately 185,000 references, illustrating the mammoth body of work dedicated to understanding the cell cycle. The cell cycle field has grown and diversified into many different areas of study, including cancer research, cytoskeleton, chromosome structure and function, and cell asymmetry. In addition, cell cycle research has begun to burrow itself into many fundamental issues of cell biology and biochemistry, such as spatial and temporal regulation of protein function and the activities of protein machines. With an explosion of provocative and paradigm shifting work in the past 20 years, research is rapidly expanding and always changing. In the following chapter, I will provide a hopefully succinct and clear presentation of the salient points of cell cycle regulation, ubiquitin-mediated protein degradation, and *Drosophila* biology required for the understanding of my thesis.

CDK/cyclin complexes: The conductors of the cell cycle symphony

The canonical cell cycle consists of four distinct phases: G1, S, G2, and mitosis. The genome is replicated in S-phase, and is segregated into the two daughter cells during mitosis. The intervening gap phases, G1 and G2, are used in certain cell types as points of cell cycle regulation. The cell cycle is generally considered a set of transitions from one stage into another. These transitions are "points of no return" in most normal cells and are areas of complex regulation. For example, at the G1-S transition the cell exits a stationary or quiescent stage of

G1 (sometimes referred to G0) and begins to replicate its DNA in S-phase. At the G2-M transition, the cell proceeds from a metastable G2 state into mitosis, elaborating a mitotic spindle and condensing its chromosomes. Finally, in the metaphase-anaphase transition, the cell pushes itself over the edge by separating and segregating its chromosomes.

These major cell cycle transitions are driven by cyclin-dependent kinase (CDK)/cyclin complexes[1]. CDKs are a conserved family of kinases that form a complex with a cyclin regulatory subunit. CDKs and cyclins come in many flavors. In metazoans, CDKs are generally grouped by homology and referred to by number (e.g. CDK1, CDK2, CDK4). Cyclins can be grouped by homology and function and referred to by letter (e.g. cyclin A, cyclin D). Specific CDK/cyclin complexes have unique functions in the cell cycle. In metazoans, "G1 cyclins" (i.e. cyclin E and D) complexed with CDK2 or CDK4 are believed to drive the G1-S transition. CDK2/cyclin E and CDK1(or 2)/cyclin A complexes are believed to drive S-phase and replication. "Mitotic cyclins" (i.e. cyclins A, B, and B3) complexed with CDK1 control entry into mitosis from G2.

Changes in the activity of specific CDK/cyclins complexes regulate different steps of the cell cycle. CDK/cyclin complexes are often referred to as clocks or timers because their activities fluctuate to push the cell cycle forward. Activation and eventual inactivation of CDK/cyclin complexes creates these oscillations in activity. In a simplistic view, the cell defines its cell cycle stage by the activity or inactivity of the CDK/cyclin complexes. In addition, the cell remembers which CDK/cyclin activities have previously oscillated and uses this

information to further establish its cell cycle state. This idea is supported a large body of work using cell fusion or cytoplasmic manipulation to transfer the program of the cell cycle state from one cell to another [1]. It is important to note that the inactivation of CDK/cyclin complexes is required for successful cell cycle progression. For example, the CDK1/cyclin B complex is activated at the G2/M transition driving the cell into mitosis. At the end of mitosis, this same CDK1/cyclin B complex needs to be inactivated in order to exit mitosis.

Ups and downs of CDK/cyclin activity

How are oscillations in CDK/cyclin complexes achieved? Free CDKs are believed to be inactive and are activated by binding to a cyclin partner and by an activating phosphorylation event [2]. The CDK-activating kinase (CAK) phosphorylates the CDK on a conserved tyrosine residue at position 160 or 161. CAK phosphorylation of CDKs appears to be constitutive in most cell types and probably does not play a regulatory role in CDK/cyclin regulation during the cell cycle, with the exception of the early *Drosophila* syncytial divisions [3]. Since cyclin binding activates CDKs, the level of cyclin binding partner plays an important regulatory role. Cyclin expression is a tightly regulated circuit that permits certain cyclins to be expressed during discrete stages of the cell cycle. For example, "G2" or mitotic cyclins activate their own transcription while inhibiting expression of G1 cyclins [4]. Thus, a switch is thrown during early S-phase phase at which G2 cyclin levels rise, reinforcing their own expression while suppressing G1 cyclin transcription. These regulatory loops stabilize one state in

[1] For an excellent review of the history and development of most models regarding cell cycle regulation, please refer to a somewhat out of date textbook from Tim Hunt and Andrew Murray

the cell cycle, and inhibit progression "backward" into a previous CDK/cyclin state.

There are three main pathways to inhibit CDK/cyclin complexes: (1) inhibitory phosphorylation, (2) cyclin-dependent kinase inhibitors or CKIs, (3) degradation of the cyclin partner [2]. Cyclin degradation will be discussed in detail in the next section. CDKs can be inhibited by phosphorylation on conserved threonine (T-14) and tyrosine (Y-15) residues at positions 14 and 15. Two different families of kinases are responsible for these inhibitory activities, wee1 and myt1 [5]. Inhibitory phosphorylation can be reversed by a dual specificity phosphatase, CDC25^{string}. Timely removal of inhibitory phosphorylation is used by certain organisms to regulate entry into mitosis and to respond to DNA damage checkpoints. In *Drosophila* and *S. pombe*, CDK1/cyclin complexes in S-phase and early G2 are inhibited by phosphorylation at T-14 and/or Y-15. Regulated CDC25^{string} expression and activation in G2 removes the inhibitory phosphates on CDKs. CDK1 is now activated and drives the cell into mitosis.

CDK/cyclin complexes can be inhibited by CKIs [6, 7]. CKIs bind and functionally inhibit CDK/cyclin complexes. Like cyclins and CDKs, there are many different types of CKIs with different specificities towards CDK/cyclin complexes. In response to internal and external signals, cellular pathways express, activate, and/or downregulate CKIs to stop and start the cell cycle accordingly. Often CKIs are used in normal cell cycle progression to prevent inappropriate CDK/cyclin activity. In mammalian cells, p27^{KIP1} and p21^{CIP1} inhibit CDK2/cyclin complexes [7]. However, p27^{KIP1} and p21^{CIP1} respond to

---

1. Murray, A. and T. Hunt, *The Cell Cycle*. 1993: Oxford Press. 251..

different pathways. $p27^{KIP1}$ is upregulated in response to extracellular anti-mitogenic signals. $p21^{CIP1}$ is expressed in G1 under normal cycling conditions and in a p53-dependent fashion during DNA damage. Also in mammalian cells, the $p16^{INK4}$ family of CKIs inhibits CDK4/cyclin D in G1. In response to growth and mitogenic signals, a signal transduction pathway results in $p16^{INK4}$ inactivation. CDK4/cyclin D is activated and drives the cell out of G1 into S-phase. Interestingly, CKIs in the $p16^{INK4}$ family are classified as tumor suppressor genes based on the findings that loss of heterozygosity (LOH) at the $p16^{INK4}$ locus is linked with cancer progression. In budding yeast, Sic1 inhibits CDC28/Clb1-6 complexes under normal cycling conditions to help suppress CDK activity during late mitosis and G1, whereas, Far1 expression in response to alpha factor exposure inactivates the CDC28/CLN1-3 complexes, resulting in an arrest in G1 [5, 6]. In *Drosophila*, the p21/p27 homolog, *dacapo*, is expressed in G1 cells inhibiting CDK2/cyclin E activity.

Recently, the *rux* gene has been identified as a CKI specific for mitotic cyclin/CDK complexes in *Drosophila*. In *rux* mutants, this critical G1 phase in the developing eye imaginal disc is not established and cells undergo a premature S-phase. The simultaneous overexpression of *rux* and cyclin A inhibits induced by cyclin A induction, indicating *rux* prevents cyclin A associated S-phase activity. In addition, when Rux is expressed during S or G2, Cdk1-dependent mitoses are inhibited. *In vivo*, Cyclin A and cyclin B bind *rux*. The expression of *rux* in embryos results in a strong reduction of Cdk1 kinase activity [8]. *In vitro* analysis demonstrates that Rux prevents activating phosphorylation of Cdk1 on T161 and that Rux also inhibits Cdk1 activity by other means. These data indicate that Rux

is a novel CKI present in a higher eukaryote which acts specifically on mitotic cyclins [9].

The cell cycle can be viewed as a balance of power between extracellular and intracellular signals, opposing kinases and phosphatases, and protein expression and degradation. In concert, these activities result in timely oscillations of CDK/cyclin activity that drive cell cycle progression.

Progress through destruction

Ubiquitin-mediated targeted protein degradation (see section below) is an essential theme in cell cycle control [10]. Wolgang Zachariae and Kim Nasmyth described the cell cycle ending with an "orgy of protein degradation" [11]. Much advancement in understanding how cell division is regulated has been made through the elucidation of the protein degradation in mitosis. The machinery responsible for this targeted degradation is the anaphase-promoting complex (APC).

Much of the early research regarding protein degradation and the cell cycle was focused on the regulation of cyclin protein levels. Cyclins were identified as a protein that oscillates during the early cleavage divisions in sea urchin [12]. Subsequent studies revealed that cyclin B protein accumulates during interphase and is abruptly degraded at the end of mitosis. In a pioneering set of experiments, cyclin B in cycling frog extracts was shown to be degraded through an ubiquitin-mediated pathway [13] [14]. Furthermore, the amino terminus of cyclin B was sufficient to confer mitotic degradation to cyclin B and heterologous proteins; whereas, a cyclin B mutant lacking its amino terminus

was stable in mitosis. A degenerate nine amino acid motif called the "destruction box" was identified within the amino terminus of cyclin B that was required for its degradation [14].

Following these seminal studies, the field of cyclin degradation has revealed much about the spatial and temporal regulation of protein destruction in mitosis. All mitotic cyclins (A, B, and B3 in higher eukaryotes; Clb1-6 in *S. cerevisiae*, CDC13 in *S. pombe*) are degraded in mitosis and contain the destruction box sequence required for targeted ubiquitin mediated degradation. In most systems, there is an ordered disappearance of the cyclins in mitosis [11, 15]. In higher eukaryotes, cyclin A is degraded at or just before metaphase. Cyclin B is degraded at the metaphase-anaphase transition. In *Drosophila*, cyclin B3 is degraded later in anaphase after cyclin B [15]. Cyclin degradation is also spatially organized [16-18]. In *Drosophila* embryos, a cyclin B and green fluorescent protein (GFP) fusion proteins disappears first at the spindle poles in metaphase, then at the interdigitating microtubules of the spindle midline, and finally within the whole cell. Experiments using stabilized versions of mitotic cyclins in many different systems have agreed that degradation of mitotic cyclins is required to exit mitosis [5, 11].

An early study suggested that there is a non-cyclin protein whose degradation is required to exit from mitosis [19]. Addition of a stabilized version of sea urchin cyclin B to cycling *Xenopus* egg extracts blocks the cycle in late anaphase/telophase. However, addition only the amino terminus of sea urchin cyclin B (which is believed sufficient to titrate and inhibit the protein degradation machinery) to the same cycling extract resulted in a metaphase block [19]. Taken together, the authors of this study suggested that degradation

of a non-cyclin substrate is required for the metaphase-anaphase transition. This study led to the search for non-cyclin proteins whose destruction is required for exit from mitosis. Interestingly, more recent evidence suggests that cyclin A or Clb5 degradation is required for the metaphase-anaphase transition [15, 20].

To date, many non-cyclin substrates have been identified as probable targets of the APC whose degradation is required to exit mitosis or stabilize of G1 state [11, 21]. The degradation of "securins", such as Pds1 in *S. cerevisiae* [22-24], is required for sister chromatid separation at the metaphase-anaphase transition. The degradation of securins is believed to promote the activity of different class of proteins, "separins", whose activity is required for dissolution of the chromatid linkages and sister chromatid separation. Proposed "securin"-like homologs have been identified in other systems. For example, the degradation of Cut2 in fission yeast [25] and *pimples* and *three rows* in *Drosophila* [26, 27] are also required for sister chromatid separation. In budding yeast, Ase1 is targeted for degradation by the APC in telophase and plays a role in spindle integrity [28]. To date, most of the non-cyclin substrates of the APC contain the canonical destruction box motif required for targeted degradation in mitosis and G1. Intriguingly, a unique motif, the KEN box, has been identified in many APC substrates to be required for their degradation in G1 and recognition by the activator protein, $CDH1^{fzr}$ [29]. Perhaps, there is large class of proteins yet to be discovered targeted for degradation by the APC. In support of this idea, recently two more proteins, geminin and Xkid, have been identified as APC targets [30, 31].

The little guy that causes so much trouble: Ubiquitin

Targeted protein degradation via the ubiquitin pathway is essential for many cellular functions, including cell cycle progression. Ubiquitin is a small, highly conserved protein that is reversibly conjugated to target proteins [32, 33]. Degradation of a protein via the ubiquitin pathway involves two steps. In the first step, successive rounds of ubiquitin conjugation and extension of the ubiquitin chain by ubiquitin conjugating enzymes results in a polyubiquitinated protein. Then, polyubiquitinated target proteins are recognized and degraded by the 26S proteasome in an ATP-dependent fashion. The 26S proteasome is a large multi-subunit complex that functions as an active protease for ubiquitin-tagged protein substrates [32]. Degradation of proteins by the 26S proteasome is not considered a regulated step in cell cycle progression because it is constitutively active and most ubiquitinated targets are degraded efficiently.

Ubiquitin is transferred to protein substrates through a complex pathway involving three essential enzyme families [10, 32, 33]. Free ubiquitin cannot be transferred directly to substrates and needs to be in the proper chemical state, or "charged". Free ubiquitin is "activated" by forming a thiolester linkage between its carboxy-terminus to a family of ubiquitin- activating enzymes, called E1 enzymes. Enzymes in the ubiquitin pathway are named according to there elution profile from an ubiquitin affinity column, E1 being the first elution fraction, etc...[32]. This first activation step is driven by ATP hydrolysis. Subsequently, ubiquitin covalently bound to an E1 is transesterified to a family of ubiquitin-conjugation enzymes, or E2 enzymes. Finally, ubiquitin is transferred from the E2 to a lysine residue in the target protein, either directly or with the assistance of an ubiquitin ligase, or E3. E3s are generally required for

ubiquitin chain elongation on targets, which increases recognition and turnover by the 26S proteasome. Most E3s do not form covalent linkages to ubiquitin. Ubiquitin chains can also be modified by several classes of deubiquitinating enzymes which remove either single ubiquitin monomers from chains or multiple ubiquitin side-chains from targets [34]. Deubiquitinating enzymes have been implicated in proofreading activities of the proteasome, recycling of ubiquitin, and regulators in certain pathways.

The most regulated step in the ubiquitin pathway is the activity of E3 enzymes which are required for target specificity. Ubiquitin mediated protein degradation is utilized in a number of signaling pathways and basic cellular functions. For example, the tumor suppressor gene, p53, and the hypoxia-induced factor 1α (HIF-1α) are normally both very unstable proteins in the cell. Their instability is dependent on ubiquitination by different E3 enzymes under normal cellular states. Then, upon DNA damage (for p53) or reduced oxygen levels (for HIF-1α) signal transduction cascades result in inactivation of ubiquitination and the stabilization of these proteins. There are many E1s, E2s, and E3s in the cell, varying in number between species. Different subsets of these families are used in specific degradation pathways. There are two distinct ubiquitin-mediated proteolysis pathways required for cell duplication: the SCF and the APC.

The dueling banjos of the cell cycle: APC and SCF

The anaphase-promoting complex (APC), or "cyclosome", is the essential E3 ubiquitin ligase required for targeted degradation of proteins in

mitosis and G1 [35-37]. The APC was identified in yeast, clam oocycte extracts, and frog egg extracts through a combination of genetic and biochemical studies (see Chapter 3 for details). The APC is believed to recognize and polyubiquitinate substrates via the destruction box or KEN box motifs. The ubiquitin ligase activity of the APC oscillates during the cell cycle, active from metaphase through G1. Ectopic activation of the APC results in the destabilization of its targets, such as mitotic cyclins [38]. Mutations in core complex subunits result in cyclin stabilization [37]. Likewise, immunodepletion of APC from mitotic extracts results in cyclin stabilization *in vitro* [35].

The composition of the APC has been investigated by immunopurification in many systems [11, 39-41]. Most subunits of the APC remain tightly bound in a large 20S complex throughout the cell cycle and are referred to as the "core" complex. The association of activator proteins, $CDC20^{fzy}$ and $CDH1^{fzr}$, is substoichiometric and regulated within the cell cycle (see Chapter 4). The APC core complex contains ≥eight subunits depending on the species[2]. Homology studies suggest that the APC core complexes in all eukaryotes have common components. In *Drosophila*, homologs to the budding yeast CDC16 and CDC27 have been identified and copurify in a large molecular weight complex [18]. Little is known about the APC complex on the molecular level. Which component contains the ubiquitin ligase activity? How it is regulated? Which component recognizes the destruction box and KEN box motifs? Future studies using purified components and genetic variants will provide insight into APC

[2] Please refer to a comprehensive review by Zachariae and Nasmyth for a detailed discussion of the constitution of the APC core complex 11. Zachariae, W. and K. Nasmyth, *Whose end is destruction: cell division and the anaphase-promoting complex.* Genes and Development, 1999. 13(16): p. 2039-58..

core activity. It is not yet clear which E1 and E2 enzymes specifically interact with the APC *in vivo* and are required for APC activity in metazoans [11].

Detailed protein sequence analysis of APC core subunits has uncovered many common sequence motifs shared between the APC subunits and other E3 ubiquitin ligases [11]. CDC16, CDC23, and CDC27 contain 9-10 copies of tetratrico peptide repeats (TPR) implicated in protein-protein interactions and are required for APC complex integrity [42, 43]. Apc2 and Apc11 are related to subunits of the SCF family of ubiquitin ligases (see below). Apc2 is a member of the "cullin" family of proteins, which includes CDC53 (SCF complex) from budding yeast [44]. CDC53's cullin domain is believed to recruit the E2 enzyme, CDC34 to the SCF. Perhaps, Apc2 fulfills the same role in recruitment of E2 for the APC. The small Apc11 subunit shares homolog with HRT1 of the SCF. Both Apc11 and Hrt1 contain a RING-H2 domain that mediates protein-protein interactions [44].

As mentioned previously, the SCF (Skp1-cullin-F-box complex) is another ubiquitin ligase required for cell cycle progression [10, 44]. The SCF targets phosphorylated substrates for degradation such as Sic1 and G1 cyclins. SCF complexes have been identified in most eukaryotes. Unlike the APC, SCF is believed to be active throughout the cell cycle. Cell cycle regulation of the phosphorylation of SCF substrates regulates their recognition and eventual ubiquitination. For example, SCF activity is required for the G1/S transition in budding yeast. The budding yeast CDK inhibitor, Sic1, is phosphorylated at the G1/S transition by CDC28/Cln complexes allowing Sic1 to be recognized by the SCF and targeted for degradation. Sic1 remains unstable until late mitosis, when the CDC14 phosphatase dephosphorylates and stabilizes Sic1 [45]. Stabilization

of Sic1 in mitosis is believed to result in CDC28 kinase inactivation and assist in activation of the APC (see Chapter 4). At the G1/S transition, Sic1 is degraded by the SCF which also assists in APC inactivation. Thus, APC and SCF activities are partially interdependent within the cell cycle.

Substrate specificity of the SCF is achieved using different F-box proteins within the core complex. For example, SCF containing the F-box protein CDC4 recognizes phosphorylated Sic1 in budding yeast. Other SCF-like ubiquitin ligases have identified in many organisms and linked to diverse cellular processes unrelated to cell cycle progression [44].

During the 5 years of my graduate work, much advancement has been made to better understand the role of targeted degradation and cell cycle progression. Many key players have been identified, such as the APC and SCF. However, the complex regulation of the APC in *Drosophila* remains to be elucidated. In this thesis, I will provide some new insights into the role of the APC and exit from mitosis during *Drosophila* embryogenesis.

The awesome power of the Drosophila embryo

Drosophila embryogenesis provides a unique system for studying the regulation of cell division. The embryo is a multicellular organism that passages through a complex program of developmental events. Most models currently used to investigate the cell cycle are single cell systems, such as yeast and mammalian tissue culture. The embryo transitions through highly regulated changes and additions to the cell cycle as the organism develops. Investigation of these changes has uncovered coupling of developmental signals to cell cycle

regulators. Each transition provides an experimentally amenable opportunity to dissect the complex control of the cell cycle.

The first thirteen mitotic cycles of a fertilized *Drosophila* embryo are synchronous nuclear divisions occurring in a common cytoplasm, or syncytium [46]. These syncytial cycles are extremely fast. Interphase length for the first nine divisions is ~4 min. Interphase lengthens in cycles[3] 9-13 to ~20 min in cycle 13. The syncytial nuclear divisions are S-phases and intervening mitoses without gap phases. The nuclear divisions begin dividing in the internal portion of the embryo and then migrate to the cortex by cycle 9 and 10. During interphase of cycle 14, the nuclei on the cortex become cellularized. Membranes invaginate from the cortex, pinching in and enveloping the layer nuclei. As will be seen in Chapter 2, experimental investigation of the unique qualities (speed, synchrony, etc...) of the syncytial cycles has uncovered important fundamentals of cell cycle control.

After cycle 13 and cellularization, the embryonic cell cycle begins to change [46]. Most of the somatic cells go through a synchronous round of S-phase in cycle 14 and arrest temporarily in G2. At this time, early gastrulation events begin and germ layers begin to form. The imposition of this G2 into the cell cycle is achieved by the downregulation of the CDC25^{string} phosphatase. Cells cannot progress into mitosis 14 because CDK/cyclin complexes are inhibited by phosphorylation at T-14 and Y-15. Regulated expression of CDC25^{string} and subsequent removal of inhibitory phosphorylation on CDK1/cyclins drives cells

[3] The specific cell divisions and stages are referred to by the cell cycle stage and the number of divisions through which the cell has progressed. For example, "G2 of cycle 15" refers to the G2 stage of a cell in its 15th cell division. This nomenclature will be used extensively throughout this thesis.

into mitosis 14 [47]. Interestingly, the expression of CDC25^{string} and the subsequent mitosis 14 occurs in a highly regulated and reproducible pattern. Different groups of cells in a stereotypical pattern enter mitosis 14 at specific times. The pattern is referred to as "mitotic domains" [48]. After mitosis 14, cells progress immediately into S-phase of cycle 15. Cycles 15 and 16 are regulated in G2 similarly to cycle 14. Elucidation of the programmed entry into mitosis 14 through CDC25^{string} has contributed greatly to the understanding of how cells regulate cell cycle progression

After mitosis 16, cells enter the first G1 phase of embryogenesis in cycle 17. The acquisition of this G1 is believed to be a result of a combination of many molecular events. Prior to G2 of cycle 16, cyclin E expression is continuously high throughout the cell cycle. Cyclin E is then downregulated and remains low into G1 of cycle 17. Concurrently at this stage, the CDK inhibitor, *dacapo*, accumulates [49, 50]. Cells exiting mitosis prior to cycle 16 are believed to be driven immediately into S-phase by high CDK2/cyclin E activity. After cells exit mitosis of cycle 16, cells cannot progress into S-phase and remain in G1 because CDK2/cyclin E is inhibited by *dacapo* and limited in expression. In addition, the APC activator, *fizzy-related*, is expressed at this stage which helps downregulate mitotic cyclins and establish the G1 state [51]. These studies have highlighted the underlying drivers controlling the G1 state in more canonical cell cycles, by investigating how cells create a G1 in cycle 17 in the *Drosophila* embryo.

It is important to note that many cells in the embryo do not follow the cell cycle program described above. For example, a subset of nuclei in the syncytial divisions remains in the interior of the embryo where they go through rounds of successive S-phases without mitosis, known as endocycles. Other nuclei destined

to become germline precursor cells, or pole cells, cellularize early and follow a unique cell cycle program [52]. In the cellularized, postblastoderm embryo, subsets of cells do not complete cycles 14-16 remaining blocked in certain stages or become endocycling cells. As the developmental program unfolds, cells begin to differentiate and assume unique identities. Often the differentiation events correlate with a change in the cell cycle program. For example, salivary gland precursor cells begin to endocycle after cycle 16, whereas nervous system precursor cells continue to cycle beyond cycle 17 [53].

The developmental program of the cell cycle in the *Drosophila* embryo is a complex web of decisions, transitions, and transformations resulting in stereotypical subsets and patterns of cells with unique identities and cell cycle profiles.

Chapter 2

An inhibitor to the APC blocks exit from mitosis in Drosophila syncytial stage embryos

Introduction

The Beauty and the Beast: Exiting mitosis in a syncytium

The first 13 nuclear divisions of the *Drosophila* embryo provide an incredible experimental context for studying basic cell biology [46]. As discussed earlier (see Chapter 1), the syncytial nuclear divisions are rapid, synchronous mitotic cycles occurring in a common cytoplasm or syncytium. This synchrony and speed of the divisions create a unique context to investigate the underlying cellular control and mechanics of cell division. In addition, *Drosophila* nuclei (~5μm) and chromosomes are quite large, simple to visualize, and have well-defined cytology. Characterization and analysis of the relevant cell cycle events in live or fixed samples using fast, reproducible and simple techniques is a key strength of this experimental system (even for a first-year graduate student). It was the beauty of the syncytial *Drosophila* embryo stained for tubulin and DNA revealing a population of cells going through mitosis that attracted me to studying the cell cycle in *Drosophila*.

In a pioneering study, Edgar et al. [3] investigated the underlying molecular mechanisms that regulate the syncytial nuclear divisions. This study uncovered a number of peculiarities of the syncytial divisions that at first glance seemed counter to the dogma of cell cycle regulation.

The rise and fall in CDK activity is, in part, believed to control a canonical cell cycle. As discussed in Chapter 1, cyclin (the activating partner of CDKs) synthesis and the removal of inhibitory phosphorylation are two mechanisms to

activate CDK kinase activity and promote entry into mitosis [1]. Then, either degradation of the cyclin partner in an APC dependent fashion [11], inhibitory phosphorylation [54], or specific CDK inhibitors [6] inactivate the CDK. Using a combination of these mechanisms, the cell creates an oscillation in CDK activity.

The early syncytial embryo appears to be devoid of oscillations in CDK activity [3]. Rigoruos analysis of cell cycle regulators can be performed, using a technique of selecting embryos for biochemistry according to cell cycle stage and age. The syncytial pre-blastoderm divisions (cycles 1-8) occur without detectable oscillations in cdc2 (CDK1) activity. Kinase activity appeared to be constant until the blastoderm division (cycles 10-13). No inhibitory phosphorylation of CDK1 could be detected until the cycle 14. Cyclin A and B levels do not oscillate with mitotic exit until the blastoderm cycles. Taken together these results suggest that the pre-blastoderm divisions occur with high CDK1 kinase activity and cyclin levels, and without inhibitory phosphorylation. How does this happen? Is there another mechanism or pathway used?

One model put forth is that there is local oscillation of mitotic CDK kinase activity (undetectable by standard biochemical methods) that drives the entry and exit from mitosis in the syncytial pre-blastoderm. The underlying idea behind this model is that the syncytial divisions are driven primarily by maternal contribution of transcripts and protein without zygotic expression. Extending this idea, Edgar et al proposed that there is an excess of cyclin A, B, and CDK1 in the initial nuclear divisions. The significant pool of cell cycle regulators, which fluctuate in activity and expression, are a minor fraction of the bulk protein. Thus, biochemical analysis of whole embryo extracts would fail to detect oscillations of a small, "specialized" pool undergoing cell cycle changes.

In support of this idea, Frank Sprenger while in the lab performed a series of experiments suggesting that cyclin destruction is required in the syncytial embryo (later published with results presented in this chapter, [55]). By removing amino terminal sequences that contain 'destruction box' sequences recognized by the APC, mitotic cyclins are rendered refractory to APC-dependent degradation and are stabilized during mitosis. Overexpressing stabilized versions of mitotic cyclins in *Drosophila* and other systems results in a mitotic block, because cyclin degradation and CDK1 inactivation is required to exit mitosis ([15], [56], Parry and O'Farrell, submitted). Syncytial embryos microinjected with a stable version of cyclin B (Figure 1) were delayed or arrested in mitosis [55]. This result suggests that cyclin degradation is still required for exit from mitosis, despite the lack of complete degradation of cyclins in the syncytial embryo. Furthermore, the requirement for cyclin degradation in mitosis, despite the lack of oscillation of bulk cyclin levels, supports the model that local oscillations of CDK1 activity drive the syncytial divisions.

In light of this result, I wanted to extend this observation to a general requirement for APC activity in the syncytial embryo.

Materials and Methods

All methods for this chapter have been previously described [19, 55].

Cyclin B Amino terminus purification and microinjections

Expression and purification of 13-110 (amino terminus of sea urchin cyclin B) and 13-110* (identical to 13-110 except for two point mutations described in the text) peptides was performed as previously described [19] except for a modification of the column chromatography. Supernatant after 85°C incubation was applied to a phosphocellulose column equilibrated in 20mM PIPES (pH6.5), 50mM NaCl. The column was washed sequentially with 3 column volumes of 100mM, 300mM and 500mM NaCl in 20mM PIPES (pH6.5). The peptide predominantly eluted in the 300mM NaCl step elution and was >90% pure by Coomasie blue staining on a SDS gel. Fractions from the 300mM NaCl elution were pooled, concentrated using a Centriprep-3 (Amicon), dialyzed overnight at 4°C against 5mM NaCl, .1mM NaPO4 (pH7.7) injection buffer, and concentrated again to a final concentration of 10mg/ml using a Microcon-3 (Amicon). All steps were analyzed using SDS-PAGE, using a Tris-Tricine gel system modified from the Schagger and von Jagow method [57] and stained with Sypro Orange (Biorad).

Sevelen embryos (0-1 hr) were prepared and microinjected as previously described [58], with 5 mg/ml peptide in 5mM NaCl, .1mM NaPO4 (pH7.7). Estimated injection volume was between 2-5% of the total volume of the embryo. Injected embryos were aged at 18°C for 30 minutes before fixation.

Fixation

Microinjected embryos require special attention, and described herein is the unique protocol used for fixation and immunostaining of microinjected embryos. Embryos after microinjection and aging were removed from glass coverslips with heptane. Using a pipetteman, embryos were transferred into a two phase solution of 5 ml heptane and 5 ml 37% formaldehyde and rocked gently for 10 min. Embryos were then transferred to a basket lined with a nitex filter and washed 3 times with phosphate-buffered saline (PBS) to remove excess fixative. To remove the vitelline membrane by hand, embryos were adhered to double-stick tape, transferred to a petri dish, and covered with PBS. Using a single tine of forceps, embryos were gently removed from the vitelline membrane, washed with PBS + 0.1% Triton X-100 (PTX), and transferred to eppendorf tube. The embryos were stained as will be described in Chapter 4.

Results

To further the observation that cyclin degradation is required to exit mitosis in the syncytial embryo despite lack of oscillation in bulk cyclins, I blocked APC activity and analyzed the consequences. Since the syncytial nuclear cycles are driven by maternally provided protein and transcripts, I was not able to use mutant strains to inactivate components of the APC. Also, these experiments were performed before the advent of RNAi technology in *Drosophila*. I set out to inactivate the APC by using a previously described peptide inhibitor, named 13-110 [19]. The 13-110 peptide fragment contains 110 residues from the amino terminus of sea urchin Cyclin B (Figure 2). The 13-110 contains a 'destruction box' sequence from Cyclin B required for recognition and ubiquitination by the APC (See Chapter 1). 13-110 is believed to titrate the APC, preventing ubiquitination of endogenous substrates and mitotic exit. In support of this, this peptide can block exit from mitosis in *Xenopus* in vitro egg extracts, arresting the cycling extracts in metaphase. As a control, a peptide containing amino acid changes in the destruction box (13-110*), which renders the full length cyclin B unrecognizable by the APC, has no effect in the *Xenopus* system.

We asked the simple question: how does introduction of an inhibitor to the APC effect the syncytial division? If the syncytial embryo uses the APC to target mitotic cyclins and other substrates for degradation, one would expect a mitotic arrest similar to stabilizing mitotic cyclins (Figure 1). The 13-110 and 13-110* peptide fragments were expressed and purified (see Figure 2b, Materials and Methods). Then, syncytial embryos (1-2 hr old) were microinjected with 1-

5mg/ml solution of the appropriate peptide, aged for different lengths of time, fixed, and immunostained for DNA, tubulin, and phosphorylated histone 3 (PH3, marks mitotic chromosomes).

Consistent with a role for APC-mediated degradation, syncytial embryos microinjected with 13-110 displayed a graded mitotic arrest near the point of injection. The nuclear divisions were blocked in mitotic-like states near the point of injection, whereas nuclei distant from the site of injection progressed to the expected nuclear density (Figure 3A). Nearly all injected embryos showed condensed chromosomes within a mitotic spindle near the point of injection, although not all arrested mitoses had the appearance of a normal metaphase. Syncytial embryos of all ages (cycles 4-13) arrested in response to the 13-110 peptide. Importantly pre-cycle 8 embryos, which ordinarily exhibit no detectable oscillations in cyclin levels or CDK1 activity [3], arrest with a high efficiency, supporting a role for oscillations in CDK1 activity during these cycles. Embryos injected with the 13-110 peptide were stained for the T7 epitope tag (data not shown), revealing a gradient of peptide with the high point at the site of injection. This result is consistent with the graded response.

As a control, embryos were injected with the 13-110* peptide which is not recognized by the APC [19]. The control 13-110* peptide did not cause a mitotic arrest under similar conditions (Figure 3B). This result supports the notion that the destruction box sequence contained within the 13-110 peptide is sufficient to interact with the APC, thus interfering with its interaction with endogenous substrates.

The effect of the 13-110 peptide over time revealed the mitotic block was not static. Using short time-points (data not shown) and injection of live embryos

(Parry and O'Farrell, data not shown) to test for timing of the block, the 13-110 peptide could arrest the first nuclear division after microinjection in mitosis. Examination of the arrested embryos suggested the graded response to the 13-110 peptide. Nuclei closest to the point of injection arrested in a metaphase-like spindle and DNA configuration. Usually, nuclei farthest from the point of injection appeared to be cycling without perturbation. The anaphase and telophase figures distal to the extreme metaphase arrested nuclei (see Figure 3A) appeared to be only delayed in mitosis and exiting mitosis into the next division. This was confirmed by live analysis (data not shown). The block or delay in many stages of mitosis resulting from injection of the 13-110 (Figure 3A) peptide differs from anaphase-block after injection of stabilized cyclin B (Figure 1B), This difference suggests that the 13-110 peptide inhibits cyclin B independent events in mitosis (See Discussion).

Longer time points (>30 min after injection) suggested that sometimes the unperturbed domain, if large enough, could continue to cycle, increasing in nuclear density, while pushing the arrested nuclei to one side of the embryo (data not shown). Also, morphology of the arrested nuclei after >15 min lost wild-type configuration; fragments of DNA with associated spindles were seen in some injected embryos. The loss of the normal mitotic morphology suggests that the APC inhibitor is not completely effective at blocking all of the molecular forces and events in mitosis. Colchicine-induced spindle checkpoint arrests (data not shown) or an hypoxic metaphase arrests (Chapter 5) have stable spindle and DNA morphology for >30 minutes.

Discussion

Inhibition of the APC via a peptide inhibitor blocks exit from mitosis during the syncytial nuclear divisions (Figure 3). The first stage of mitosis sensitive to the 13-110 peptide is the metaphase-anaphase transition. Anaphase, and perhaps telophase, was also severely delayed, suggesting that APC is required in later steps of mitosis. The result that the APC inhibitor causes a metaphase arrest is consistent with other studies in *Drosophila* and other systems. Stabilizing known substrates of the APC in *Drosophila* such as cyclin A and *Pimples* block metaphase [15, 27]. Taken together with results presented here, the first step requiring the APC in mitosis is most likely the metaphase-anaphase transition.

The observed accumulation of anaphase and telophase figures suggests that there are additional roles for the APC in the exit from mitosis, consistent with studies using stabilized versions of *Drosophila* mitotic cyclins. The degradation of cyclin B is required for transition through anaphase in syncytial embryos (Figure 1, [55]) or cellularized embryos [15] .
Similarly, degradation of cyclin B3 is required for late mitotic events such as completion of telophase and chromosome decondensation. Unlike injection of the 13-110 peptide and inhibition of the APC, stabilization of individual mitotic cyclins B or B3 does not perturb events prior to anaphase, such as the metaphase-anaphase transition. Injection of the 13-110 peptide delays anaphase and telophase in syncytial embryos which is consistent with interrupting cyclin B and B3 degradation.

Taken at face value, the result that inhibition of APC results in metaphase arrest is not earth shattering. However, until this study, in was unclear how the pre-blastoderm syncytial divisions could progress without oscillations of cyclin levels or CDK1 kinase activity [3]. Together with results using stabilized mitotic cyclins, we propose that cyclin degradation is required during the syncytial cycles despite the lack of oscillations of cyclin protein or CDK1 activity [3, 55].

Two critical observations made after these experiments support the previously proposed model that there are local oscillations in CDK1 activity in the syncytial embryo. Tin Tin Su and Shelagh Campbell observed that there is a graded loss of PH3 (phosphorylated histone 3) staining, which is a marker for CK1 activity, on anaphase chromosomes [55] only during the syncytial nuclear divisions. PH3 staining decreases at the leading edges of anaphase chromosomes as they move towards the spindle poles. The loss of PH3 staining suggests that there is a local decline in CDK1 activity in the syncytial nuclear divisions. In a later study from Jordan Raff and colleagues [18], a fusion protein of cyclin B and green fluorescent protein (cycB-GFP) disappeared in a localized manner during mitosis. In blastoderm syncytial embryos near the end of metaphase, the spindle-associated cyclin B-GFP disappears in a wave that starts at the spindle poles and spreads to the spindle equator. When the cyclin B-GFP on the spindle is almost undetectable, the chromosomes enter anaphase. Local degradation of cyclins can produce local oscillations in CDK1 activity. Although the components of the core APC do not appear localized in *Drosophila* [18], studies from other systems suggest that APC activators and core APC components can be localized [11, 21, 59, 60].

Combining all these results, we propose that local APC activity causes an oscillation in CDK1 activity, driving syncytial nuclei out of mitosis (See Figure 4). This model reconciles the results that APC and cyclin degradation are still required despite the lack of oscillations in cyclin levels in the early syncytial embryo. We suggest that the local pool of cyclins associated with the mitotic apparatus is the relevant cyclin associated with CDK1, and that this represents a small undetectable fraction by Western blot that oscillates in the early cycles. As the number of nuclei increase with each division, this pool increases in proportion to the bulk cyclin level. Thus, in later syncytial cycles, total cyclin levels oscillate as a result of the increase in local cyclin degraded. We propose that cyclins are targeted for destruction first at the spindle poles, then along the spindles toward the center of the spindle. PH3 staining (a measure of CDK1 activity) is lost as leading edge of anaphase chromosomes near the spindle poles, where APC is active and can degrade cyclins, resulting in a loss of CDK1 activity. The observation of the disappearance of cyclin B-GFP from the spindle poles in a localized fashion supports the idea that local degradation can occur.

Figure 2-1

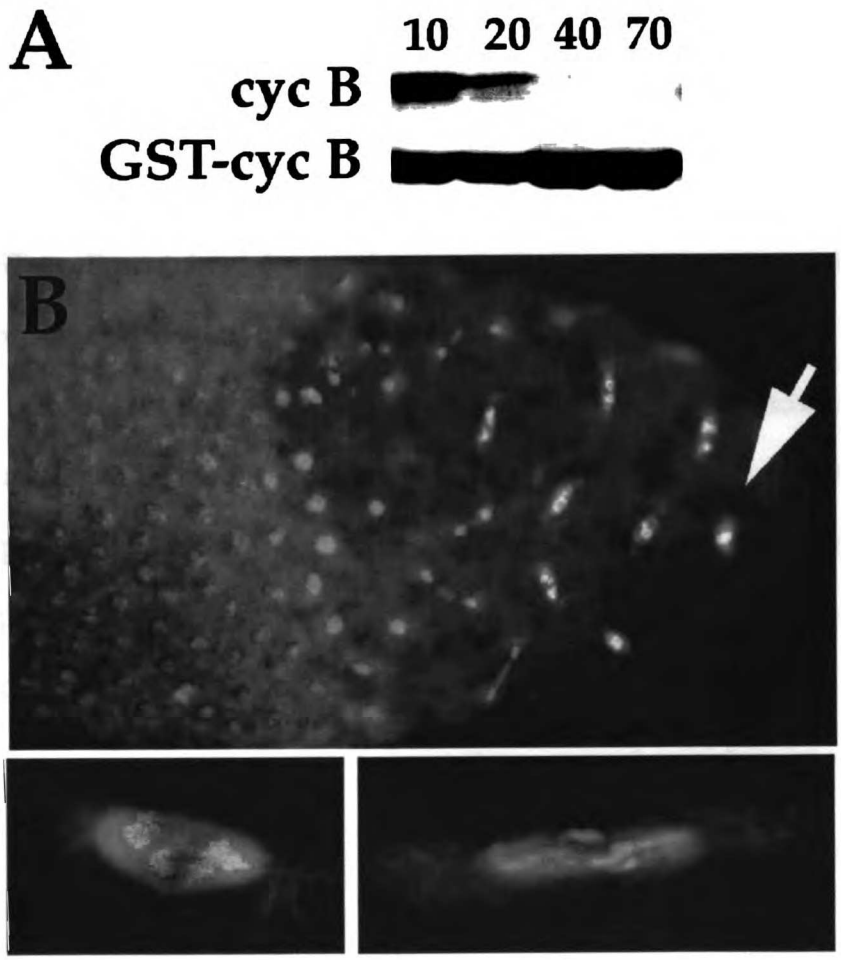

Figure 2-1[4]

(Panel A) Approximately equal amounts of ^{35}S labeled full length Drosophila cyclin B (cyc B) or a fusion of glutathione S-transferase and cyclin B (GST-cyc B) was incubated with mitotic Xenopus egg extracts for 10, 20, 40, and 70 minutes. The products of the reactions were separated and analyzed by SDS-PAGE and western blotting or autoradiography. GST-cycB was stable in similar conditions and protein levels did not decline, even after a 70 min incubation.

(Panel B) GST-cycB protein at 6mg/ml was microinjected into syncytial embryos. The embryos were then aged for 30 min, fixed, and stained for tubulin (blue) and DNA (red). Mitotic exit was blocked close to the site of injection indicated by the arrow. The nuclei continued to divide at a distance from the injection, indicated by the interphase morphology and higher density of nuclei to the left in Panel B. The insets give examples of mitotically blocked nuclei with organized mitotic spindles and condensed DNA masses.

[4] Experimental results presented in Figure 1, Panels A and B, were previously published 55. Su, T.T., et al., *Exit from mitosis in Drosophila syncytial embryos requires proteolysis and cyclin degradation, and is associated with localized dephosphorylation.* Genes and Development, 1998. 12(10): p. 1495-503. and performed by F. Sprenger.

Figure 2-2

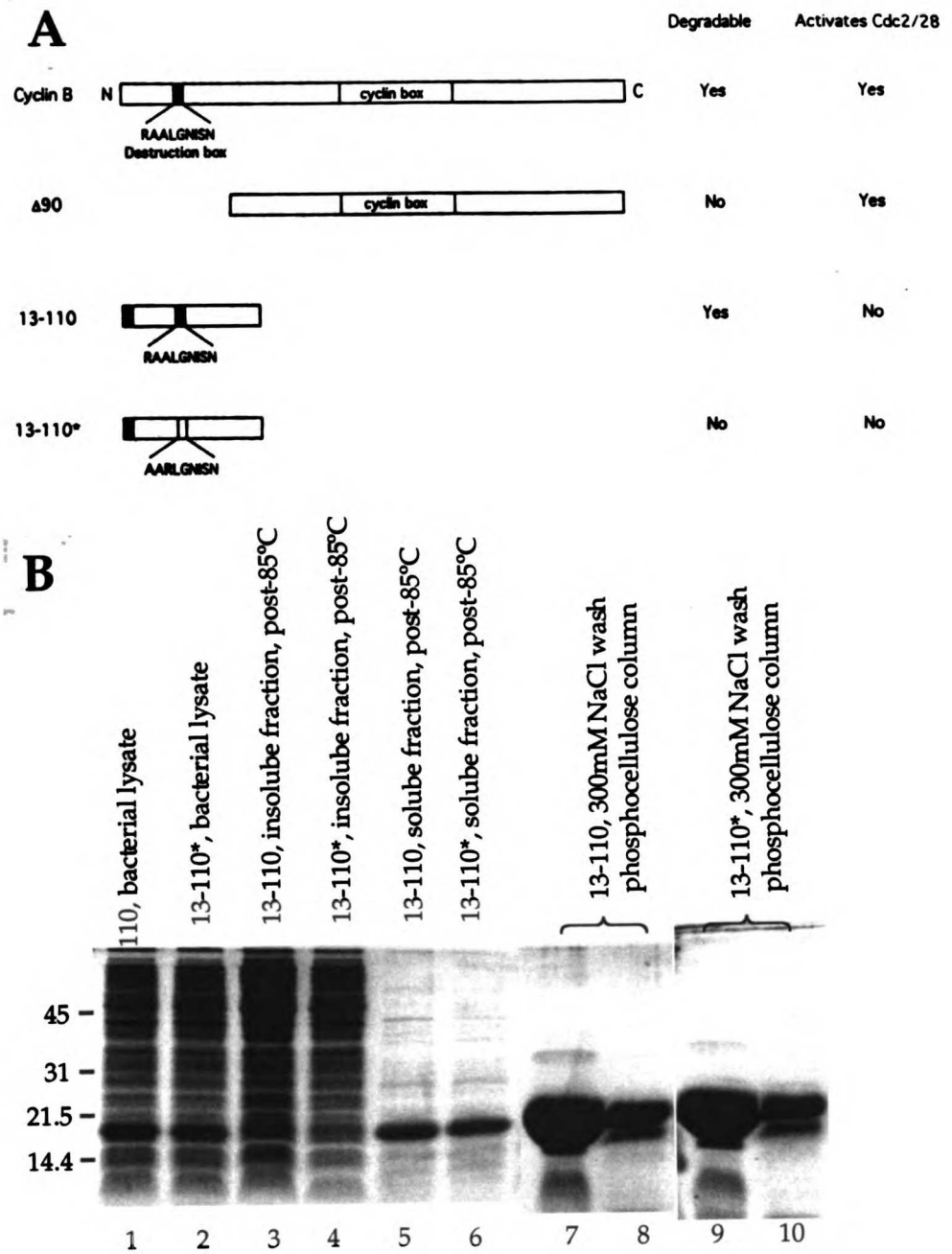
A
Degradable
Activates Cdc2/28
Cyclin B
N
cyclin box
C
Yes
Yes
RAALGNISN
Destruction box
Δ90
cyclin box
No
Yes
13-110
Yes
No
RAALGNISN
13-110*
No
No
AARLGNISN
B
110, bacterial lysate
13-110*, bacterial lysate
13-110, insolube fraction, post-85°C
13-110*, insolube fraction, post-85°C
13-110, solube fraction, post-85°C
13-110*, solube fraction, post-85°C
13-110, 300mM NaCl wash phosphocellulose column
13-110*, 300mM NaCl wash phosphocellulose column
45
31
21.5
14.4
1
2
3
4
5
6
7
8
9
10

Figure 2-2

(Panel A) The relative structure and characteristics of the 13-110 peptide, 13-110*, full length and a truncated form (Δ90) of sea urchin cyclin B are diagrammed. The table also indicates the ability of these constructs to be degraded in Xenopus mitotic egg extracts and to activate Cdc2 kinase activity.

(Panel B) Steps in the purification of the 13-110 and 13-110* peptides were analyzed by SDS-PAGE and Coomasie blue visualization of protein. Lanes 1 and 2 are whole cell lysate after induction of the corresponding peptides. Lanes 3 and 4 are the insoluble fractions (resolubilized in SDS-PAGE loading buffer) after the 85°C incubation and centrifugation that do not contain the peptides. 13-110 and 13-110* peptides are greatly enriched and soluble after 85°C treatment, lanes 5 and 6. Lanes 7-10 are NaCl elution fractions from the final purification step of a phosphocellulose column, highly enriched for the 13-110 and 13-110*. These fractions were pooled and processed for microinjection.

Figure 2-3

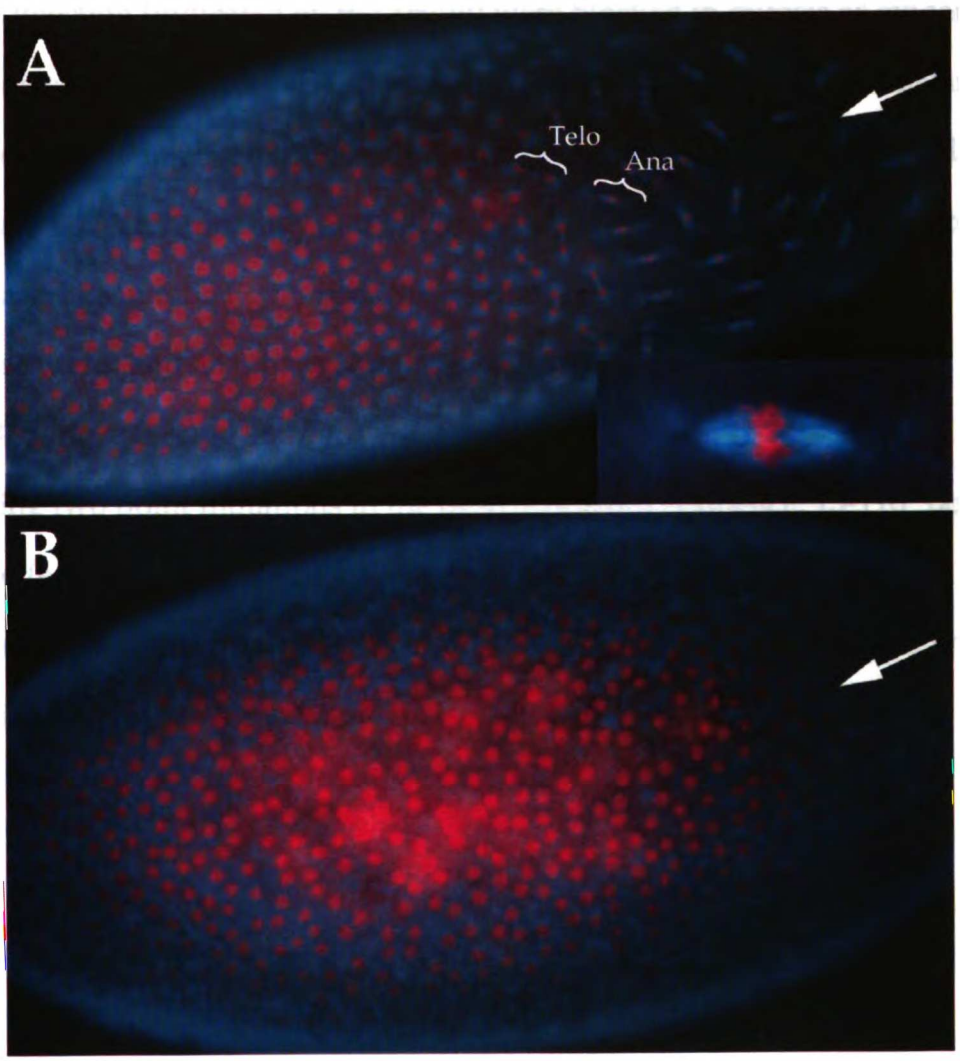

Figure 2-3

(Panel A) Syncytial stage embryos were microinjected with 13-110 peptide, aged 30 min, fixed, and stained for microtubules (blue) and DNA (red). Nuclei at the point of injection (indicated by the arrow) were blocked in mitosis as evidenced by organized microtubules and condensed DNA morphology. Nuclei distant from the point of injection continued to divide unperturbed, displaying a diffuse interphase DNA morphology and higher density. The inset gives an example of a metaphase-like mitotic figure near the point of injection. Brackets identify telophase (Telo) and anaphase (Ana) nuclei.

(Panel B) Syncytial stage embryos were microinjected with 13-110* peptide containing two point mutations in the destruction box sequence. 13-110* peptide had no effect on nuclear divisions. Nuclei maintained a consistent density throughout the embryo and appeared to be synchronous in the cell cycle with diffuse interphase DNA morphology.

Figure 2-4

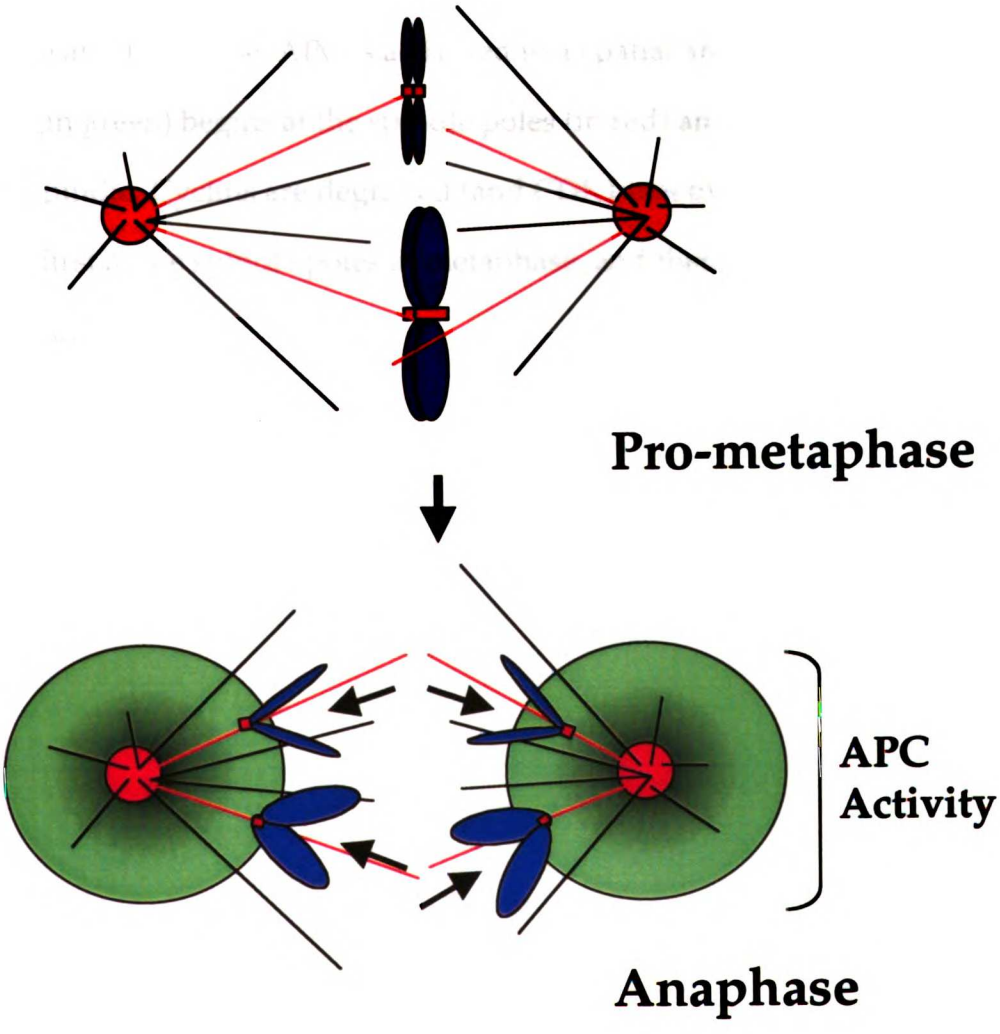

Figure 2-4

Figure 4 depicts a model for localized CDK1 activity in mitosis. In prophase and early metaphase, APC activity is low everywhere in the cell. CDK1 activity remains high and promotes the early mitotic events. In metaphase through anaphase and telophase, APC is activated in a spatial and temporal pattern. APC activity (in green) begins at the spindle poles (in red) and then radiates into the mitotic spindle. Cyclins are degraded (and CDK1 inactivated) in a corresponding pattern, first at the spindle poles in metaphase, and then at the interdigitating microtubules.

Chapter 3

The development of an in vitro assay for Drosophila APC

Introduction

The awesome powers unite

As discussed in Chapter 1, the APC is an essential E3 ubiquitin ligase activity required for exit from mitosis and maintenance of G1 [11, 21]. The APC recognizes and polyubiquitinates substrates, targeting them for degradation by the proteasome. In the past 10 years, many groups have used different assays to measure or infer APC activity. APC activity can be measured directly in an *in vitro* assay, or activity can assessed by monitoring the protein levels of its substrates.

Since APC activation results in disappearance of mitotic cyclins and other substrates, assays that monitor the protein levels of cyclins provided a preliminary readout of APC activity. Stringent tests can be applied to these assays that ensure the fluctuations in cyclins are APC-dependent, such as using mutations in core APC components or removing the destruction box on the substrate. Monitoring endogenous or exogenously introduced cyclins is an assay used to determine APC activity in most systems from yeast to frogs to human cell lines. In *Drosophila*, immunostaining of embryos and larval tissues or Western blotting are common tools employed to measure APC activity. Instead of looking at cyclins directly, cyclin degradation can also be assayed by using a fusion of LacZ to the S. cerevisiae mitotic cyclin, Clb2 [37]. This fusion protein is targeted to degradation by the APC and is biologically inactive in the cell. These procedures fall prey to the caveat that APC activity is inferred. Changes in

substrate levels can also result from changes in transcription or the activity of the proteasome.

APC activity can also be probed more directly in an ubiquitination assay. The polyubiquinating activity of the APC is the essential regulated step governing cyclin degradation [10, 14]. Many assays that measure the covalent attachment and elongation of ubiquitin chains onto mitotic substrates have been reported [35, 36]. Through monitoring the polyubiquitination activity of extracts toward an *in vitro* substrate, the N-terminal peptide of sea urchin cyclin B, two independent studies purified the APC from frog and clam extracts. Although, some studies have used different substrates to assay the ability of the APC to differentially ubiquitinate substrates under different conditions. APC ubiquitination assays are widely used in most model systems and have contributed vastly to our understanding the complex regulation of APC and mitotic events.

Biochemical assays of substrate ubiquitination have certain advantages. APC activity is measured directly and the assay can be shown to be destruction box dependent. However, biochemical assays have their limitations. Measured activity might not reflect *in vivo* activity, necessitating strict correlation with *in vivo* observations. Also, most spatial and temporal resolution is lost by measuring activity from extracts. Finally, most established assays do not use endogenous (same species) substrates. The most commonly used substrate is the amino-terminus of sea urchin cyclin B. By not using endogenous substrates, specificity and differential timing issues cannot be addressed.

In most experimental systems, the combination of *in vivo* monitoring of endogenous APC substrates and biochemical assays towards APC ubiquitin

ligase activity has resulted in our core understanding of the APC and its regulation. To complement other techniques, I developed an APC ubiquitination assay in *Drosophila*.

Materials and Methods

Embyro manipulation, genetics and live-genotype sorting

Embryos were collected, aged, and heat-shocked using standard techniques [61]. Sevelen embryos were used as wild-type genotype. HS-CYCE, HS-FZY, HS-FZR were gifts from C. Lehner [62]. *fzr*$^{-}$/FM7-GFP deficiency stock was generated using Df(*1*)*bi-D3*/FM7 stock previously described [51]. *fzy*^{1}/CyO-GFP, *cycE*^{AR95}/CyO,Kr-GFP and cycE^{AR95}/CyOKr-GFP;HS-RUX were constructed using standard Drosophila genetic techniques. The CyO,Kr-GFP and FM7, Kr-GFP balancer lines [63] were a gift from T.Kornberg. Embryos were sorted according to genotype using the UAS-GFP expression driven by the Kr-GAL4 on the CyO and FM7 balancer chromosomes. Mutant embryos do not express GFP in the Krupel pattern, whereas heterozygote and homozygous balancer sibling embryos displayed low and high GFP expression. Embryos 4-5 hr old were dechorionated, submerged in Embryo Bath (0.7% NaCl, 0.05% Triton X-100), assessed for GFP expression using a UV dissection microscope (Zeiss M2BIO) with a GFP excitation filter, and sorted by hand with a glass capillary pipette and manual suction. Sorted embryos were then heat-shocked on grape juice plates and/or aged in aerated microcentrifuge tubes, rocking at room temperature.

Extract preparation

Extracts were prepared using modifications of two protocols [64], [65]. Embryos were dechorionated with 50% bleach and suspended in Lysis buffer (50mM HEPES, 150mM KCl, .1%NP-40, 1mM EGTA, 80mM β-glycerophosphate, pH 7.5)

with protease and phosphatase inhibitors added just prior to use. Embryos were sonicated three times with 1sec pulses from a micro-sonication tip. Extracts were centrifuged at 14,000Xg to remove insoluble protein and particulate matter. Soluble protein extracts were aliquoted, measured for protein concentration, and stored at –80°C.

Expression and Purification of ^{125}I-labeled 13-110, UBA1, and UBC4

Purified UBA1, UBC4, and 13-110 were originally supplied as gifts from the laboratory of D. Morgan and A. Murray, and later generated in our laboratory as needed. ^{125}I-labeled 13-110 was generated by iodinating 13-110 peptide (see Chapter 2) using a standard chloramine T trihydrate chemical linkage scheme. *S. cerevisiae*, His-tagged UBA1 was expressed and purified from *S. cerevisiae* using protocol from the laboratory of R. Deshaies. *S. cerevisiae* UBC4 was expressed and purified from *E. coli* using a modified protocol from the laboratory of D. Morgan. Conditions for ubiquitination assays were similar to previous studies [65]. Exact quantification of the amount of ^{25}I-labeled 13-110, UBA1, and UBC4 used in each reaction was not performed. However, it was empirically determined that similar concentrations of the constituents to those used in Charles, J. et al. (1998) was optimal (see Figure 1).

APC Ubiquitination Assay

APC was immunoprecipitated by incubating 25-300µg (100µl final volume) of soluble extract with rabbit polyclonal antibodies to Drosophila CDC27 (a gift from J. Raff) for 60 min at 4°C. 20µl of a 1:1 mixture of Protein A-agarose to Lysis Buffer was added. The mixture was incubated for an additional 30 min. Immunoprecipitants were washed 2 times with Lysis buffer, one time with QA

High Salt (20mM Tris-HCl, 250mM KCl, 1mM $MgCl_2$, pH 7.6), and one time with QA (20mM Tris-HCL, 100mM KCl, 1mM $MgCl_2$, pH 7.6).

Ubiquitination assays were performed using embryonic extracts (data not shown) or immunoprecipitates. Briefly, immunoprecipitants were incubated at room temperature for 5-30 min (20 min standard reaction time) with 1mM ATP, 1nmol or 1 μg of bovine ubiquitin (Sigma), 3.5pmol UBA1, 47 pmol UBC4, and 0.2 μl of ^{125}I-labeled 13-110. The reaction was stopped by addition of 7.5 μl SDS-PAGE gel loading buffer, containing SDS and β-mercaptoethanol. The entire reaction was electrophoresed on either 12.5% or 7-20% gradient SDS-PAGE gels. The gels were dried on a standard gel dryer (Bio-Rad model#583) and exposed to film for varying amounts of time at -80°C.

Results

Our original rationale for setting up an assay for APC activity was to complement many *in vivo* observations of mitotic cyclin levels that implied changes in APC activity. Although *in vivo* observations are quite powerful, there are specific limitations to directly assessing the activity of APC in *Drosophila*. Until recently [27, 66], mitotic cyclins were the only identified targets of the APC in *Drosophila*, containing a canonical destruction box that is responsible for their instability in mitosis and G1. [15]. The presence or absence of mitotic cyclins implies APC activity. However, the direct role of the APC in cyclin turnover during embryogenesis cannot be directly tested because of the lack of mutants in core APC components. Without mutations in the APC core complex, the turnover of cyclins cannot be directly correlated to APC activity. In view of these limitations, I developed an assay to measure the ubiquitination activity of the APC directly.

Getting to know your assay

As a starting point for probing assay conditions, I used a polyubiquitination assay established by the laboratories of D. Morgan and A. Murray (see Materials and Methods) to measure APC activity [65, 67]. This assay measures the ability of immunopurified APC or protein extracts to provide the essential E3 enzymatic activity required to efficiently polyubiquitinate the amino terminus of sea urchin cyclin B (13-110). The 13-110 peptide contains the

destruction box sequence required for successful ubiquitin-targeted degradation (see Chapter 2) and serves as a specific substrate for APC in frogs, budding yeast, flies, and humans. Briefly, *S. cerevisiae* E1 and E2 enzymes (Uba1 and Ubc4), ATP, ubiquitin, and ^{125}I-labeled 13-110 are incubated with immunoprecipitants of APC or cell extracts. Reactions are then electrophoresed to separate the polyubiquitinated species. High APC activity results in increased polyubiquitinated 13-110, which is an observable ladder and smear of multi-ubiquitinated species separated by SDS-PAGE.

In order to immunoprecipitate and isolate APC, I reproduced previous results using antibodies specific to APC core components [18]. Using buffer conditions similar to those used in the APC assay, a polyclonal antibody to *Drosophila* CDC27 efficiently co-precipitated Drosophila CDC16 (data not shown). This results suggests that CDC27 and CDC16 are in a complex which corresponds with data from other systems. Importantly, the buffer and wash conditions for the ubiquitination assay are permissible for APC core complex immunoprecipitation. For all APC assay experiments, antibodies to CDC27 were used to immunoprecipitate the core APC.

Luckily, initial assay tests of APC immunoprecipitates from 7-8 hr old embryonic extracts indicated robust APC activity (data not shown). This fortuitous success indicated that I would be able to measure APC activity without great pains in determining optimal conditions. Subsequent tests indicated that Uba1, Ubc4, ATP, ubiquitin, and the ^{125}I-labeled 13-110 were not rate limiting at the concentrations (data not shown) used for all experiments. To confirm the polyubiquitin ladder is dependent on the destruction box of the substrate, competition experiments were performed with an unlabelled 13-110

peptide which contains two point mutations in the destruction box sequence rendering it unrecognizable by APC (13-110*, see Chapter 2). 5-fold excess, unlabelled13-110* did not competitively inhibit the ubiquitination of ^{125}I-labeled 13-110 compared to an unlabelled wild-type 13-110 (data not shown), indicating the reaction is specific for the destruction box contained within the 13-110 peptide.

In order for a biochemical assay to be useful, it must be capable of measuring changes in input enzymatic activity. The ubiquitination assay was tested for its ability to measure dynamic changes in APC activity. Increasing the amount of extract used to immunoprecipitate APC increased the resulting polyubiquitination activity (Figure 1, lanes 1-5). In addition, increased time of the reaction increased the resulting activity. Taken together, these conditions allowed for the detection of changes of activity over a reasonable range of input activity. Importantly, the reactions were not saturated at the concentrations of APC or times used in subsequent reactions (data not shown) because an increase in input APC or time resulted in greater accumulation of polyubiquitinated products. Finally, I tested the relationship between time of reaction together with the amount of input APC. Assays were performed using short reaction times and high amounts of input APC or long reaction times with low amounts of input APC (data not shown). Both conditions resulted in similar output activity. The data suggests that the time and input APC variables are independent and neither is rate limiting.

While performing these experiments a background or contaminating activity was detected that appeared to add a single ubiquitin to the 13-110 peptide (Figure 1, lane 1). This contaminating activity required ATP, ubiquitin,

Uba1, and Ubc4 (data not shown). The contaminating activity is believed to fractionate or co-purify with either Uba1 or Ubc4. Fortunately, the activity did not influence the efficiency of the input APC to generate higher molecular weight conjugates (data not shown) in this reaction.

Mutants in ubiquitin were used to determine the identity of the electrophoretically distinct species of 13-110 (Figure 2). Methylated ubiquitin (Me-Ub) and the ubiquitin variant (K48R) with a point mutation at position 48 (K→R) block extension of the ubiquitin side-chains from the primary ubiquitin, inhibiting polyubiquitination. Both Me-Ub and K48R blocked the appearance of high molecular weight ubiquitin conjugates (Figure 2). The ubiquitin variants have slightly different electrophoretic mobilities compared to the bovine ubiquitin used normally. Knowing the predicted molecular weight of ubiquitin-13-110 conjugates [MW (ubiquitin) =7kD, MW (13-110)=17-18kD], the identity of the initial ubiquitin-13-110 conjugates were determined along with background bands from the iodination step (Figure 2).

The Developmental Age Conundrum

All initial experiments were performed using APC immunoprecipitated from 7-8 hr old embryonic extracts. At this stage in embryogenesis, many cells have entered the first G1 stage during cycle 17 and express high levels of *fzr*. The robust observed APC activity in 7-8 hr old embryonic extracts is consistent with high *fzr*-related dependent G1 activity.

Detectable APC activity in earlier stages of development did not match predicted outcomes. APC was immunoprecipitated from various stages of development (1.5- 8.5 hr old embryos) and assayed for APC activity (Figure 3,

lanes 1-6). Unexpectedly, measured activity was low in stages prior to 6.5 hr old compared to older stages. We estimate a >5-fold difference in activity between early stage extracts and G1 of cycle 17 extracts. This result was surprising because cells at early stages degrade mitotic cyclins and should have high APC activity.

One explanation for this discrepancy in activity is that extracts are made from a population of embryos containing cells in different stages of the cell cycle. APC activity is thought to fluctuate during the cell cycle, peaking for only a short period in mitosis (these stages have no G1). Perhaps, the output activity measured is a merge of the inactive and active states from different cells and/or embryos. The later stage embryos have a high population of G1 cells in which APC activity is high. We tested this model by comparing activity from extracts made from embryos with a high population of cells in G2 to extracts (low APC activity) from embryos with the majority of cells in mitosis (high APC activity). Embryos in G2 of cycle 14 have >90% of cells in G2 where APC activity is predicted to be low. To generate a condition with the high APC activity in embryos, a stabilized version of cyclin B was expressed, arresting most cells in mitosis of cycle 14. Endogenous mitotic cyclins continue to be degraded, suggesting APC is active. Despite the predicted physiological difference in APC activity between G2 and mitotic embryos, measurable APC activity remained equally low in G2 of cycle 14 and mitotic arrested cycle 14 extracts (data not shown). This result is not consistent with the proposed model of cell cycle status influencing the lack of activity measured from early stages.

The low activity in early stage embryos could be the result of inappropriately exposing the APC complex to activators and inhibitors while

making extracts and disrupting the natural cellular state of the cell or embryo. For example, an inhibitor to the APC can be normally compartmentalized separate from the APC. When the cells are lysed the inhibitor can now ectopically act on the APC. In support of this inhibitor model, early stage embryonic extracts appear to contain an "inhibiting" activity (Figure 3, lanes 7-12). Active APC from G1 of cycle 17 stage embryos was immunoprecipitated and then mixed with buffer alone, syncytial stage or G2 of cycle 14 stage extracts for 30 minutes. The immunoprecipitants were washed and measured for APC activity. G1 of cycle 17 APC activity is lower after exposure to early stage extracts (lane 8and 9), but not by buffer alone (lane 7). The possibility that the G1 of cycle 17 APC bound to the antibody was competed away by excess inactive early stage APC was eliminated (Figure 3, lanes 10-12). Instead of immunoprecipitated APC, G1 of cycle 17 extract was mixed with buffer, syncytial stage, or G2 of cycle 14 extract. All of the APC in the mixture was immunoprecipitated by adding a vast excess of CDC27 antibody and Protein A beads. Consistent with the previous experiment, G1 of cycle 17 APC activity is lower upon exposure to early stage extracts. The source of the inhibition will be discussed later (see Section- "CycE?" and Discussion). Finally, the inactivating activity in early stage extracts can be removed by boiling (data not shown), suggesting that the inactivating activity is protein-based and is not a salting or small molecule contaminant.

fizzy and fizzy-related: the Ying and Yang of APC activators

A final model explaining the abrupt increase in measurable APC activity is that the APC assay detects only *fizzy-related* dependent activity. This model is supported by experiments using identical reagents and assay conditions in *S.*

cerevisiae. The these conditions detected Cdh1-dependent APC activity and not CDC20-dependent activity [67]. *fzy* and *fzr* are unique with regards to their embryonic expression pattern. *fzy* is expressed at all embryonic stages until after G1 of cycle 17. *fzr* expression begins early in 5-6 hour old embryos in a small subset of cells. Expression increases in the bulk of the embryo as cells enter G1 of cycle 17 at 6-8 hr. The *fzr* expression profile is similar to the increase in APC activity in this assay.

The model that the APC assay detects only *fzr* activity was tested by altering of *fzy* and *fzr* via overexpression and mutation and analyzing the resulting APC activity. Loss of *fzr* results in ectopic mitotic cyclin accumulation and an extra cell cycle instead of a G1 arrest during cycle 17. Mutations in *fzy* result in a mitotic delay in the epidermis during cycle 16 and the perdurance of mitotic cyclins during mitosis. APC activity was compared between mutant *fzy* and *fzr* extracts to their heterozygous siblings (Chapter 3, Figure 4, lanes 11-14). *fzy* or *fzr* mutant and heterozygous embryos were sorted live using GFP-expressing balancer chromosomes (see Materials and Methods). Extracts were made at the developmental stage when the *fzy* and *fzr* mutants first deviate from the wild-type cell cycle [51], [15]. In support of the assay being *fzr*-dependent, APC activity was lower in *fzr* mutants (80% decrease). Interestingly, activity was slightly lower in *fzy* mutants (20% decrease) compared to heterozygous controls. The small decrease in APC activity seen in *fzy* mutants could be a result of cells delayed in metaphase of cycle 16, preventing the increase of *fzr* expression in G1 of cycle 17. These results suggest that the ubiquitination assay requires *fzr* and perhaps *fzy*.

To further test if the APC assay was responsive to *fzy* activity, *fzy* was overexpressed (see below HS-FZY) in *fzr* mutant embryos (data not shown). The rationale behind this experiment was to remove the influence of *fzr* by mutation and assay the ability of *fzy* to modify APC activity. Similar to *fzr* mutant embryos, uninduced *fzr* mutant embryos carrying *fzy* on a heat-shock inducible transgene displayed a significant decrease in APC activity compared to heterozygous siblings. Overexpression of *fzy* in *fzr* mutant embryos did not increase APC activity. This result suggests that in the absence of *fzr*, *fzy* cannot change APC activity in this assay. The data are consistent with the APC assay being *fzr*-dependent (see Discussion).

APC activity was measured following overexpression of *fzy* and *fzr*. Overexpression of *fzr* in the *Drosophila* embryo during G2 of cycle 16 (prior to the bulk expression of endogenous *fzr* in G1 of cycle 17) down-regulates cyclins A, B, and B3 and inhibits mitosis [51]. Ectopic *fzy* expression does not appear to modify the cell cycle profile or change cyclin levels, but overexpression does rescue the mutant phenotype (C. Lehner, personal communication, data not shown). This suggests that *fzy* expression alone is not rate-limiting in the *Drosophila* embryo.

fzy and *fzr* were overexpressed using transgenic lines carrying either *fzy* or *fzr* under the control of the heat shock inducible, hsp70 promoter (HS-FZY or HS-FZR). Figure 4 shows the effects of *fzy* or *fzr* overexpression in G2 of cycle 14 (lanes1-4) and in G1 of cycle 17 (lanes 5-8). In G2 of cycle 14, *fzy* overexpression had no effect on measurable APC activity. Whereas, *fzr* overexpression greatly increased (>5-fold) measurable APC activity. Western blots and in situ hybridization experiments confirmed overexpression under these circumstances

(data not shown). In G1 of cycle 17, both *fzy* and *fzr* overexpression resulted in higher APC activity. The increase in APC activity resulting from *fzy* overexpression was variable. Controls for the heat shock protocol were also variable. Despite the variability, *fzr* overexpression at all stages tested resulted in increased APC activity and *fzy* overexpression in G2 of cycle 14 failed to change APC activity. The effects of *fzy* overexpression on APC activity in later stages needs to be more rigorously examined.

Could it be? Cyclin E is inhibitory?

Cyclin E has been implicated as a negative regulator of the APC (see Chapter 4). The effect of ectopic cyclin E expression on measurable APC activity was tested. Cyclin E was ectopically expressed in G1 cycle 17 under the control a heat shock inducible promoter (HS-CYCE). Using similar conditions, Knoblich et. al [62] observed mitotic cyclin accumulation, suggesting the APC was inactivated by cyclin E. However, no change was observed in APC activity when cyclin E was overexpressed (Figure 5, lanes 5&6). Parallel Western blotting confirmed that cyclins A and B accumulated under these experimental conditions. The data present a contradiction between the predicted decline in APC activity upon cyclin E overexpression and the measured APC activity. APC inactivation by cyclin E could occur in a short, transient period because ectopic cyclin E drives G1 cells through an ectopic cell cycle [62]. To test this, APC activity was measured at different times after cyclin E induction (data not shown) and no difference was observed (data not shown). It is not clear why under these

circumstances, the measurable APC activity does not change and remains to be tested.

To further test the role of cyclin E as a negative regulator of the APC, APC activity was measured in embryos mutant for cyclin E. Development and the cell cycle profile are normal in cyclin E mutant embryos (*cyclin E^{AR95}*) through mitosis of cycle 16 [62]. Maternally provided cyclin E function is believed to support cell cycle progression until this stage. After this point, most cells fail to enter S-phase of cycle 17 in *cyclin E^{AR95}* embryos. APC activity was measured in cyclin E mutants (Figure 5, lanes 2&4) and compared to heterozygous siblings (Figure 5, lanes 1&3). Measurable APC activity was increased about 4-5 fold in *cyclin E^{AR95}* embryos in an early stage during S-phase 15 (compare lanes 1 and 2). This result correlates with new data (see Chapter 4) that suggests *cyclin E^{AR95}* embryos are deficient in at least a subset cyclin E functions much earlier in development, as early as mitosis of cycle 14. It is important to note that there is no change in endogenous mitotic cyclin levels or cell cycle progression at this stage in *cyclin E^{AR95}* embryos. The increase in APC activity in *cyclin E^{AR95}* suggests that cyclin E has an inhibitory role in the in this assay and could contribute to the inhibitory activity present in early stage extracts (See Discussion).

Discussion

This chapter is a summary of results elucidating the *in vitro* activity of *Drosophila* APC. An ubiquitin ligase assay of immunopurified APC was designed to monitor APC activity from *Drosophila* embryonic extracts. The APC assay was ATP and ubiquitin dependent (data not shown, Figure 2). Importantly, substrate ubiquitination required the destruction box sequence suggesting the activity was specific for APC targets (data not shown). Robust activity was detected from late embryonic stages (Figure 1 and 2). Measured activity was low in early, pre-cycle 17 embryonic extracts and did not correlate to cell cycle stage (Figure 2). An inhibitory activity in early stage (<4 hr old) embryonic extracts was detected that could partially inactivate measured activity from late stages (Figure 2).

APC activity was measured under different conditions (Figure 4 and 5). Overexpression of *fzr* increased activity. Conversely, activity was low from *fzr* mutant embryos. *fzy* overexpression could not increase APC activity in cycle 14 and cycle 15 embryos and had variable effects in G1 of cycle 17. *fzy* mutant embryos had slightly decreased activity. Overexpression of cyclin E in G1 of cycle 17 had no effect on measurable APC. Interestingly, embryos mutant for cyclin E (*cyclin* E^{AR95}) had lower APC activity, suggesting an inhibitory role for cyclin E.

Which APC is being measured?

The data presented in this chapter supports the hypothesis that the measured *in vitro* APC activity detects primarily *fzr*-dependent activity. Measurable APC activity increases with developmental time and correlates to the bulk increase in *fzr* expression. FZR protein is assumed not to be present at the early stages. Attempts to produce antibodies to FZR have failed, thus leaving this notion untested. APC activity changes upon genetic modulation of *fzr*, supporting the model of the assay being *fzr*-dependent. It is not clear if the low activity in early stage extracts is *fzr*-dependent APC. There are a few cells expressing *fzr* at this stage [51] that could contribute to this activity. A homolog to *fzr* has been identified from the Drosophila genome, which could also be differentially regulated and expressed, contributing to measurable APC activity. However, there are no reports regarding the *fzr* homolog as of yet.

APC activity was low in early stage extracts where physiological APC should be active. We believe this assay does not detect *fzy*-dependent activity. Without data regarding the *fzr* homolog, we assume that the the early cell divisions in *Drosophila* embryos contain only *fzy*-dependent APC activity. RNAi experiments targeted towards *fzy* causes an arrest of the early cell divisions (data not shown). *fzy* is highly expressed in early embryonic stages while *fzr* expression is undetectable in most cells [68]. Perhaps *fzy*-dependent APC activity is difficult to measure and the small activity measured from early embryos is *fzy* activity. However, at this stage no measurable changes can be seen under conditions when *in vivo* data suggests a change in APC activity. For example, APC activity does not change in mitotically arrested extracts, remaining low. Furthermore in early stage embryos, *fzy* overexpression does not increase APC activity. APC activity is slightly decreased in *fzy* mutants. This experiment is

difficult to interpret. The difference in activity could be because cells are delayed in mitosis 16, preventing cells to progress into G1 where measurable APC is high. Finally, APC activity does not increase when *fzy* is overexpressed in *fzr* mutant embryos (data not shown). This result suggests that in the absence of *fzr*, *fzy* cannot change APC activity in this assay. For reasons that are not clear, this APC assay cannot detect *fzy*-dependent APC activity. *fzy* activity could be lost due to experimental caveats or an inhibitory activity to *fzy* could be present (see below).

What is the inhibitory activity in early stage extract?

When extracts are generated, the physiological cell cycle state is lost. Compartmentalization is lost, cellular structures are disrupted, and molecules are permitted to mingle when normally they are kept separate. The results of which could be a set of biochemical activities that do not reflect physiological activities.

An inhibitor in early extracts is believed to contribute to the low measurable activity in the APC assay. When an extract or immunopurified APC containing active APC is mixed with early stage extracts, the activity is decreased (Figure 2). This inhibitory activity has not been identified. Cyclin E levels are high in early stages and do not fluctuate until G2 of cycle 16 when cyclin E levels decline. An intriguing idea is that the constant presence of cyclin E in early stage embryos suppresses measurable APC activity. This model is supported by the observation that measurable APC activity increases in cyclin E mutant embryos (Figure 5). It has not been tested if the increase in APC activity in *cyclin* E^{AR95} embryos is *fzr*-dependent.

Although this *in vitro* APC assay does not appear to measure *fzy*-dependent activity, we can successfully measure *fzr*-dependent activity. This assay will be useful in the future to probe the role of cyclin E as an inhibitor to the APC (perhaps through *fzr*), the regulation of *fzr*, and perhaps the regulation of *fzy*.

Figure 3-1

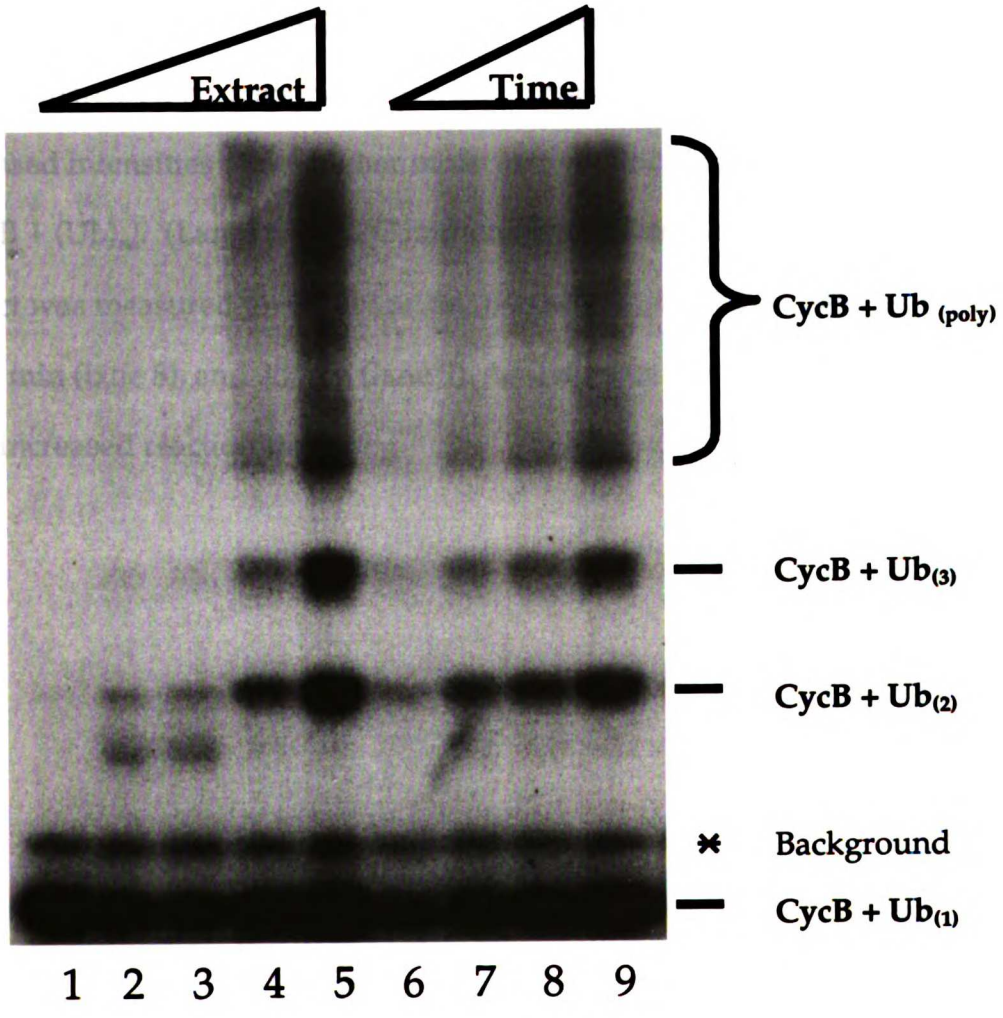
Extract
Time
CycB + Ub (poly)
CycB + Ub(3)
CycB + Ub(2)
Background
CycB + Ub(1)
1 2 3 4 5 6 7 8 9

Figure 3-1

(Lanes 1-9) APC activity was measured under different conditions. (Lanes 1-5) APC was immunoprecipitated from different amounts of 7-8 hr extract (0, 25, 50, 100, and 200μg, respectively) and incubated with ^{125}I-13-110 for 20 min. APC activity increased correspondingly with increased extract as visualized by the increased intensities of the higher molecular weight polyubiquitinated species [Cyc B + $(Ub)_n$]. (Lanes 6-9) APC immunoprecipitated from 100μg of 7-8 hr extract was measured for its ubiquitination activity for 1 min (lane 6), 5 min (lane 7), 15 min (lane 8), and 30 min (lane 9). APC activity increased correspondingly with increased reaction times.

Figure 3-2

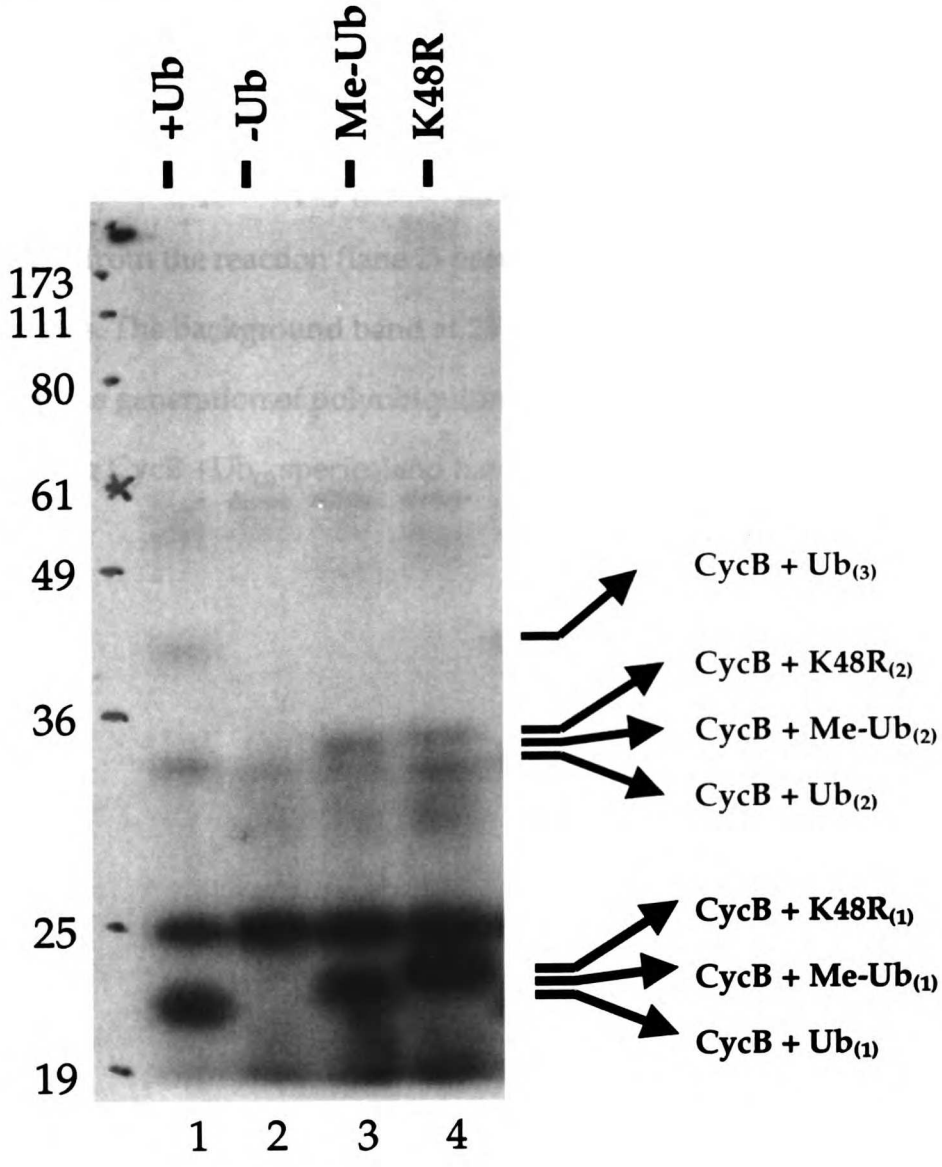
+Ub
-Ub
Me-Ub
K48R
173
111
80
61
49
36
25
19
1
2
3
4
CycB + Ub(3)
CycB + K48R(2)
CycB + Me-Ub(2)
CycB + Ub(2)
CycB + K48R(1)
CycB + Me-Ub(1)
CycB + Ub(1)

Figure 3-2

The polyubiquitinated species in the APC assay were characterized. APC was immunoprecipitated from 5.5-6.5 hr old embryonic extracts. Immunopurified APC was incubated in the standard reaction (see Materials and Methods, lane 1), without ubiquitin, with methylated ubiquitin (Me-Ub, lane 3), or a variant of ubiquitin refractory to ubiquitin chain elongation (K48R, lane 4). Different ubiquitin-13-110 species [CycB + $Ub_{(n)}$] are indicated by arrows. Removing ubiquitin from the reaction (lane 2) prevents the appearance of ubiquitin-13-110 conjugates. The background band at 25 kD remains. Me-Ub and K48R efficiently prevent the generation of polyubiquitinated species (no high molecular weight "smear" or CycB +$Ub_{(3)}$ species)and have no effect the addition of one ubiquitin.

Figure 3-3

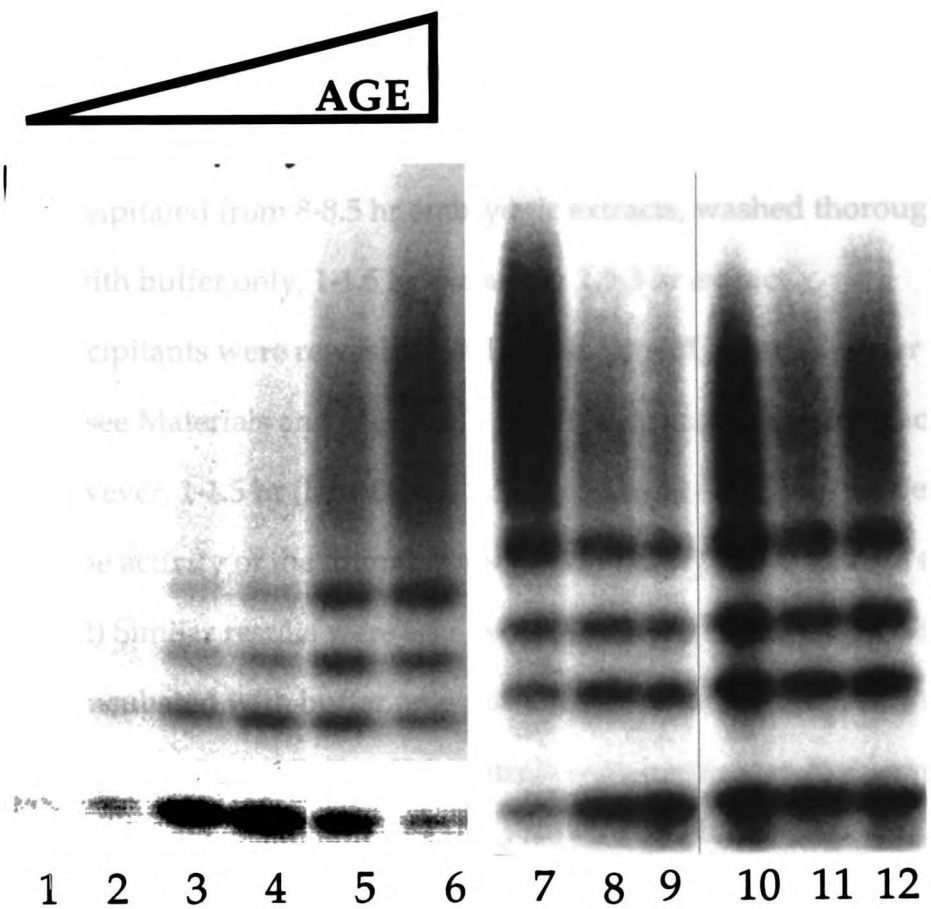

Figure 3-3

(Lanes 1-6) APC ubiquitination activity was measured under standard reaction conditions from different stage extracts: 1-1.5 hr (lane 1), 2.5-3 hr (lane 2), 3.5-4.5 hr (lane 3), 4.5-5.5 hr (lane 4), 6.5-7.5 hr (lane 5), 8-8.5 hr (lane 6). Ubiquitination activity increased with age. Measurable activity of the developmental ages tested is lowest at 1-1.5 hr and highest at 8-8.5 hr.

(Lanes 7-12) Mixing experiments were performed to test for a presence of an "inhibitor" present in early stage extracts. (Lanes 7-9) APC was immunoprecipitated from 8-8.5 hr embryonic extracts, washed thoroughly, and incubated with buffer only, 1-1.5 hr extract, or 2.5-3 hr extract. Immunoprecipitants were rewashed and tested for APC activity under standard conditions (see Materials and Methods). Buffer only had no effect on activity (lane 7); however, 1-1.5 hr (lane 8) and 2.5-3 hr (lane 9) old embryonic extracts decreased the activity of the immunoprecipitated APC from late stage extracts. (Lanes 10-12) Similar results were seen when 8-8.5 hr old embryonic extract was mixed and incubated with buffer only (lane 10), 1-1.5 hr old extract (lane 11), and 2.5-3 hr old extract (lane 12). Parallel controls were performed to eliminate dilution and antibody competition during immunoprecipitations and ubiquitination reactions. APC activity decreased when 8-8.5 hr old extract was incubated with 1-1.5 hr and 2.5-3 hr old extract compared to buffer only (compare lanes 11 and 12 to lane 10).

Figure 3-4

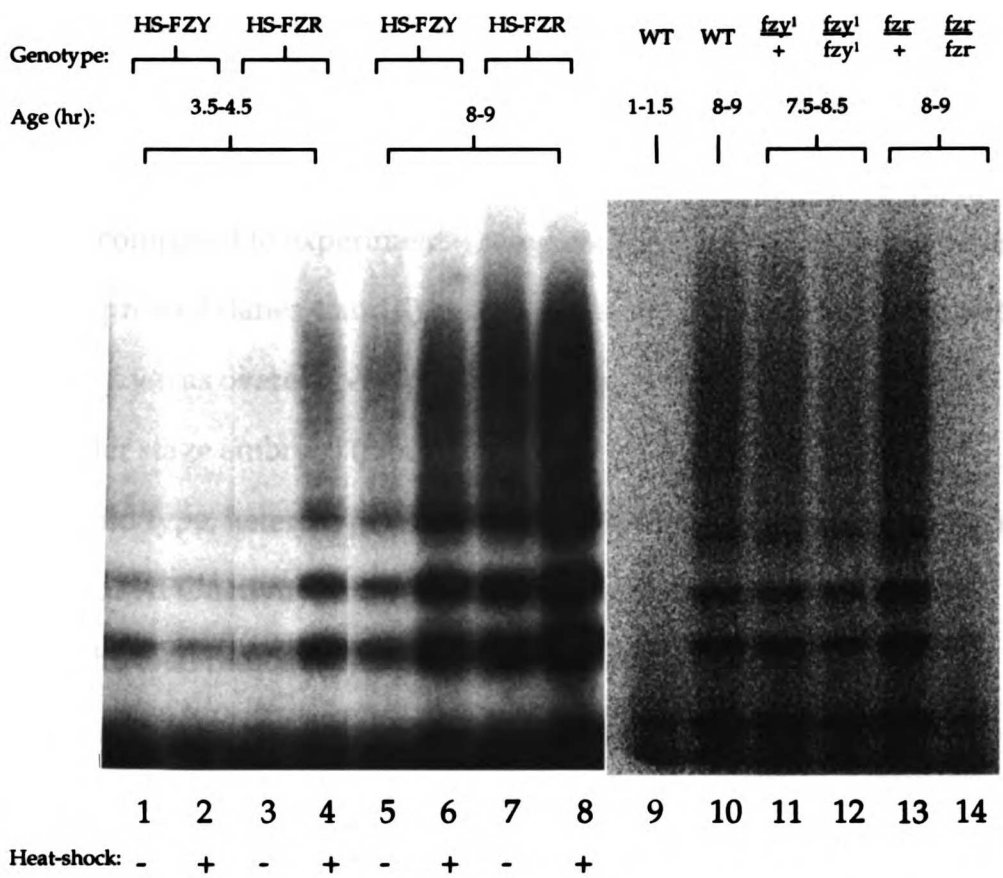
Genotype:
HS-FZY
HS-FZR
HS-FZY
HS-FZR
WT
WT
fzy1 +
fzy1 fzy1
fzr +
fzr fzr
Age (hr):
3.5-4.5
8-9
1-1.5
8-9
7.5-8.5
8-9
1 2 3 4 5 6 7 8 9 10 11 12 13 14
Heat-shock: - + - + - + - +

Figure 3-4

APC activity was measured following modulation of *fzy* and *fzr* in embryonic extracts either by overexpression (lanes 1-8) or by mutation (lanes 9-14).
(Lanes 1-8) Embryos carrying *fzy* or *fzr* transgenes under the control of the heat shock promoter (HS-FZY and HS-FZR) were heat shocked to overproduce the corresponding gene product (lanes 2, 4, 6, and 8) at the indicted developmental ages. Parallel experiments were performed without heat shock as a control (lanes 1,3, 5, and 7). Then, APC activity was measured under standard conditions and controls were compared to experimental samples. APC activity increased when *fzr* was overexpressed (lanes 4 and 9) at both ages tested. APC activity did not increase when *fzy* was overexpressed in early stage embryos (lane 2); but did increase in older stage embryos (lane 6).
(Lanes 9-14) Wild type, heterozygous and mutant *fzy* and *fzr* embryonic extracts were probed for APC activity under standard conditions. Activities were measured as the total radioactive signal contained in each lane for the >20 kD high molecular weight products, quantified by phosphoimaging. In wild-type embryos, measurable APC ubiquitination activity was significantly higher from older, 8-9 hr old extracts (lane 10) compared to early stage, 1-1.5 hr embryonic extracts (lane 9). *fzy* and *fzr* heterozygous or mutant extracts were generated using GFP balancer chromosomes and a live embryo sorting technique (see Materials and Methods). Activity decreased slightly (~20%) in *fzy* mutants (lane 12) compared to heterozygous sibling extracts (lane 11). In *fzr* mutant extracts (lane 14), activity decreased ~80% compared to heterozygous siblings (lane 13).

Figure 3-5

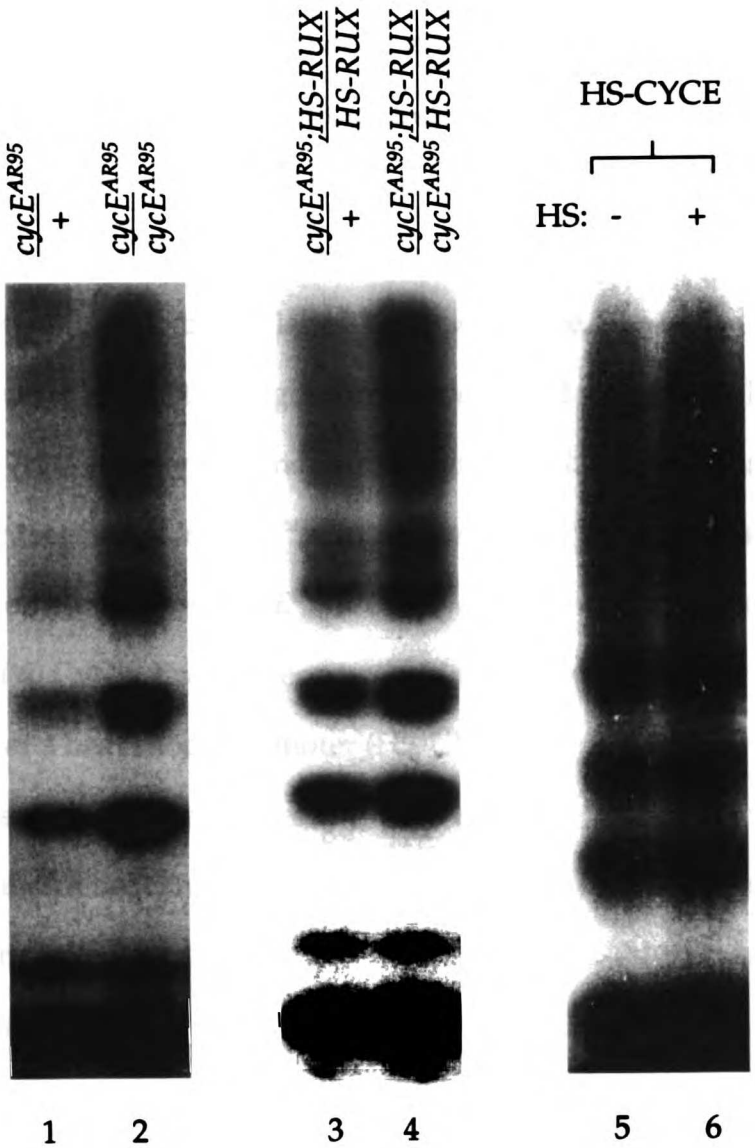
cycE^AR95 / +
cycE^AR95 / cycE^AR95
cycE^AR95;HS-RUX / +
cycE^AR95;HS-RUX / cycE^AR95 HS-RUX
HS-CYCE
HS: - +
1 2 3 4 5 6

Figure 3-5

APC activity was measured in different cyclin E mutant backgrounds (lanes 1-4) or upon cyclin E overexpression (lanes 5 and 6).

(Lanes 1-4) APC activity was measured from heterozygote and $cycE^{(AR95)}$ homozygous mutant embryonic extracts. Embryos were sorted live according to genotype (see Materials and Methods), extracts were made at 5-6 hr old, and ubiquitination activity was measured under standard conditions. Measurable APC activity was increased ~4-5 fold (as measured in parallel dilution experiments) in $cycE^{(AR95)}$ mutant embryonic extracts (Lane 1) compared to heterozygous sibling extracts (lane 2). *rux* was overexpressed in $cycE^{(AR95)}$ embryos mutant and heterozygous embryos (see Materials and Methods of Chapter 4). APC activity was measured under similar conditions as lanes 1 and 2. APC activity increased in $cycE^{(AR95)}$ mutant embryos overexpressing *rux* (lane 3) compared to heterozygous $cycE^{(AR95)}$ embryos overexpressing *rux* (lane 4).

(Lanes 5 and 6) Cyclin E was overexpressed in embryos carrying *cyclin E* under the control of a heat shock promoter (HS-CYCE, [62]). Cyclin E was overexpressed in 7-8 hr embryos and allowed to recover for 2 hr. APC activity was measured in heat shocked (lane 6) and non-heat shocked controls (lane 5). There was no detectable change in measurable APC activity as a result of cyclin E overexpression.

Chapter 4

CDKs negatively regulate APC activity

Introduction

Untangling the web of APC regulation

The regulation of the APC in and out of mitosis is a complex web of regulatory modules. There are many known mechanisms that contribute to APC activity: expression and phosphorylation of activator proteins, phosphorylation of core APC components, and binding of inhibitory protein complexes [11, 21]. As of yet, the precise set of interactions and protein states that regulate the APC throughout the entire cell cycle have not been clearly worked out. In addition, regulation of the APC might be unique in different organisms and developmental contexts. In general, APC is believed to be inactive during S-phase and G2 during when CDK/cyclin activity is high. Then, sometime around the metaphase-anaphase transition APC is activated (perhaps to a subset of substrates) and remains active through mitosis into G1.

Genetic and biochemical studies in recent years have identified $CDC20^{fzy}$ and $CDH1^{fzr}$ as substoichiometric activators of the APC. In *Drosophila*, *fzy* was first identified to be required for mitotic cyclin degradation and sister chromatid separation [15, 68]. The *fzy* homolog in *S. cerevisiae*, CDC20, has subsequently been shown genetically and biochemically to activate the APC [38, 69]. *fzr* was later identified in *Drosophila* to be required for cyclin degradation in G1 and the maintenance of a G1 state [51]. Concurrently, *fzr* related homologs (CDH1 or HCT1) were identified in frogs and budding yeast and similarly are required for cyclin degradation and can activate the APC [38, 70]. $CDC20^{fzy}$ and $CDH1^{fzr}$

homologs have been identified and characterized in many other species, including frogs and humans. In general, both CDC20^{fzy} and CDH1^{fzr} bind and activate the APC. CDC20^{fzy} is believed to activate the APC in mitosis to a subset of substrates (Pds1 and Clb5 in budding yeast) and is required for sister chromatid separation. CDH1^{fzr} is activated late in mitosis and is active through G1. There is some evidence that CDC20^{fzy} and CDH1^{fzr} target the APC to different substrates [38], but the universality of this idea remains to be tested. In the embryonic cell cycles *Xenopus* and *Drosophila*, CDH1^{fzr} is not expressed. These divisions are thought to be entirely CDC20^{fzy} dependent.

CDC20^{fzy} is regulated by protein expression, phosphorylation, and interaction with the checkpoint proteins [11, 21]. CDC20 protein levels oscillate with the cell cycle, remaining low in G1 through late G2. CDC20 itself is a target of the APC [38, 69]. CDC20^{fzy} is also inhibited by the spindle assembly checkpoint. CDC20^{fzy} in some systems has been shown to be phosphorylated during late G2 and early mitosis [71-73]. It is unclear if CDC20^{fzy} phosphorylation has a function [60], although in certain circumstances it can be inhibitory [73]. Finally, MAD2 binds and inhibits CDC20^{fzy} activation when the checkpoint is activated and perhaps under normal circumstances in the beginning of mitosis [74-76]. In *Drosophila*, *fzy* regulation has not been directly investigated. Unlike most organisms, *Drosophila fzy* protein levels do not fluctuate with the cell cycle [68].

Many exciting recent studies have shown that CDH1^{fzr} is regulated primarily through phosphorylation [71, 77-79]. In budding yeast, CDH1 is phosphorylated by CDC28 in S-phase through early mitosis, preventing its binding to APC. In mitosis, CDH1 is dephosphorylated by CDC14 [45, 77],

permitting CDH1 to bind and activate the APC. In the case of CDH1, CDK activity negatively regulates APC, explaining an early observation that inappropriate CDK inactivation leads to cyclin degradation [80]. Negative regulation of CDH1^{fzr} by phosphorylation appears to be a conserved mechanism [71, 79].

In *Drosophila*, a series of experiments has implicated cyclin E as a negative regulator of *fzr*-dependent APC activity [51, 62]. Overexpression of cyclin E in G1 stage embryos results in ectopic mitotic cyclin accumulation [62]. Coexpression of cyclin E suppresses the ability of ectopic *fzr* to downregulate mitotic cyclins in G1 cells, presumably by suppressing *fzr*-dependent APC activation [51]. Ectopic *fzr* expression has no effect on cell cycle progression until G2 of cycle 16 when endogenous cyclin E levels decline. Conversely, when *fzr* is overexpressed prior to G2 of cycle 16 in cyclin E mutants, mitotic cyclins are downregulated. In this case removing cyclin E function by mutation allow ectopic *fzr* to activate the APC. These results suggest that cyclin E is capable of inhibiting *fzr*-dependent APC activity in a similar fashion to the budding yeast suppression of CDH1 by CDC28.

Studies have shown phosphorylation of the core APC complex can activate the APC. In an early study, CDK1 activity was shown to be required for cyclin degradation in *Xenopus* egg extracts [81]. Many core components of the APC (CDC27, CDC16, CDC23, and APC1) are phosphorylated *in vitro* and *in vivo* during mitosis [11]. In more recent studies using APC ubiquitination assays, phosphorylation of the APC by CDK1/cyclin B-type complexes appears to activate the APC [79, 82-84]. Inactive interphase APC can be phosphorylated and activated by CDK/cyclins. Conversely, active mitotic APC complexes can be

treated with phosphatases and inactivated (activity is restored by treatment of APC with CDK/cyclin complexes). A molecular model of how phosphorylation of the APC at specific sites (probably by CDK/cyclin complexes) allows the APC to interact with activators such as $CDC20^{fzy}$. In support of this, "phosphorylated" APC can more efficiently bind and be activated by $CDC20^{fzy}$ [60, 71, 84, 85].

Many other kinases seem to influence APC activity. CDC5 in S. cerevisiae and Plx1 (Polo-like kinase) have been shown to activate the APC [65, 69, 84]. Genetically and biochemically, PKA has been shown to negatively regulate APC activity, perhaps by phosphorylation of the APC core complex [86, 87].

Despite the wealth of data regarding the regulation of APC activity, many questions remain. What is the molecular circuit leading to $CDC20^{fzy}$ activation? What regulates the spatial and temporal degradation of APC targets? How do positive and negative phosphorylation events of APC and its regulators coordinate APC activity? Do checkpoint pathways play a role in APC regulation during a normal cell cycle?

Tipping the Scale over to the APC

Recent work in the O'Farrell lab has uncovered a role for mitotic cyclins in the inhibition of APC activity. While probing the function of the mitotic cyclin inhibitor, *roughex (rux)*, in the *Drosophila* embryo, Nikita Yakubovitch observed that cyclin A is downregulated in G2 of cycle 16 cells when *rux* is overexpressed (data not shown). Similarly, when *rux* and cyclin A are coexpressed in G1; a transient nuclear localization can be observed, followed by degradation of cyclin A [88]. In G1 of cycle 17, turnover of mitotic cyclins is high. Prior to cycle 16,

when *rux* is overexpressed cyclin A is functionally inhibited and becomes nuclear [8, 9]. But, cyclin A remains stable at early stages. It appears that functional inhibition of mitotic cyclins prior to G2 of cycle 16 does not result in cyclin A turnover; however, rux overexpression in later stages results in cyclin A degradation.

To explain these data, it was proposed that high cyclin E and mitotic cyclin levels together inhibit the APC. Cyclin E levels are continuously high in the embryo until G2 of cycle 16 [62]. When cyclin E levels are high, the APC is held inactive during interphase by both mitotic cyclins and cyclin E. Upon *rux* overexpression, mitotic cyclins are inhibited; however, the APC is still inhibited by high cyclin E in the early embryo. When cyclin E levels decline in G2 of cycle 16, *rux* overexpression results in APC activation because both mitotic cyclins and cyclin E are low. In support of this model, preliminary experiments suggested that cyclin A disappears upon *rux* overexpression in cyclin E mutant embryos ($cycE^{AR95}$).

In this chapter, data is presented exploring the role of CDK/cyclin complexes in APC regulation. To further the above observations, the levels of mitotic cyclins were assessed upon *rux* overexpression in cyclin E mutant embryos ($cycE^{AR95}$). In addition, I attempted to identify the players participating in APC regulation by CDK/cyclins by testing the role of *rca1* as a negative inhibitor of *fzy*.

Materials and Methods

Fly and embryo manipulation, fixation, and immunostaining

All genetic backgrounds were generated using standard Drosophila genetic techniques [61]. The fly stocks used in this chapter were (1)*cycE*^{AR95}/*CyO*; HS-RUX/HS-RUX, (2) *fzy*^{1}/*CyO*, (3) *rca1*$^{1.2}$/*CyO*, or (4) *rca1*$^{1.2}$, *fzy*^{1}/*CyO* and were all constructed by standard genetic techniques. The HS-RUX stock was a gift from B. Thomas and *rca1*$^{1.2}$/CyO was a gift from L. Zipursky. All embryo collection, aging, manipulation, and fixation was performed as previously described [55, 64].

Embryos were fixed with 3.7% formaldehyde for 20 min for cyclin A, B, and B3 staining.

Cyclin B3 immunostaining was performed as previously described [15, 55]. Cyclin A and B embryonic immunostaining was as a modification of the tyramide signal amplification (TSA) scheme from NEN Life Science Products (Cat. #NEL700). Antibodies used in this chapter were to Drosophila cyclin A (rabbit polyclonal, UCSF#25), cyclin B (monoclonal F2F6) or cyclin B3 (rabbit polyclonal, gift from C. Lehner). Primary antibody incubations were usually performed overnight. Secondary antibodies (horseradish peroxidase coupled anti-rabbit or anti-mouse) were incubated for >3 hr. TSA reactions were 2.5 min at room temperature. The tyramide amplified signal was visualized using a final incubation with fluorscein or rhodamine coupled strepavidin conjugates (>3 hr). DNA was visualized using HOECHST 33258 (Molecular Probes).

Extract preparation and western blotting

Embryonic extracts of $cycE^{AR95}/cycE^{AR95}$; HS-RUX/HS-RUX or $cycE^{AR95}$/*CyO-GFP*; HS-RUX/HS-RUX were generated by sorting embryos live as described in Chapter 3 and lysing embryos directly in SDS-PAGE sample loading buffer. Western blots were performed as previously described [3]. Proteins were separated on a 10% SDS protein gel, transferred to PVDF membranes, and probed for Drosophila cyclin A.

In vitro transcription/translation reactions and immunoprecipitation reactions

^{35}S-methionine labeled or unlabeled FIZZY, FIZZY-RELATED, and RCA1 were produced using the in vitro coupled transcription/translation reticulocyte system from Promega (Catalog #L4600). The vectors containing T3 or T7 promoters for expression used in these reactions have been previously described [15, 51, 89] and were gifts from C. Lehner and L. Zipursky. Coupled reactions to produce labeled or unlabeled protein were performed for 3 hr at 37°C. Coupled in vitro transcription/translation reactions were diluted in APC lysis buffer and mixed for 1 hr at 4°C. Antibody incubation, protein A coupling, and subsequent wash steps were performed exactly as described in Chapter 3. Precipitants were resuspended in SDS-PAGE sample loading buffer containing β-mercaptoethanol and loaded onto 8 or 10% SDS protein gels. Gels were dried for 60 minutes and radiolabel signal was visualized by autoradiography or phosophoimaging.

Xenopus RCA1 microinjections

Purified *Xenopus laevis* RCA1, or emi1, and MBP alone were gifts from P. Jackson. *Xenopus* RCA1 was purified as fusion protein with MBP, and microinjected into

Drosophila embryos at 10mg/ml. MBP alone at similar concentrations was used as an additional control.

All microinjections and subsequent embryo manipulation was performed according the protocol in Chapter 2.

RESULTS

To probe the role of dual inhibition of the APC by cyclin E and mitotic cyclins, *rux* was overexpressed in cyclin E mutant ($cycE^{AR95}$) embryos during G2 of cycle 14[5]. $cycE^{AR95}$ homozygous or heterozygous embryos carrying the *rux* gene under the control of a heat shock inducible promoter were heat shocked when cells are in G2 or mitosis of cycle 14 (2.5-3 hr old). *rux* overexpression in heterozygote ($cycE^{AR95}$/*CyO*) sibling embryos was similar to overexpression in a wild-type background (Figure 1, panel 1, C and D). Cyclin A and perhaps cyclin B appeared to become nuclear. Normally, both are cytoplasmic. The levels of cyclins A and B did not change in heterozygote siblings upon *rux* overexpression (Figure 1, data not shown).

In homozygous $cycE^{AR95}$ embryos, *rux* overexpression caused mitotic cyclins to be downregulated (Figure 1, panel 1, E and F). It is important to note that $cycE^{AR95}$ embryos without *rux* overexpression develop normally until G1 of cycle 17. Figure 1 shows that in $cycE^{AR95}$ most cells do not stain positively for mitotic cyclins A and B after *rux* overexpression. This effect is not completely penetrant. Some $cycE^{AR95}$ embryos displayed varied levels of cyclin A and B within the collection. In addition, most $cycE^{AR95}$ embryos had cells that retained positive cyclin A and B staining. Time course experiments indicated that mitotic

[5] These experiments were initially performed by S. Vidwans or N. Yakubovitch (data not shown).

cyclins began to disappear within 30 min of heat-shock, reaching maximal downregulation at 60 min (data not shown). Then, cyclins reaccumulate by 90 min after heat-shock. The reaccumulation of mitotic cyclins is proposed to be due to the instability of *rux*, resulting in only a pulse of *rux* overexpression. Cyclin B3 disappeared and reaccumulated with similar kinetics (data not shown). Western blots confirmed that cyclin protein levels were lower (data not shown). Serial dilution Western blot analysis revealed that cyclin A protein levels decreased ~5-fold (Figure 1, panel 2).

This result suggests that cyclin E and mitotic CDK/cyclins play a dual role in inhibiting APC normally. Only by inhibiting both cyclin E (by mutation) and mitotic CDK/cyclin (by *rux*) does APC become inappropriately active. It has not been tested if the disappearance of mitotic cyclins in the above circumstance is by proteolysis and APC-dependent (see Discussion). We favor a post-translational downregulation model because cyclins are normally stable at this point.

To test if the APC activity increases in $cycE^{AR95}$ embryos when *rux* is overexpressed, APC activity was measured via the ubiquitination assay presented in Chapter 3. Activity was compared in homozygous versus heterozygous $cycE^{AR95}$ embryonic extracts upon *rux* overexpression (Chapter 3, Figure 5, lanes 3 and 4). Activity increased in $cycE^{AR95}$ homozygotes compared to heterozygotes upon *rux* overexpression. However, this increase was similar to that in $cycE^{AR95}$ homozygotes alone in which mitotic cyclins are stable. It appears that the increase in $cycE^{AR95}$ alone masks a potential difference upon rux overexpression, so we cannot use the APC assay in this circumstance.

Parallel work in the lab revealed that in addition to cyclin downregulation of mitotic cyclins, $cycE^{AR95}$ embryos go through a round of endoreplication when

rux is overexpressed. Upon *rux* overexpression in $cycE^{AR95}$ embryos, mitosis is bypassed and most cells go through a single endoreplication cycle. The observed endocycle is consistent with cyclin downregulation. These cells then progress into mitosis after cyclins reaccumulate with twice their normal DNA content. The future fate of theses cells has not been investigated. The endoreduplication cycle in this circumstance provides insight into the block to re-replication by CDK/cyclin complexes. However, it will not be discussed further.

Does rca1 fit into the APC regulation picture?

Work from P. Jackson's lab elucidating the role of Emi1 from *Xenopus* has led us to investigate the role of the Drosophila homolog, *rca1*, in APC regulation. Emi1 appears to play a role in regulating the APC. Depletion of Emi1 from cycling *Xenopus* egg extracts prevents accumulation of cyclin B and prevents entry into mitosis, suggesting ectopic APC activation. Addition of excess Emi1 protein or a non-degradable version of Emi1 to cycling extracts blocks exit from mitosis and cyclin B degradation, presumably because of APC inhibition. Emi1 binds $CDC20^{fzy}$ and prevents in from activating the APC *in vitro*. Emi1 contains 5 CDK consensus phosphorylation sites. An allele of Emi1 with mutated CDK phosphorylation sites blocks cyclin B degradation and mitotic exit. The model put forth is that Emi1 binds and inactivates $CDC20^{fzy}$ during interphase and early mitosis. Also, phosphorylation of Emi1 by CDK/cyclin influences its activity either by its interaction with $CDC20^{fzy}$ or by regulating its degradation during late mitosis.

In a collaboration with P. Jackson's laboratory, I tested the role of Emi1 as an inhibitor of the APC. *Drosophila* syncytial embryos were microinjected with

wild type or mutant Emi1 protein. Following a similar protocol to that presented in Chapter 2, approximately 0.5-1.0 ng of protein was injected into cycle 10-12 syncytial embryos. The embryos were analyzed for cell cycle progression by immunostaining for tubulin and DNA. Injection of buffer alone or a mutant Emi1 that cannot interact with $CDC20^{fzy}$ results in equal distribution of embryos containing mitotic or interphase nuclei (see Figure 2; nuclear divisions are synchronous at this stage). In contrast, microinjection of wild-type Emi1 causes an increase in embryos in mitosis or causes a delay in mitosis near the point of injection (see Figure 2). Live imaging of microinjected embryos (data not shown) suggests that embryos delay in the first mitosis after injection. The data suggest that *Xenopus* Emi1 inhibits *Drosophila* APC because Emi1 microinjection shows a similar phenotype to microinjection of an APC inhibitor (see Chapter 2).

The role of *Drosophila rca1* as an inhibitor of the APC was then tested. *rca1* is the *Drosophila* homolog to *Xenopus* Emi1 [89]. *rca1* overexpression in the developing eye causes ectopic S-phase and cyclin A accumulation. The embryonic phenotype of *rca1* is indistinguishable from *cyclin A* mutants, suggesting that *rca1* is required for cyclin A function [89]. This data fits a model that *rca1* is an inhibitor of APC, because overexpression causes an upregulation of cyclin A perhaps by inhibition of the APC. *rca1* mutants appear to lack cyclin A function, consistent with inappropriate APC activation. However, cyclin A protein level is normal in *rca1* embryos, which is not consistent with *rca1* having a role in APC regulation.

Inspired by the *rca1* phenotype and Emi1 microinjection results, I tested if *rca1* interacts with *fzy* genetically and biochemically. Polyclonal antibodies were generated to peptide fragments of *rca1* (residues 5-25 and 390-410). Both

antibodies recognize a band corresponding to RCA1 in Western blots (data not shown) that increases in intensity upon overexpression of *rca1*. RCA1 and FZY proteins were generated in vitro through a reticulocyte coupled transcription/translation system (see Materials and Methods). ^{35}S-labeled RCA1 from retic lysates was efficiently immunoprecipitated using *rca1* antibodies (Figure 2, panel B, lane 1 and 2). The *in vitro* interaction between RCA1 and FZY was tested by co-immunoprecipitation experiments. ^{35}S-labeled FZY was incubated with increasing amounts of RCA1, then, RCA1 was immunoprecipitated. ^{35}S-FZY was not detected above background to be associated with RCA1 (Figure 2, lanes 3-6). In addition, there was no interaction detected in reciprocal immunoprecipitation and Western blotting experiments probing interaction of endogenous *rca1* and *fzy* from embryonic extracts (data not shown). Taken together, this data suggests that there is not a detectable biochemical interaction between *rca1* and *fzy*.

To complement biochemical interaction studies, genetic epistasis between *rca1* and *fzy* experiments was performed. Embryos doubly mutant for *rca1* and *fzy* were compared to individual mutants (Figure 3, panel A). *rca1* embryos arrest in G2 of cycle 16 whereas *fzy* embryos arrest in mitosis of cycle 16 (Figure 3, panel 2). If *rca1* inhibits *fzy* activity during interphase, the arrest phenotype of the *rca1* mutant could be a result of high *fzy* activity. Perhaps, by lowering the dose of *fzy* in a *rca1* mutant, the arrest can be bypassed. Similar predictions can be made also for *rca1* mutations modifying the *fzy* arrest. *rca1, fzy* double-mutant embryos arrest in G2 of cycle 16 with similar morphology to *rca1* and *cyclin A* mutant. *rca1* appears to be epistatic to *fzy*. *fzy* cannot modify the *rca1* mutant phenotype, suggesting that there is no genetic interaction.

Taken together, the data suggest that Drosophila *rca1* and *fzy* do not interact in the same way as Emi1 and CDC20 in *Xenopus*. This is supported by the observation *rca1* embryos have normal cyclin A levels [89], contrary to what is expected if APC were ectopically active in *rca1* mutants. There are alternative explanations to the data: simple experimental caveats, requirement of an addition protein for biochemical interaction or *rca1* having an alternative function unsuppressed by *fzy*.

Discussion

Mortal enemies- CDK activity negatively regulates APC activity

In this chapter, we provide evidence that APC activity is negatively regulated by the dual activity of CDK2/cyclin E and CDK1/mitotic cyclins (Figure 1). When *rux* is overexpressed in $cycE^{AR95}$ homozygous embryos during G2 of cycle 14, mitotic cyclin levels decline dramatically (Figure 1, panel 1 and 2). This effect is not seen when *rux* is overexpressed in $cycE^{AR95}$ heterozygous embryos or an otherwise wild-type background (Figure 1, panel 1, C and D). We propose that both CDK1/mitotic cyclin and CDK2/cyclin E complexes inhibit or prevent activation of the APC. When mitotic cyclin/CDK complexes are inhibited by *rux* and cyclin E/CDK2 activity is abrogated through mutation, APC is ectopically activated. This result supports previous work suggesting cyclin E regulates mitotic cyclin levels and can suppress the overexpression effects of *fzr* [51, 62]. The result is unique, in that it is the first documentation of mitotic cyclin/CDK activity inhibiting cyclin turnover (presumably the APC) in *Drosophila*.

Why both E and mitotic cyclins?

Cyclin E and mitotic cyclins have distinct functions in the Drosophila cell cycle [90]. Cyclin E is involved in S-phase progression and perhaps mitotic cyclin stability through regulation of *fzr* [51, 62]. Mitotic cyclins are responsible for initiating many mitotic events and S-phase progression (cyclin A) [91, 92]. Cyclin

E and A have overlapping functions in S-phase control. So, why do these different classes of cyclins with different expression patterns and functions both work together to inhibit the APC?

One model is that the different CDK/cyclin complexes inhibit unique steps or forks of the regulatory pathway. For example, CDK2/cyclin E could inhibit the *fzr* regulation of the APC [51] and CDK/mitotic cyclins could inhibit *fzy* regulatory pathway [72, 73]. One complex could phosphorylate the APC core complex, while the other complex could inhibit upstream activating events. Finally, different CDK/cyclin complexes might inhibit the APC in different subcellular locations in the cell (e.g. the nucleus and cytoplasm).

A different model is that the first 16 cell cycles of embryogenesis are unique with regards to CDK/cyclin expression. Both sets of CDK/cyclins are present and capable of inhibiting the APC in interphase of cycles 1-16. Cyclin E levels do not oscillate during the first 15 divisions [62] and can inhibit the APC constantly, whereas mitotic cyclins oscillate in cycles 9-16 [3] but can inhibit the APC in interphase. Normally, the cell does not need both CDK/cyclin complexes to suppress APC activity. However, in the embryonic cycles, these complexes have non-overlapping functions that are independent of APC inhibition and are required to successfully passage through these stages of embryogenesis. So, the developmental context necessitates the presence of both sets of CDK/cyclin complexes to passage through these stages independent of APC regulation. For example, mitotic cyclins are required for mitotic entry and continuously high cyclin E levels are thought to suppress the acquisition of a G1 state.

How is the APC being inhibited by these CDK/cyclin complexes?

The short answer is that we do not know. A simple interpretation of the result is that normally in interphase cells there is a dual inhibition of the APC by both sets of CDK/cyclin complexes. When *rux* is overexpressed in $cycE^{AR95}$ embryos, these CDK inhibitory activities are eliminated and the APC is ectopically activated. In other systems, the APC has been shown to be positively and negatively regulated by phosphorylation [11, 21]. This regulation can occur at the level of core APC complex phosphorylation or by phosphorylation of activators. *fzr* is not expressed in G2 of cycle 14 and we do not think that inhibition is through *fzr* at this stage. In support of this, *fzr* expression remains low upon *rux* overexpression in $cycE^{AR95}$ embryos (data not shown). Unlike other systems, *fzy* expression is continuously high throughout the cell cycle at this stage [68]. Without the characterization of other APC activators (i.e. a *fzr* homolog), we assume a *fzy*-dependent APC is normally inhibited by CDKs at this stage. When *rux* is overexpressed in $cycE^{AR95}$ embryos, the ectopic APC activity should also be *fzy*-dependent. Genetic tests of the *fzy*-dependence are difficult because the *fzy* mutants are normal until later in embryogenesis presumably because of maternally supplied fzy function. As of yet, we do not know how CDK/cyclin complexes inhibit the APC during these stages and remains to be tested. The inhibition could be at the level of *fzy* function, the core APC, or by some other novel pathway such as *rca1* (see above).

It will be interesting to test if all of the mitotic cyclin/CDK complexes inhibit the APC. Currently, we believe that CDK/cyclin A is the primary mitotic cyclin that inhibits the APC. Evidence from other system implicates cyclin A function in negative regulation of the APC [72, 93]. In *Drosophila*, cyclin A can block re-replication [94] and might have an unique role in regulation of APC. The

roles of the individual mitotic cyclins in APC inhibition will be tested further. Preliminary experiments suggest that prolonged cyclin B3 activity does not inhibit the APC (data not shown).

Figure 4-1

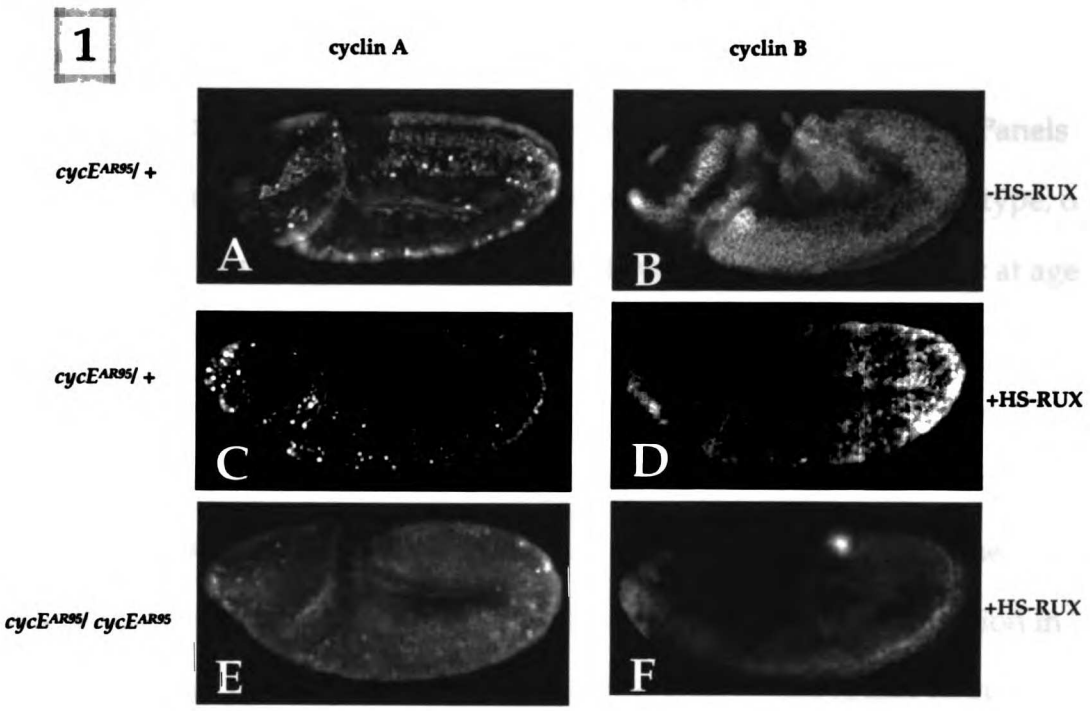
1
cyclin A
cyclin B
cycE^AR95/ +
-HS-RUX
A
B
cycE^AR95/ +
+HS-RUX
C
D
cycE^AR95/ cycE^AR95
+HS-RUX
E
F

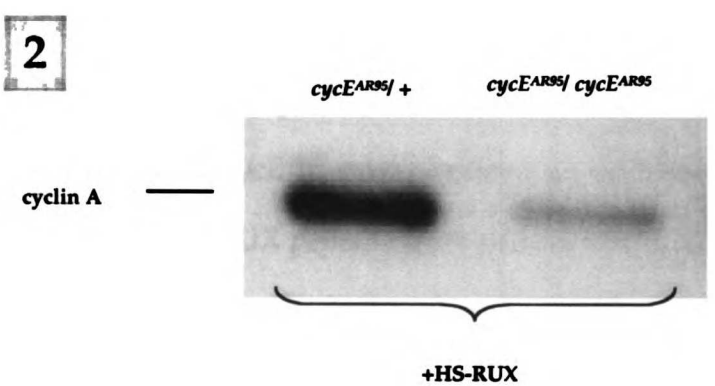
2
cycE^AR95/ +
cycE^AR95/ cycE^AR95
cyclin A
+HS-RUX

Figure 4-1

(Box 1) Levels of mitotic cyclins A and B were probed after induction of *rux* in $cycE^{AR95}$ mutants. Embryos from $cycE^{AR95}$ /+; HS-RUX parents were immunostained for cyclins A (panels A, B, E) or cyclin B (panels B, D, F). Panels A and B shows the normal distribution of mitotic cyclins A and B in wild type, or heterozygous and homozygous $cycE^{AR95}$ embryos without induction of *rux* at age 3.5-4 hr old. (Panels C-F) Embryos laid by $cycE^{AR95}$; HS-RUX parents were heat shocked at age 2.5-3 hr old to induce *rux* expression, allowed to recover for 45 min and immunostained for mitotic cyclins A and B. $cycE^{AR95}$ mutant embryos were distinguished using a LacZ marker on the CyO balancer chromosome. Panels C and D shows the pattern of mitotic cyclins upon *rux* overexpression in wild type or heterozygous $cycE^{AR95}$ embryos ([9], nuclear cyclin A and both cytoplasmic and nuclear cyclin B). Panels E and F are $cycE^{AR95}/cycE^{AR95}$ embryos after *rux* overexpression. Mitotic cyclins A and B are low and undetectable in most cells of the embryos.

(Box 2) The level of cyclin A protein was probed via Western blot analysis after overexpression of *rux* in $cycE^{AR95}$ mutant embryos. 4.5-5 hr old embryos laid from $cycE^{AR95}$ /CyO-GFP; HS-RUX parents were sorted live by genotype, heat shocked, allowed to recover, and used to make extracts (see Materials and Methods). The amount of cyclin A protein in $cycE^{AR95}$ heterozygous and homozygous embryos was probed by serial dilutions and Western blot analysis. Cyclin A protein level

Figure 4-2

A

Microinjection of Xenopus RCA1 into *Drosophila* syncytial embryos

	Mitosis*	Interphase	Delayed/ Other†
+Buffer only (%)	45	42	13
+Xenopus RCA1 (%)	71	8	22

*all nuclei of embryo synchronously in a specific stage of mitosis (prophase, metaphase, anaphase, telophase)
†injection artifact

B

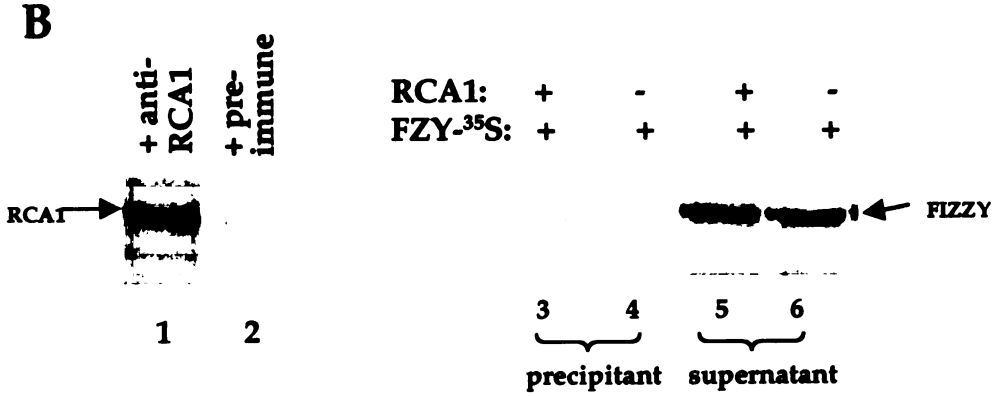

Figure 4-2

(Table A) The effect of *Xenopus* RCA1 was investigated by microinjection into *Drosophila* syncytial stage embryos. Syncytial embryos were microinjected with purified Xenopus RCA1 protein or buffer only, aged for 30 min, fixed, and stained for DNA and microtubules (see Chapter 2 for protocol after microinjection). Embryos were classified according to cell cycle state. The nuclear divisions are synchronous. "Mitotic" or "Interphase" embryos have almost all nuclei displaying mitotic or nuclear morphology. "Delayed/Other" embryos have a delay of cell cycle progression at the point of injection or display morphology consistent with microinjection artifacts. Injection of Xenopus RCA1 increased the representation of embryos in mitosis compared to embryos injected with buffer only.

(Box B) The biochemical interaction of Drosophila RCA1 and FZY was probed by co-immunoprecipitation reactions. (Lanes 1 and 2) *In vitro,* transcribed and translated ^{35}S-labeled *Drosophila* RCA1 was immunoprecipitated from a reticulocyte lysate (see Materials and Methods) using polyclonal antibodies specific to the amino and carboxy termini of RCA1 (Lane 1) compared to the pre-immune sera control (Lane 2). (Lanes 3-6) ^{35}S-labeled *Drosophila* FZY was incubated with 10-fold more unlabeled RCA1. RCA1 was immunoprecipitated as in lane 1. An almost undetectable level of ^{35}S-FZY coimmunoprecipitated with RCA1 (lane 3), which did not change if RCA1 was not added to the reaction (lane 4). Lanes 5 and 6 are 10% loads of the material that remained in the supernatant from the immunoprecipitations in lanes 3 and 4, respectively.

Figure 4-3

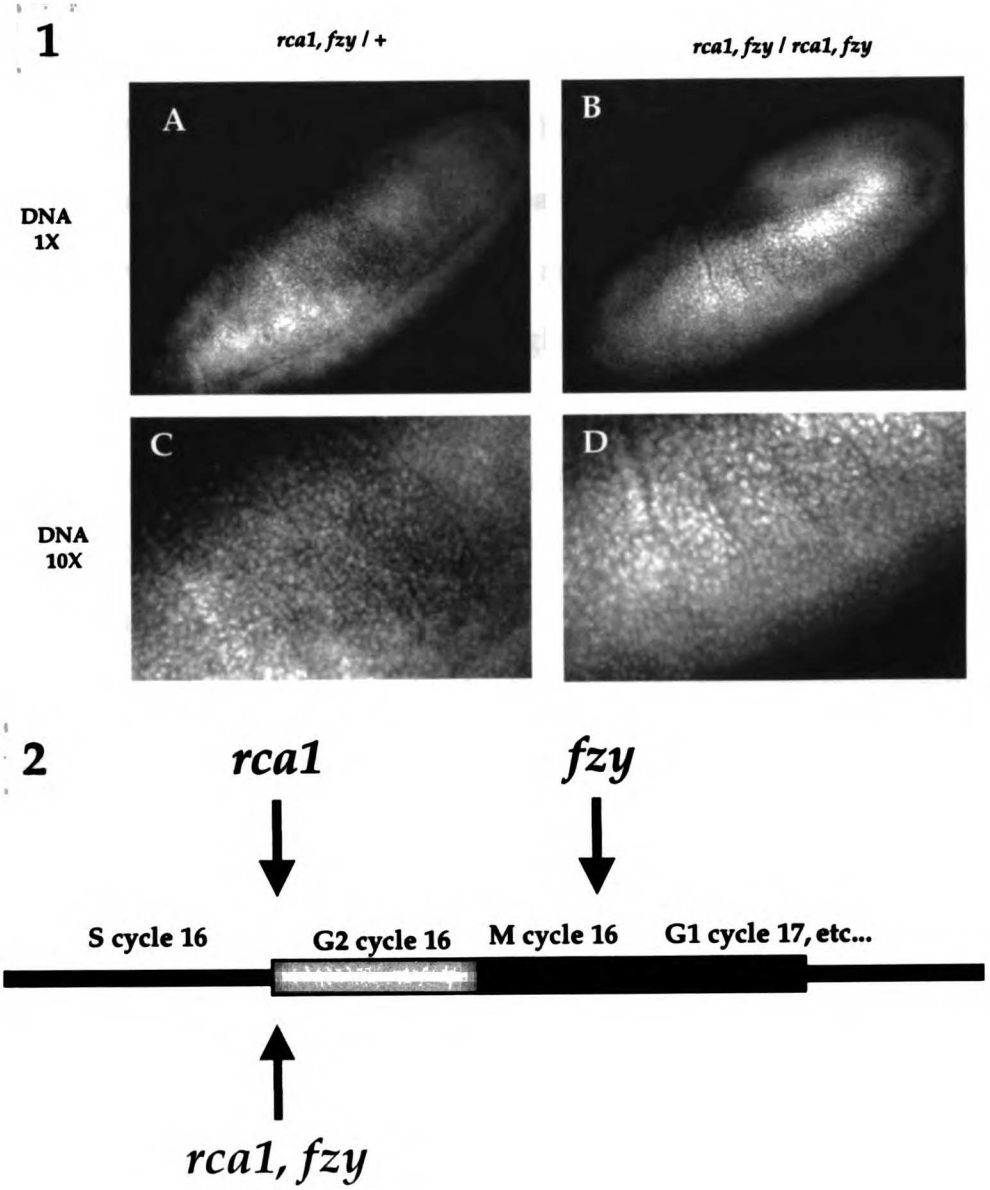
1
rca1, fzy / +
rca1, fzy / rca1, fzy
A
B
DNA
1X
C
D
DNA
10X
2
rca1
fzy
S cycle 16
G2 cycle 16
M cycle 16
G1 cycle 17, etc...
rca1, fzy

Figure 4-3

(Box 1) A genetic interaction between *rca1* and *fzy* was tested. Embryos from *rca1, fzy*/CyO parents were collected, aged until 8-9 hr old, fixed, and stained for DNA to assess cell density. Heterozygous or wild type embryos (panel A and C) were identified by a LacZ marker on the balancer chromosome and compared to homozygous *rca1, fzy* double mutants (panel B and D). Panels A and B are ventral views of the epidermis. Panels C and D are magnifications of the same embryos in A and B, highlighting the higher cell density in panel C compared to panel D.

(Box 2) A linear timeline of the epidermal *Drosophila* embryonic cell cycles depicts S-phase of cycle 16 through G1 of cycle 17 and the arrest points (arrows) of the corresponding single and double mutants. *rca1* mutants arrest in late S or G2 of cycle 16. *fzy* mutants delay in mitosis of cycle 16. Judging by larger cells, lack of mitotic figures, and timing of embryo collection, *rca1, fzy* double mutants arrest with a phenotype similar to *rca1* single mutants, suggesting an S or G2 cycle 16 arrest

Chapter 5

Hypoxia and Nitric Oxide Induce a Rapid, Reversible Cell Cycle Arrest of the Drosophila Syncytial Divisions

Introduction

Oxygen is essential for the life of most multi-cellular organisms. Limitations in oxygen have profound physiological and health consequences in humans. Prolonged or severe decreases in physiological oxygen resulting from ischemia are a major contributor to morbidity and mortality in stroke and cardiac infarction [95]. Cells in pre-tumorous growths are often deprived of oxygen as a result of insufficient and inefficient vascularization, and this hypoxia (low oxygen) is postulated to play a role in limiting tumor progression [96]. The outcome of hypoxia can differ dramatically. For example, a turtle can survive months of hypoxic conditions, whereas the cells of the human brain begin to die following a few minutes of hypoxia [97]. These outcomes presumably depend on the cellular responses to hypoxia, which range from metabolic adaptation to quiescence to apoptosis [98]. Among the cellular responses to hypoxia is an arrest of the cell cycle [96, 98]. Hypoxia is reported to arrest mammalian cells during G1, mid S phase, and G2/M. Analysis of the response to hypoxia in *Drosophila* has similarly revealed an arrest of the cell cycle in mid S-phase and mitosis [99, 100]. Despite the importance of these cellular responses, the signals mediating responses to hypoxia are ill defined and the factors influencing the type of response are poorly understood. What allows some cells to survive when others die?

In this study, we examined the responses to hypoxia during *Drosophila* embryogenesis. The development of *Drosophila* from egg to larva is remarkably fast and dynamic. Development begins with 13 rapid mitotic divisions in a

common cytoplasm, referred to as the syncytial stage. Next, cell membranes invaginate and form around the nuclei, referred to as cellularization. Following cellularization, the germ layers are formed during gastrulation, the body plan is defined and tissue types begin to form. Finally, about 24 h after fertilized oocyte deposition, the embryo hatches into a larva. The ability to survive hypoxia is likely to be an important adaptive mechanism in an organism whose eggs develop on rotting fruit where microbial proliferation can deplete oxygen. It was previously reported that *Drosophila* embryos progress from being sensitive to hypoxia to being remarkably resistant [100]. The early syncytial stage embryo is quite sensitive and can only survive a brief period of hypoxia. However, starting at about 2 h after cellularization, embryos survive almost complete anoxia. Cellularized, stage 9 embryos arrest upon depletion of oxygen, remain quiescent for a week and successfully resume development upon restoration of oxygen[6].

Recent work has suggested that the survival of *Drosophila* larvae and older embryos during hypoxia involves active responses that induce widespread changes in behavior, cell cycle progression and development [99-101]. These responses appear to be governed, in part, by nitric oxide [99]. Nitric oxide (NO)[7] is a signaling molecule in mammals that contributes to neuronal signaling, the innate immune response and regulation of blood vessel tone. In *Drosophila*, NO has also been shown to influence synaptogenesis during the development of the nervous system [102], to negatively regulate the cell cycle during imaginal disc growth [103], and to be involved with an S-phase block and a change in larval

[6] Wingrove, JA and O'Farrell, PH, unpublished observations

[7] The abbreviations used are: NO, nitric oxide; N_2, nitrogen; SNAP, sodium nitroacetylpenicillamine; DNP, dinitrophenol; CN^-, cyanide; GFP, green fluorescent protein; PBS, phosphate buffered saline: PTIO, 2-Phenyl-4,4,5,5-tetramethylimidazoline-1-oxyl-3-oxide.

behavior in response to hypoxia [99]. NO involvement in the response to hypoxia in *Drosophila* has parallels with one of its roles in vertebrates in which it induces vasodilation and increased blood flow in response to local limitations in oxygen [104].

Exceptional features of the syncytial embryo such as the synchrony and speed of the nuclear divisions and the clear cytology provide an ideal system for characterization of the effect of hypoxia and NO on cell cycle progression. We examined the kinetics of the hypoxic arrest in real time, demonstrated a comparable arrest by NO and characterized the reversal of these arrests at the level of metabolism, the cell cycle and development. Rapid and reversible arrest of the nuclear divisions occurred at two stages, interphase and metaphase. The phenocopy of the hypoxia arrest by treatment with NO suggests a role for NO in the hypoxic response. Also, measurements of ATP levels and cyanide treatments of embryos reveal metabolic changes that could contribute to the cell cycle arrest in response to hypoxia. By following recovery after prolonged hypoxia, we showed that the failure of syncytial embryos to hatch after exposure to hypoxia was due to detrimental effects on development and did not reflect an inability of the embryo to recover metabolically or restore cell cycle progression.

Materials and Methods

Embryo collection, fixation, and staining

Sevelen was used as a wild-type stock. All embryo collections, fixations, and stainings were performed as previously described [55, 61]. ≥95% of the embryos in the collections was of the proper age with a contamination of other unfertilized or older stage embryos (Data not shown). Fixed images were acquired using an upright fluorescent microscope (Leica DMRD).

Hatching assay

Hatching assays were performed by first washing treated embryos with a NaCl/Triton solution (0.7% NaCl, 0.03% Triton X-100). A known number of embryos were then placed on a grape juice agar plate, incubated for 24-30 h at 24°C, and counted for the number of eggs that hatched into larvae.

Hypoxic, NO, and cyanide treatments

For all experiments, nitrogen (N_2) and oxygen (O_2) gas was mixed to achieve desired oxygen levels. The mixture was humidified and output oxygen measured using an oxygen sensor (Reming Bioinstruments, Model PROOX 110).

Different stage embryos were collected, dechorionated with 50% bleach, and resuspended in an aerated NaCl/Triton solution. A phosphate-buffered saline (PBS) solution was perfused with mixed N_2/O_2 air at least 15 min prior to treatment in order to equilibrate the solution to desired oxygen concentrations. Embryos were made hypoxic by replacing the NaCl/Triton solution with deoxygenated PBS + 0.05% Triton X-100. For NO and cyanide treatments, 10mM SNAP (s-nitroacetylpenicillamine) or 0.2% sodium cyanide in PBS was used. Embryos were then rocked in an eppendorf tube containing the specified PBS solution, while lightly blowing N_2/O_2 gas mixture into the eppendorf tube to replace the oxygenated air (for hypoxia treatments only). To return to normoxic conditions, the deoxygenated PBS was replaced with the NaCl/Triton solution and rocked gently. Prolonged exposures to hypoxia were performed as previously described [99].

Real-time analysis of living Drosophila embryos

Embryos were collected from a transgenic line expressing a fusion protein of histone 2A and green fluorescent protein (GFP) [105]. Embryos were dechorionated with 50% bleach, aligned on a glass coverslip and placed under halocarbon oil or PBS to prevent dehydration. The GFP fluorescent signal was visualized in real time using an Olympus IX-70 microscope and images recorded using Delta Vision Version 2.10 software (Applied Scientific, Inc.). While monitoring chromosome dynamics live, embryos were made hypoxic by blowing a stream of N_2/O_2 gas onto specific embryos through a Pasteur pipette. Embryos

were treated with NO donors or CN^- by removing the PBS solution and replacing it with 10mM SNAP or 0.2% sodium cyanide dissolved in PBS.

Preparation of embryonic extracts for ATP determination

Embryonic extracts were made by resuspending 25-100μl of embryos in 200-1000μl of Glycine buffer (O.2M glycine, 50mM $MgCl_2$, 4mM EDTA, pH 7.4) contained within a 1.5 ml eppendorf tube. The embryo/buffer solution was then sonicated on ice with 1 s pulses from a microtip of a Branson Sonifier (Model 185). Extracts were centrifuged for 5 min at 14,000 RPM (16,000 RCF). The soluble supernatant was saved and protein concentration determined using the BCA assay (Pierce). Extracts were diluted to 2mg/ml in Glycine buffer and boiled for 45 s to precipitate protein. After a 15 min centrifugation, supernatants were transferred to fresh tubes, diluted, and measured for ATP concentration (see below).

Luciferase-luciferin Assay for ATP levels

The Luciferase-luciferin assay for ATP levels was modified from a protocol provided with the Luciferase-luciferin mix (Sigma cat#L0633). Briefly, 20μl of diluted extract with protein removed (see above) was mixed with 100μl 1mg/ml Luciferase-luciferin mix, diluted in water. The mixture was placed in a small scintillation vial and photon counts were measured using the "single-photon monitor" mode of a Beckman scintillation counter (Model LS 1801). Amounts of ATP in extracts were calculated using a standard curve generated from known ATP standards. All data is represented as a percentage of the "normoxic" control,

which is a sample treated under similar conditions but kept under normal ambient oxygen conditions.

Software image processing and graphing

All images and graphs were processed using Adobe Photoshop Version 5.0 and Adobe Illustrator Version 8.0. All graphs were plotted in Kaleidagraph Version 3.0.5 (Abelbeck Software).

Results

Consistent with previous studies [99, 100], syncytial (1-2 h old) are considerably more sensitive than cellularized (7-8 h old) embryos to the hypoxia treatments used during this study (Figure 1). Older embryos in the original collection are sufficient to account for the low level of syncytial stage embryos (3±1%) that survive 24 h of hypoxia. In contrast to this sensitivity of syncytial embryos, 82±5% of cellularized embryos (7-8 h old) made hypoxic for 24 h survive to hatch into larvae (Figure 1). The decline in hypoxia sensitivity begins as embryos pass two developmental milestones, cellularization and the beginning of gastrulation ([99, 100] and data not shown).

Hypoxia arrests the syncytial nuclear divisions in metaphase and interphase

A transgenic line expressing a fusion protein of histone 2A and green fluorescent protein (referred to as HIS-GFP, [105]) was used to visualize chromosome condensation and movements. Visualization and imaging of embryos prior to hypoxia allowed precise staging of the cell cycle. Hypoxia was imposed without interruption of imaging by blowing a stream of gas (humidified nitrogen or air/nitrogen mixtures) on the embryos. This approach allowed us to determine how hypoxia influences individual events during mitosis and to define the detailed kinetics of arrest and release from hypoxia even over the short (7-8min at 22°C) time course of a normal mitosis (Figure 2). We limited observations to embryos beyond the 9th mitotic cycle because the behavior of the

HIS-GFP severely limits the quality of the imaging at earlier stages. Figure 2 gives an example of a syncytial nuclear division from interphase through mitosis and into the following interphase. It is important to note that metaphase is short, lasting only 2-3 min (Figure 2).

The nuclei of embryos made hypoxic in prophase progressed at normal rates through prophase and prometaphase, and achieved a normal alignment of the chromatin on the metaphase plate (Figure 3A&B). However, progress to anaphase was blocked. The arrest in metaphase persisted for the duration of the hypoxic treatment (≤25 min). While blocked in metaphase, the nuclei adopted a hypercondensed morphology (compare Figure 3, panel B to C). Upon restoration of oxygen, the nuclei delayed 2-8 min in metaphase and then exited mitosis with kinetics similar to controls. In contrast to a previous report [100], using real-time observation we observed that the metaphase-anaphase transition is the only observed arrest point in mitosis. Nuclei made hypoxic in late metaphase/anaphase did not arrest in mitosis. However, progression through anaphase was slowed. Nonetheless, the nuclei reached telophase, the chromatin decondensed and the nuclei took on an interphase-like morphology (data not shown).

The metaphase arrest is not unique to the syncytial cycles. Analysis of the later stage, cellularized embryos (stages 8-12) showed that hypoxia induced an identical type of arrest at metaphase. The kinetics of the arrest and its reversal resembled that of the syncytial embryos (data not shown).

As previously reported, hypoxia also causes interphase cells to arrest with an unusual nuclear morphology [99, 100]. We examined the kinetics of this response. Interphase cells made hypoxic did not progress into mitosis and

remained in interphase (data not shown). The interphase nuclei increased in volume, and chromatin became hypercondensed within 2-3 min of hypoxia. Like the metaphase arrest, this arrest was reversed by restoration of oxygen. Control embryos gassed with ambient air did not arrest.

Hypoxia blocked specific stages of the cell cycle, while other steps appeared normal or slowed. The specificity and reversibility of the arrest in metaphase suggest that the arrest behaves like a checkpoint. By observing the response to oxygen deprivation in live embryos, the specificity of the metaphase arrest in mitosis is more clearly illustrated.

NO causes an arrest of the syncytial nuclear divisions

NO, which usually acts to signal between cells [104], has been implicated in the S phase arrest in cellularized embryos and larvae [99]. We tested its effect on mitosis in the syncytial embryo. HIS-GFP embryos were treated with a NO producing agent, SNAP (s-nitroacetylpenicillamine), in a saline solution while visualizing cell cycle stage as described above. Treatment of syncytial embryos with 10mM SNAP caused a reversible arrest of interphase (data not shown) and metaphase (Figure 4) with similar kinetics and morphology to that seen with hypoxia. Figure 4 shows an embryo treated with the NO donor, SNAP, as the nuclei entered prophase. Nuclei progressed normally into metaphase, but remained blocked in metaphase for the duration of the SNAP exposure (10 min). The nuclei arrested in metaphase adopted a hypercondensed chromatin morphology similar to hypoxic arrested metaphase nuclei (Figure 4C). The effects of NO were reversible; nuclei exited mitosis normally within 3 min after removal of SNAP (Figure 4D). Similar effects in blocking the metaphase-

anaphase transition were also observed in older, cellularized embryos exposed to NO donors (data not shown).

The data show that NO can provoke an arrest of the cell cycle in the syncytial embryo that resembles the arrest caused by hypoxia. The possible role of NO as a mediator of the hypoxic response is presented in the Discussion section.

Effects of hypoxia on ATP levels

We sought to determine whether the arrest of embryogenesis protects the embryo from a drop in ATP levels during hypoxia. Generally, oxidative phosphorylation uses molecular oxygen as the final electron acceptor in the coupling of electron transport and the conversion of ADP into ATP. Pronounced reductions in oxygen levels should slow the generation of ATP, leading to a drop in ATP levels in the absence of compensating responses. Levels of ATP were monitored as a measure of the ability of *Drosophila* embryos to accommodate reduced oxygen availability. Using a modification of a luciferase-based assay, total ATP levels were measured in embryonic cell extracts from different stage embryos under various treatment conditions.

Syncytial (1-2 h old) and cellularized embryos (>3.5 h old) were made hypoxic with ≤0.1% O_2 for different lengths of time and total ATP levels were determined (Figure 5A). ATP levels decreased within 5 min of treatment at all stages examined. However, a difference between the rates of ATP decline was observed between cellularized and syncytial stage embryos. In syncytial stage embryos, ATP levels dropped to 65±4% of control embryos within 5 min and continued to decline to 38±2% (Figure 5A) at 30 min of hypoxia (the minimal

level observed is 29±1%, see Figure 7). In contrast, in cellularized, older embryos, ATP levels appeared to level off at 75% of controls within 15 min (Figure 5A), and did not further decline after prolonged hypoxic treatments of >90 min (data not shown). These results suggest that cellularized embryos are better equipped to metabolically adjust to hypoxia than syncytial embryos.

Since both syncytial and cellular embryos arrest in metaphase with similar kinetics, it is unlikely that the dissimilar drop in ATP levels directly causes the metaphase arrest in both stages. It remains possible that a decline in ATP levels arrests syncytial embryos while a distinct mechanism mediates the similar metaphase arrest of the later stage embryos. If the decrease in ATP levels caused the cell cycle and developmental arrest of syncytial embryos, the decline in ATP levels and the responses ought to be tightly correlated during this stage.

To test if there is a correlation in ATP levels and the observed effects of hypoxia, we compared the threshold in oxygen concentrations at which responses (cell cycle and developmental arrests) are triggered to concentrations that cause ATP decline in syncytial embryos. Treatment of syncytial embryos with 2% O_2, failed to arrest the cell cycle or development, and survival was not decreased. Conversely, exposure to 1% O_2 arrested the cell cycle and development at all stages tested (data not shown). Likewise, embryonic and larval survival was decreased. Thus, a transition in response to oxygen deprivation occurred between 1% and 2% O_2. ATP levels were determined for embryos exposed to different O_2 levels. ATP levels declined in response to <0.1% and 1%, but not to 2% O_2 treatments (Figure 5B). These results suggest a parallel between the oxygen requirements for sustaining ATP levels and for continued

development and cell cycle progression in the syncytial embryo. However, a more detailed analysis of the correlation would be necessary to examine the parallel in the rates of the decline of ATP and the timing of the metaphase block at different O_2 concentrations. At the level of the present analysis, the correlation is unclear. That is, at 5 min after imposition of hypoxia, the ATP levels declined about 12% in 1% O_2 while the drop was 35% in <0.1% O_2, yet both of these treatments resulted in a metaphase arrest. However, our ability to score a difference between the rate at which nuclei arrest is limited. Metaphase arrest is observed about 4 min after the beginning of the hypoxic treatment. We do not know when during the 4 min between the imposition of hypoxia and the metaphase block, oxygen concentration is sensed and elicits an arrest. We can however conclude that if the decline in ATP mediates the response to oxygen, cells would have to respond to a remarkably small decline in ATP (i.e. considerably less than the 12% decline seen at 5 min).

The kinetics of ATP recovery was assayed after 30 min of <0.1% O_2 treatment (Figure 5C). ATP levels quickly (within 5 min) recovered to maximal levels. ATP levels are fully recovered by the time cell cycle progression is renewed. These data can not discount the possibility that the restoration of ATP levels is responsible for the reversal of the arrest (See Discussion).

Inhibition of oxidative phosphorylation is sufficient to arrest the nuclear divisions

Since ATP declines in response to hypoxia, a failure to maintain ATP levels (and other metabolites) could contribute directly or indirectly to the

hypoxic responses (i.e. cell cycle arrest). Results from a previous study have shown that treatment of syncytial embryos with DNP (dinitrophenol) caused a mitotic arrest, among other effects [101]. To test if an inhibition of oxidative phosphorylation in the absence of hypoxia is sufficient to arrest the syncytial nuclear divisions, an inhibitor of oxidative phosphorylation, cyanide (CN^-), was used to decrease ATP levels.

Cyanide was titrated to a concentration that effectively reduced ATP levels with similar kinetics to that of hypoxia (Figure 6). Dechorionated embryos treated with 0.02% CN^- were assayed for ATP levels compared to control, untreated embryos. With 0.02% CN^- treatment, ATP levels declined with similar kinetics to hypoxia (56% for CN^- to 52% for hypoxia after 15 min of treatment, Figure 5&6). Using the HIS-GFP syncytial embryos, the effect of CN^- treatment on the syncytial nuclear divisions was determined. As in the case of hypoxia and NO addition, administering 0.02% CN^- at prophase and interphase blocked the nuclear divisions in metaphase and interphase, respectively. Hence, inhibiting oxidative phosphorylation in the absence of hypoxia is sufficient to arrest the cell cycle. The reversibility was not tested since CN^- is an irreversible inhibitor.

In summary, hypoxia, NO, and inhibition of oxidative phosphorylation are each sufficient to arrest the syncytial nuclear division in interphase and metaphase. It was also shown that hypoxia and CN^- cause a decline in ATP levels. Treatment of syncytial stage embryos with the NO donor, SNAP also caused a decline in ATP, but the decline was delayed (Figure 6). There was ~5-10 min lag before the decline in ATP levels. Since the arrest of the cell cycle by NO occurs within a minute, there is discordance between ATP decline and the

biological response upon treatment with the NO donor. This disparity suggests that NO has an ATP independent mode of controlling cell cycle progress (See Discussion).

Recovery and subsequent developmental failure following prolonged hypoxia

As shown above, normal cell cycle, development, and ATP levels are rapidly restored following short, sub-lethal exposures to hypoxia. We examined these same parameters after prolonged hypoxia to investigate the basis for the unique vulnerability of syncytial embryos exposed to hypoxia. Figure 1 shows that 13.5 h and 24 h exposures to <0.1% O_2 reduce the survival of syncytial stage embryos to 23±1% and 3±1% of control embryos, respectively. The same treatments do not significantly reduce the survival of older embryos.

To assay the recovery of ATP metabolism after a lethal exposure to hypoxia, syncytial embryos were made hypoxic for 13.5 h and shifted to an oxygenated saline solution for 3 h. ATP levels dropped to 29±1% of control embryos after 13.5 h of hypoxia, but returned to 93±6% of the normoxic controls within 3 h of oxygen restoration (Figure 7). Similar results were observed with 24 h hypoxic treatments of syncytial embryos (data not shown). We conclude that ATP levels recover rapidly following hypoxia, and that a persistent failure of ATP metabolism does not contribute to the embryonic lethality of prolonged hypoxia.

To test for restoration of cell cycle progression following prolonged hypoxia, syncytial embryos were made hypoxic for 13.5 h, returned to normoxic conditions for 3 h, and then fixed and assessed for their cell cycle and developmental state by visualizing the DNA (not shown) and microtubules

(Figure 8). Embryos fixed early during hypoxia and at the end of hypoxia showed the same distribution of metaphase and interphase arrest types with hypercondensed DNA morphology. There was no evidence of progression of the cell cycle or development during this prolonged hypoxia. Upon oxygen restoration, some embryos (<30%) failed to re-initiate nuclear cycles or did so abnormally. These embryos remained either uncellularized with aberrant DNA masses and spindle morphology, or remained arrested with no morphological defects (Figure 8, panel A). In contrast, the majority of the embryos (>70%) re-initiated mitotic cycles and reached a cell density comparable to control embryos not subjected to the 13.5 h of hypoxia (Figure 8B-D). Although <30% of the embryos demonstrated defective cell divisions after prolonged hypoxia, this cannot account for the >75% decrease in survival. These data suggest that most syncytial stage embryos still remain competent to re-enter the cell cycle even after a lethal, prolonged period of hypoxia.

The ability of embryos to recommence development following prolonged hypoxia was tested by examining their progression to later stages of development, including cellularization, gastrulation and germband extension. Upon reperfusion of oxygen, some embryos (<30%) re-initiated mitotic division but exhibited early developmental defects, failing to cellularize either partially or completely (Figure 8A). Another group of embryos (<30%) exhibited normal morphologies but appeared to have been delayed. They became cellularized but not germband extended (Figure 8B). Another group (~30%) had extended germbands and appeared to be at stages comparable to the control embryos (Figure 8C vs. 8D); however, these embryos displayed variable abnormalities in morphology and cell density. It is not clear whether the few embryos that

survived arose from only one of these classes. We conclude that a lethal exposure to hypoxia does not preclude further development of syncytial embryos, but the ensuing development is highly abnormal.

In summary, at least a significant fraction of syncytial embryos exposed to prolonged hypoxia are competent to restore their ATP levels, re-enter the cell cycle and resume development. Based on the observed morphological defects, we infer that defects in development are responsible for much of the lethality of the prolonged hypoxia. In contrast, older embryos exposed to prolonged hypoxia show few morphological defects upon restoration of oxygen, which are presumably corrected as these embryos develop into normal flies (data not shown).

Discussion

Despite the key role that oxygen plays in the life of most organisms, little is known about the cellular mechanisms and factors governing survival of oxygen deprivation. We provide evidence that hypoxia and NO, elicit a number of responses in syncytial and cellularized *Drosophila* embryos, including checkpoint-like arrests of the cell cycle and development.

Hypoxia reversibly blocks the metaphase-anaphase transition

The gap phases in the cell cycle seem like natural times for cells to arrest. Indeed, cells arrest at these stages when quiescence is induced by nutritional or growth factor deprivation. However, hypoxia appears to act at additional stages [96, 99]. Studies using mammalian cell lines have reported situations in which hypoxia causes cells to accumulate with G1, S, or G2/M DNA content. In *Drosophila* embryos, hypoxia arrests cells within S phase and within mitosis during syncytial stages [100, 101]. Using real-time methods, we have characterized the effects of hypoxia on each step of mitosis.

Following the undisturbed progression through prophase, hypoxic nuclei arrest in metaphase with a hypercondensed morphology (Figure 3C). Many important steps of mitosis (nuclear envelope breakdown, mitotic spindle assembly and breakdown, centrosome migration, chromosome movements, and cytokinesis) proceed normally or are only slightly delayed in the absence of oxygen. In contrast, the events of the metaphase-anaphase transition, such as

sister chromatid segregation and separation, are specifically blocked. We have followed metaphase-arrested cells in living embryos for more than 20 min, and the arrest persisted. Analysis of fixed embryos shows that metaphase arrested cells are still present after 13.5 h of hypoxia. We conclude that a step required for the metaphase/anaphase transition is efficiently blocked during hypoxia.

The metaphase block is reversible: upon oxygen restoration the nuclei re-entered the cycle after ≥2 min (Figure 3). The delay in onset of anaphase increases with the duration of hypoxia (Figure 3B-C). Presumably, recovery and completion of metaphase events occur during this time. Despite increased recovery time, syncytial embryos re-enter the cell cycle after a prolonged (≥13.5 h) and lethal exposure to hypoxia (Figure 8).

In addition to a metaphase arrest, a previous study of fixed preparations had suggested that a prophase arrest occurred during hypoxia [100]. In contrast, by following cells from the moment of oxygen depletion, we show that prophase cells continue to metaphase with no obvious delay. We attribute the presence of prophase-like cells in the fixed preparations of this previous study to interphase cells, which upon hypoxia assume a hypercondensed DNA morphology similar to prophase nuclei.

The remarkable speed of the metaphase arrest allows us to estimate how quickly the embryo responds to hypoxia. Prophase nuclei ordinarily progress through metaphase into anaphase in 4 min. Since prophase nuclei arrest at metaphase when made hypoxic, we conclude that nuclei respond within this 4 min between the end of prophase and the beginning of anaphase. The failure of metaphase nuclei to arrest could be explained if the time required to respond to

hypoxia is equivalent to the length of metaphase, or if the oxygen requiring step is at the beginning of metaphase.

The specificity and reversibility of the arrest in metaphase suggests that the arrest behaves like a checkpoint. Checkpoints prevent progression of the cell cycle during stress by blocking at precise stages such as the metaphase-anaphase transition or S-phase [106]. Most cell cycle checkpoints involve signaling networks that sense a stress (i.e. DNA or mitotic spindle damage) and modulate the activity of certain cell cycle regulators. For example, the spindle assembly checkpoint is thought to sense damage to or improper formation of the mitotic spindle and block the metaphase-anaphase transition by stabilizing substrates whose degradation is normally required to exit mitosis [11]. We suggest arrest at the metaphase-anaphase transition acts as checkpoint protecting the cell from segregation errors that might occur if cells progress through anaphase in the absence of oxygen. This interpretation is supported by the slowed and abnormal anaphase that occurs in the few hypoxic cells that escape the checkpoint (data not shown).

Nitric oxide mimics hypoxia

NO exposure of cellularized *Drosophila* embryos and larvae induces responses characteristic of hypoxia and inhibition of NO generation suggests that it mediates at least some of the responses to hypoxia [99, 103]. To extend the tests of the ability of NO to phenocopy hypoxia, we asked if NO would induce a metaphase arrest.

Using NO donors and inhibitors, we tested whether NO can mimic hypoxia and is required for the normal responses to hypoxia. Exposure to a nitric

oxide donor, SNAP, arrested syncytial embryos with kinetics, specificity and morphology that resemble the hypoxic arrest (Figure 4). NO provokes a response that accurately mimics the response to hypoxia. Pretreatment of syncytial embryos with an inhibitor to nitric oxide, PTIO (2-Phenyl-4,4,5,5-tetramethylimidazoline-1oxyl-3-oxide), suggests a requirement for NO in the hypoxic interphase arrest. HIS-GFP, syncytial embryos were microinjected with PTIO as a pretreatment and assayed live for their response to hypoxic treatments. When the nuclei were synchronously in interphase, the embryos were exposed to hypoxia. During hypoxia, interphase nuclei of PTIO-treated embryos progressed slowly to assume a more compact shape and assemble a mitotic spindle (data not shown). This terminal mitotic-like state suggests that PTIO partially bypasses the block in interphase by hypoxia, and suggests that NO mediates at least part of the hypoxia effect on the cell cycle in syncytial embryos as it does in older embryos.

The role of NO in the metaphase arrest is less clear. NO can induce a metaphase arrest, but we have been unable to bypass the hypoxia-induced metaphase arrest with inhibitors of NO. Furthermore, as discussed below, cyanide induces a similar metaphase arrest, suggesting that progress through mitosis is sensitive to disruption of metabolism (Figure 6). Our finding that NO induces a mitotic block prior to any decline in ATP (Figure 6) suggests that NO can induce this arrest in the absence of a decline in metabolism. Nonetheless, since we were unable to completely bypass the block caused by hypoxia there presumably are other contributors to the block. Perhaps nitric oxide does not ordinarily mediate the metaphase arrest or if it does, it might act redundantly with another effector.

In addition to NO, previous findings with dinitrophenol treatment and our analysis of cyanide show that poisoning metabolism induces cell cycle arrest similar to that caused by hypoxia (Figure 6, [101]). Perhaps the perturbation of metabolism might be another contributor to the hypoxic arrest. Since reductions in ATP levels during hypoxia are very small at the time of the initial arrest of the cell cycle, it seems implausible that ATP levels make an important contribution to the arrest signal. Nonetheless, we can not fully exclude this possibility, nor can we argue against the possibility that reduction in metabolic activity might create some signal other than ATP that might contribute to the response. One could experimentally test the role of energy metabolism in the hypoxic response if it were possible to impose hypoxia without disrupting energy metabolism. The *Drosophila* embryo is not amenable to this, and we were not able to reverse effects of hypoxia by introducing ATP into the embryo (data not shown). Nonetheless, the effects of cyanide and the hypoxia-induced ATP decline suggest that reduced energy metabolism could contribute to the observed cell cycle arrests. We favor an interpretation that decreased oxidative phosphorylation acts in coordination with, or redundantly to signaling systems such as that activated by NO to induce the responses during hypoxia.

Homeostatic regulation of ATP improves as embryogenesis progresses

Hypoxia is predicted to compromise energy metabolism. Induced quiescence might reduce energy consumption and thereby protect the embryo from the consequences of the decreased energy metabolism. We examined the ability of the embryo to maintain ATP levels in the face of hypoxia. ATP levels

decline during hypoxia and recover rapidly upon restoration of oxygen, but the rate and the extent of ATP decline in cellularized embryos was much less than in syncytial embryos. We conclude that late embryos have a more robust ability to accommodate the reductions in oxidative phosphorylation that occur during hypoxia. While it was intriguing to speculate that this difference might contribute to the improved ability of the older embryos to survive hypoxia, our characterization of the recovery and eventual death of embryos does not support this idea (see below).

How do syncytial embryos die?

For a rapidly developing embryo to survive hypoxia it must recover metabolically and developmentally. For unknown reasons, cellularized embryos accommodate and survive prolonged hypoxia significantly better than syncytial embryos (Figure 1, [99, 100]).

Syncytial stage embryos develop rapidly with little zygotic transcription, they may not be able to compensate metabolically as well as older embryos. Indeed, early embryos show a greater decline in ATP levels during hypoxia (Figure 5). However, despite a decline in ATP levels to less than 30% of controls after 13.5 and 24 h of hypoxia, the syncytial embryos are not metabolically crippled. Upon oxygen restoration, ATP levels are quickly restored (Figure 5). Metabolically, the syncytial embryo recovers.

Initially, we speculated that the extraordinarily fast nuclear divisions of the syncytial embryos (8-20 min) would not permit arrest and/or recovery from the hypoxic arrest. This is not true: hypoxia reversibly arrests the nuclear divisions just as efficiently as it arrests the slower cell cycles of late stage

embryos. Also, embryos re-enter the cell cycle and continue to develop after prolonged hypoxia. However, these recovered embryos exhibit defects of varying severity marked by failure of, or aberrations in cellularization and gastrulation (Figure 8). We conclude that the decrease in survival of syncytial embryos is not from an inability to overcome the arrest of embryogenesis. Rather, prolonged hypoxic treatments decrease the ability of the embryo to faithfully execute the processes of development, resulting in lethality.

Many cellular processes such as energy metabolism and the cell cycle are slowed or blocked by hypoxia. Abnormal development of the syncytial embryo could result from the prolonged period of virtual suspended animation during hypoxia. The syncytial embryo could be particularly sensitive to this slowing of development. Older, cellularized embryos might be more resistant to hypoxia because patterning signals have already begun to be interpreted and the cell membranes might limit the inappropriate diffusion of molecular signals. This hypothesis remains to be tested.

Acknowledgements

We would like to thank Renny Feldman, Simon Prochnik and Devin Parry for critical reading of the manuscript. We would also like to thank Robert Saint for providing the HIS-GFP transgenic fly stock. And finally, we would like to especially thank James Wingrove for his support, help, and assistance during all stages of the project.

Figure 5-1

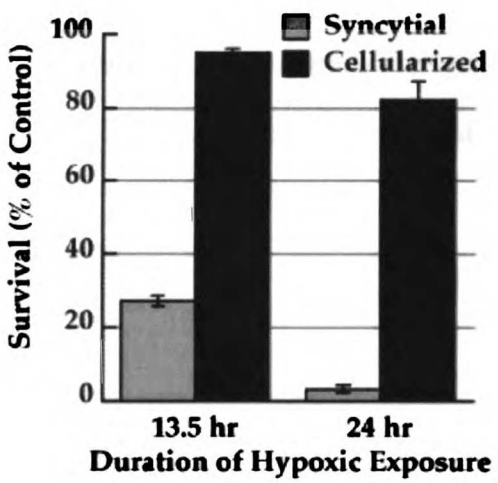
Syncytial
Cellularized
Survival (% of Control)
100
80
60
40
20
0
13.5 hr
24 hr
Duration of Hypoxic Exposure

Figure 5-1 – *Survival of syncytial and cellularized embryos after hypoxia*
Syncytial (1-2 h old) and cellularized (7-8 h) stage *Drosophila* embryos were made hypoxic and then assayed for survival. Embryos were incubated for 13.5 or 24 h in a saline solution perfused with <0.1% O_2 in a O_2/N_2 mixture (a 200 fold reduction in O_2 levels), and then placed on an agar plate under normal ambient oxygen levels (normoxic). Embryonic survival after hypoxia was scored as the number of embryos that hatched into larvae. The bar graph is the percentage of embryos exposed to hypoxia that hatched into larvae compared to control embryos without treatment. 27±1% and 3±1% of syncytial embryos survived to hatching after 13.5 and 24 hr exposures to hypoxia, respectively. In contrast, 95±1% and 82±5% of older, cellularized embryos survived to hatching after 13.5 h and 24 h hypoxic treatments. The error bars represent standard error.

Figure 5-2

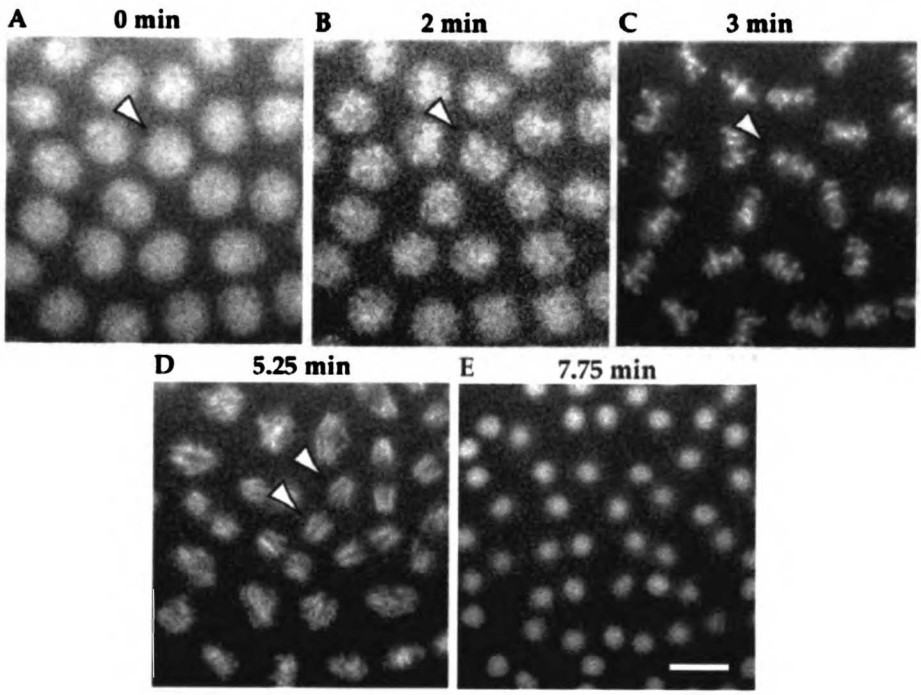

Figure 5-2 – Live, real-time visualization of chromatin dynamics and cell cycle progression

Syncytial stage embryos expressing a fusion protein of histone 2A and green fluorescent protein (HIS-GFP) were used to visualize chromatin in living embryos. *(Panel A-E)*, A representative example of the syncytial, synchronous, nuclear divisions, progressing through mitosis with normal morphology and timing is shown. Decondensed DNA in interphase nuclei *(A)* began to condense as nuclei progressed into prophase (*B*). The condensed chromatin aligned along the mitotic spindle in metaphase. *(C)*. Normal metaphase persisted 2-3 min (*C, D*), followed by the separation and segregation of the DNA masses during anaphase *(D)*. Finally, the chromatin decondenses in late telophase *(E)* and the cycle began again. The arrows indicate a single nucleus followed through mitosis, total length ~8 min. The scale bar in *panel E* corresponds to 10 μm.

Figure 5-3

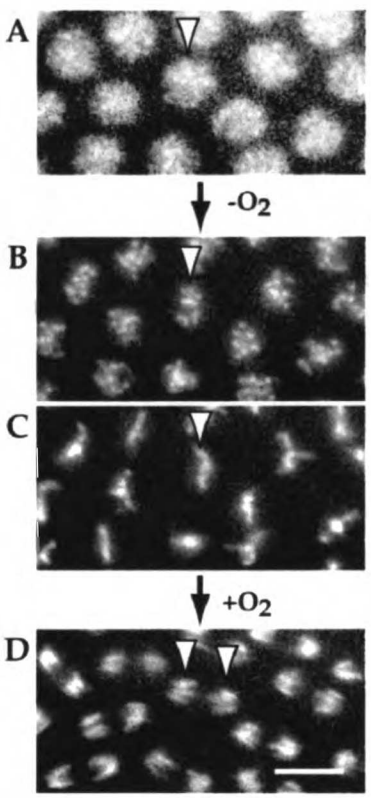

Figure 5-3 – Hypoxia reversibly blocks the metaphase-anaphase transition
HIS-GFP syncytial embryos were made hypoxic while visualizing chromosome dynamics in real-time. Nuclei entering prophase *(A)* under normal oxygenated conditions were made hypoxic by blowing a stream of <0.1% O_2 on the entire embryo. The hypoxic nuclei progressed normally into metaphase *(B)* and remained blocked in metaphase for the duration of the treatment (10 min), adopting a stereotypical hypercondensed DNA morphology *(C)*. Normally, metaphase is 2-3 min. Upon reoxygenation with ambient air; the nuclei delayed 4 min in metaphase and then progressed with normal kinetics through anaphase *(D)* and into the next nuclear cycle. The arrows indicate a single nucleus during the treatment and scale bar in *panel D* corresponds to 10 μm.

Figure 5-4

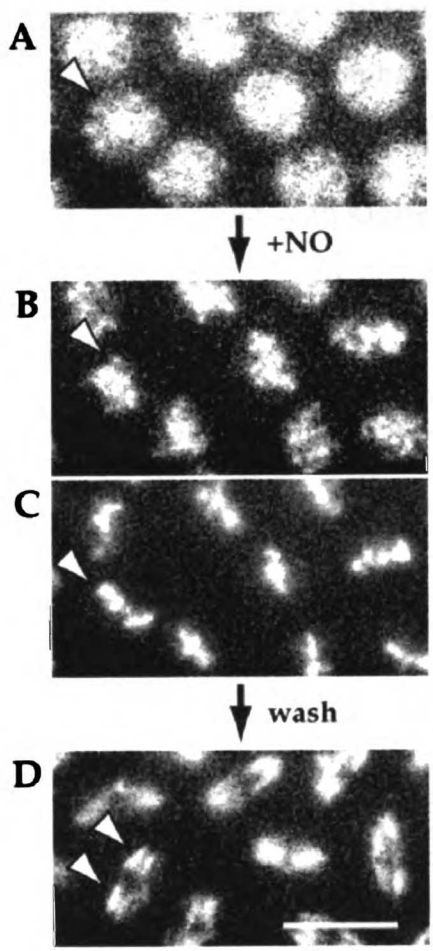

Figure 5-4 – NO treatment arrests the syncytial nuclear division in metaphase HIS-GFP syncytial embryos were used to monitor the effect of NO treatment on the progression of the nuclear divisions in the absence of hypoxia in real-time *(see Figure 3)*. When the nuclei were in prophase, as indicated by condensed chromatin *(A)*, the embryos were treated with 10mM SNAP, an NO-donor, in saline solution. Nuclei progressed normally into metaphase *(B)*, but remained blocked in metaphase with hypercondensed DNA *(C)* for the duration of the 10 min treatment. The embryos were then washed with saline solution to remove the NO-donor. Nuclei exhibited a 3 min delay, and then exited mitosis normally. Anaphase was synchronous and with normal morphology and timing after the wash *(D)*. The arrows follow a single nucleus through the treatment. Scale bar in *panel D* corresponds to 10 μm.

Figure 5-5

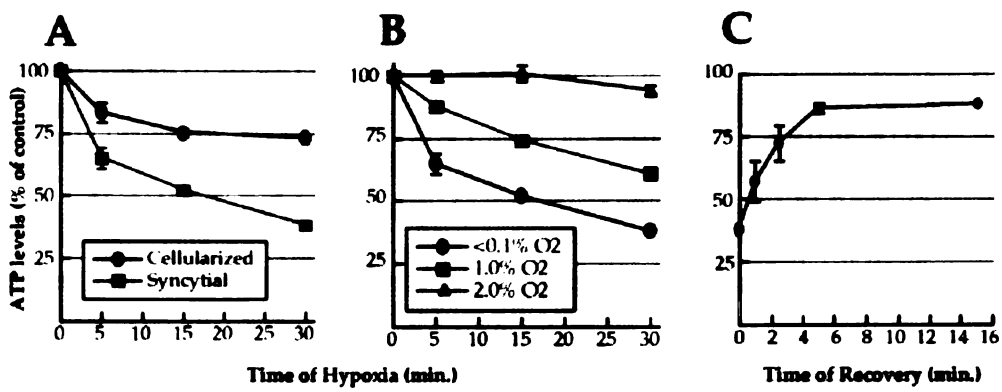
A
B
C
ATP levels (% of control)
100
75
50
25
0 5 10 15 20 25 30
Cellularized
Syncytial
<0.1% O2
1.0% O2
2.0% O2
Time of Hypoxia (min.)
0 2 4 6 8 10 12 14 16
Time of Recovery (min.)

Figure 5-5 – ATP levels in response to hypoxic treatment

In *panels A-C* embryos were treated with hypoxia and assayed for total ATP levels during or after hypoxic treatment. The amount of ATP levels are represented as the percentage of control, untreated embryos and plotted over time of hypoxic exposure or recovery. *(A)*; Syncytial (1-2 h old) and cellularized, older embryos (4-8 h) were made hypoxic with <0.1% O_2 and assayed for total ATP levels. ATP levels showed declines for both syncytial and cellularized stages, but at different rates, reaching 38±2% and 73±2% after 30 min of hypoxia, respectively. *(B)* Syncytial embryos were made hypoxic with different mixtures of O_2/N_2 to achieve final oxygen concentrations of <0.1%, 1.0%, and 2.0% O_2. ATP levels declined for <0.1% and 1.0% O_2 (38±2% and 61±2% after 30 min, respectively), but did not significantly declined upon exposure to 2.0% O_2 (94±2% after 30 min). *(C)*; Recovery of ATP levels in syncytial stage embryos after 30 min of hypoxic exposure was tested. Embryos were made hypoxic for 30 min with <0.1% O_2, and then transferred to oxygenated saline solution to recover. ATP levels declined to 38±2% of controls during the hypoxic treatment *(see also A, B)*, and recovered immediately after reoxygenation, returning to 86±2% after 5 min. Error bars represent standard error.

Figure 5-6

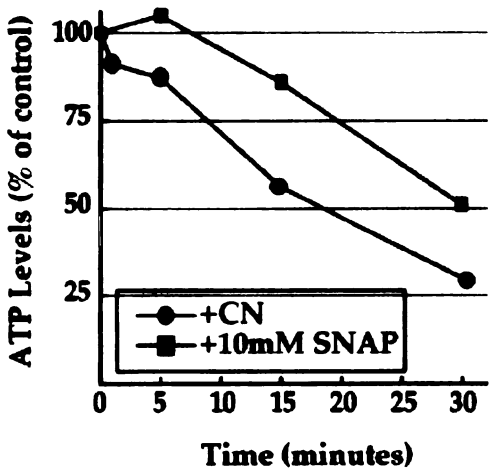
ATP Levels (% of control)
100
75
50
25
+CN
+10mM SNAP
0
5
10
15
20
25
30
Time (minutes)

Figure 5-6 – ATP levels upon treatment with an inhibitor to oxidative phosphorylation and an NO donor

ATP levels were assayed in syncytial embryos treated with cyanide (CN^-), an irreversible inhibitor of oxidative phosphorylation, or the NO donor, SNAP. Figure 6 is a plot of ATP levels (represented as the percentage of the normoxic, untreated control embryos) versus time of treatment. During 0.2% CN^- treatment, ATP levels declined with an intermediate rate compared to exposure to <0.1% and 1.0% O_2 *(see figure 5B)*, decaying to 30% of untreated controls after 30 min. During treatment with 10mm SNAP, ATP levels remained high after 5 min (105% of untreated controls), and then began to decline after 15 min (86% of untreated controls).

Figure 5-7

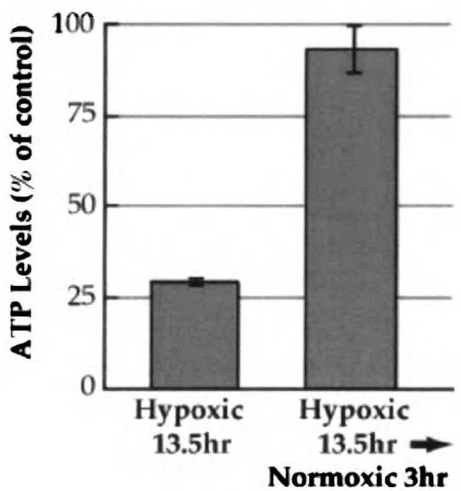
ATP Levels (% of control)
100
75
50
25
0
Hypoxic 13.5hr
Hypoxic 13.5hr
Normoxic 3hr

Figure 5-7 – Recovery of ATP levels after prolonged hypoxia

ATP levels were assayed during recovery from prolonged, lethal exposures to hypoxia. Syncytial embryos were exposed to <0.1% O_2 for 13.5h, then transferred to an oxygenated saline solution to recover for 3h. ATP levels were assayed immediately after the hypoxic exposure (*column 1* - "Hypoxic 13.5 h") and after the 3h recovery (*column 2* – "Hypoxic 13.5 h Normoxic 3h"). ATP levels declined to 29±1% after 13.5 h of hypoxia, and recovered to 93±6% of controls 3 h after reoxygenation. Error bars respresent standard error.

Figure 5-8

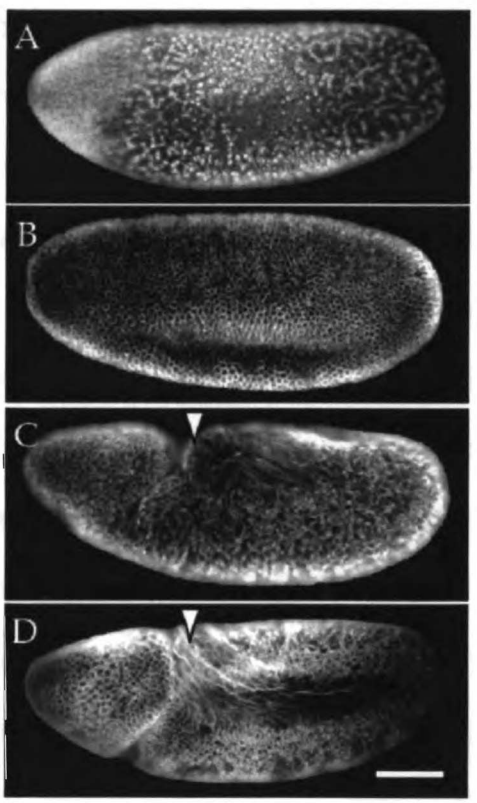

Figure 5-8 – Cell cycle progression and development after prolonged hypoxia Syncytial embryos were made hypoxic for 13.5h with <0.1% O_2 and allowed to recover in oxygenated saline solution for 3h. Embryos were then fixed and stained with antibody specific to α-tubulin to monitor cell cycle progression and morphology (*A-D*). *(A-C)* Examples of classes of observed phenotypes are shown, including an untreated control with normal morphology and cell density *(D)*. *(A)* shows an example of an embryo that has failed to cellularize or undergo any scorable gastrulation events. In addition, the nuclear division cycles appear to be delayed or blocked, asynchronous, and display aberrant mitotic spindle morphology. *(B)* This embryo is an example of a class of embryos that has attained proper cell density and demonstrates normal morphology and cellularization. However, development was delayed and gastrulation events or germband extension are not detectable (compare to *D*). *(C)* This embryo is typical of a class that appears to have advanced the most during recovery. Almost normal cell density was achieved and gastrulation has begun, however there is aberrant morphology and perturbed germband extension (see arrow). *(D)* An untreated control embryo that has cellularized, begun to gastrulate and germband extend (see arrow). Scale bar in *panel D* corresponds to 65 μm.

Conclusions and Perspectives

Why do it everywhere, when you can do it locally?

In this thesis, I explored the complex web of activities that govern the embryonic cell divisions of the *Drosophila* embryo. Changes in the activity of CDKs drive some of the major cell cycle transitions. In order to exit mitosis, the cell requires the inactivation of mitotic cyclin/CDK activity via degradation of the cyclin partner. The E3 ubiquitin ligase, APC, targets proteins for degradation including the mitotic cyclins in mitosis and G1 via polyubiquitination. To better understand the role of CDK oscillations and the activity of the APC in cell cycle regulation, I investigated their role in the developing *Drosophila* embryo.

I began my research by dissecting the mechanism of how the syncytial nuclear division exit mitosis. The first 13 nuclear divisions of the Drosophila embryo are synchronous, nuclear divisions that occur without detectable oscillations in bulk CDK activity. At the time of this work, divisions without oscillations in CDK1 activity seemed counter intuitive. Moreover, one's first reaction to the result was a simple question...how do the nuclei exit mitosis? Through my experiments using an inhibitor to the APC and the work of Frank Sprenger, Tin Tin Su, and Shelagh Campbell, evidence was put forth establishing the requirement for changes in CDK activity despite the lack of bulk oscillations. Cyclin degradation and CDK1 inactivation are required during the early syncytial divisions. The data led to a model that local changes in CDK1 activity drive exit from mitosis in the syncytial embryo. In my opinion, this study is

relatively unappreciated in the cell cycle field as one of the important studies investigating the idea of localized control of cell cycle regulators.

Subsequent studies have highlighted the importance of spatial regulation of cell cycle events. Cyclin B was shown to be degraded locally at the spindle poles and interdigitating microtubules in the *Drosophila* embryo. Similar studies have examined local cyclin degradation in other systems. Activators and core components of the APC are localized to the spindle poles and kinetochores, providing an ideal mechanism for spatially distinct degradation of substrates during mitosis. Finally, a wealth of studies have localized checkpoint components and suggested their activities have discrete, localized effects within mitosis. I believe that the conversion of the classical genetic and biochemical studies identifying the key cell cycle regulators with spatial and temporal information of their activities is the most exciting avenue of the cell cycle field in the years to come.

Mutual inhibition of the APC and CDKs

In Chapter 3 and 4, I provide evidence that CDKs negatively regulate the APC in perhaps a novel fashion. APC activity increases in cyclin E mutants as measured by an *in vitro* ubiquitination assay. Furthermore, abrogation of CDK activity by *rux* overexpression and mutation of cyclin E in the Drosophila embryo results in cyclin downregulation and presumably APC activation. In support of a role for cyclin E in APC regulation, a previous study from C. Lehner and colleagues suggested that cyclin E can inhibit *fzr* activation of the APC. Work from budding yeast has established a pathway that regulates the *fzr* homolog, CDH1, through phosphorylation by CDC28. Interestingly, *fzr* is not

expressed in the early *Drosophila* embryo which suggests that CDK1/mitotic cyclins and CDK2/cyclin E can regulate a *fzy*-dependent APC.

In view of the evidence from recent studies, I propose *fzy* regulation is *Drosophila* will be unique. This result is one of the few examples of regulation of *fzy*-dependent APC by CDK activity. Work from other systems suggests that $CDC20^{fzy}$ is regulated primarily through protein expression. *fizzy* protein levels do not appear to change during the early embryonic cell cycles. In addition, the few studies investigating *fzy* phosphorylation in other systems have implicated cyclin A associated activity. In the *Drosophila* embryo, both mitotic cyclins and cyclin E inhibit the APC, perhaps through *fzy*.

I believe the combination of our work and the work from other labs will set the stage for future investigations. There are still two general avenues to investigate with regards to CDK inhibition of APC activity. The first is how do CDKs inhibit the APC. Do the CDKs act through inhibition of an activator, activation of an inhibitor, or on the core APC complex? Secondly, and more interesting, what flips the switch that inhibits CDK activity and activates the APC? One of the key issues in cell cycle regulation is how the cell activates the APC and inhibits the CDKs. In *Drosophila*, cyclin E appears to be continuously high during the early cell divisions. Is there an unique circuit that bypasses the influence of cyclin E to flip the switch?

Hypoxia, Metaphase, and Complexity

Cells sense and respond to oxygen levels. There is a range of cellular outcomes to hypoxia including metabolic changes, cessation in proliferation, and apoptosis. I initially began investigating the effects of hypoxia on mitosis to

uncover a novel checkpoint pathway. Following up on initial observations by Victoria Foe and Jeffrey Ubersax, I characterized the reversible block of the metaphase-anaphase transition using live visualization of cell divisions in the *Drosophila* embryo. The hypoxic metaphase block appears to be a checkpoint-like response to an environmental stress. In addition, ATP levels decline dramatically in the syncytial embryo upon oxygen deprivation which probably contribute to the metaphase arrest. To probe the molecular players that sense hypoxia and govern the observed responses, I showed that NO can phenocopy the hypoxic metaphase arrest with similar kinetics and reversibility. Inhibitors to NO did not bypass the hypoxic metaphase arrest, which suggests that there are other contributors to the block in mitosis besides NO.

The dissection of the hypoxic response in *Drosophila* embryos illustrates the potential complexity of biological signaling and cellular responses. In most of my biology courses, we have been taught about simple response pathways that sense and act to signals essentially in a vacuum, independent of other cellular influences. This is not the case with hypoxic responses. Reductions in oxygen have a wide range of outcomes on the cell (and organism) which are interdependent. Other experiments in the lab have shown that transcription and translation are blocked by hypoxia. Future work aimed at understanding the hypoxic response pathways will need to consider all of the influences in concert in order to decipher individual phenotypes. For example, how can a cell respond to hypoxia without transcription, translation, and energy supplies? I believe that the truly exciting issues regarding hypoxia will emerge once we understand how all of the responses influence each other and who are the shared players.

References

1. Murray, A. and T. Hunt, *The Cell Cycle*. 1993: Oxford Press. 251.

2. Morgan, D.O., *Principles of CDK regulation*. Nature, 1995. **374**(6518): p. 131-4.

3. Edgar, B.A., et al., *Distinct molecular mechanism regulate cell cycle timing at successive stages of Drosophila embryogenesis*. Genes and Development, 1994. **8**(4): p. 440-52.

4. Amon, A., et al., *Mechanisms that help the yeast cell cycle clock tick: G2 cyclins transcriptionally activate G2 cyclins and repress G1 cyclins*. Cell, 1993. **74**(6): p. 993-1007.

5. Morgan, D.O., *Cyclin-dependent kinases: engines, clocks, and microprocessors*. Annual Review of Cell and Developmental Biology, 1997. **13**(9): p. 261-91.

6. Peter, M. and I. Herskowitz, *Joining the complex: cyclin-dependent kinase inhibitory proteins and the cell cycle [comment]*. Cell, 1994. **79**(2): p. 181-4.

7. Vidal, A. and A. Koff, *Cell-cycle inhibitors: three families united by a common cause*. Gene, 2000. **247**(1-2): p. 1-15.

8. Sprenger, F., N. Yakubovich, and P.H. O'Farrell, *S-phase function of Drosophila cyclin A and its downregulation in G1 phase*. Current Biology, 1997. **7**(7): p. 488-99.

9. Foley, E., P.H. O'Farrell, and F. Sprenger, *Rux is a cyclin-dependent kinase inhibitor (CKI) specific for mitotic cyclin-Cdk complexes*. Current Biology, 1999. **9**(23): p. 1392-402.

10. King, R.W., et al., *How proteolysis drives the cell cycle.* Science, 1996. **274**(5293): p. 1652-9.

11. Zachariae, W. and K. Nasmyth, *Whose end is destruction: cell division and the anaphase-promoting complex.* Genes and Development, 1999. **13**(16): p. 2039-58.

12. Evans, T., et al., *Cyclin: a protein specified by maternal mRNA in sea urchin eggs that is destroyed at each cleavage division.* Cell, 1983. **33**(2): p. 389-96.

13. Murray, A.W., M.J. Solomon, and M.W. Kirschner, *The role of cyclin synthesis and degradation in the control of maturation promoting factor activity.* Nature, 1989. **339**(6222): p. 280-6.

14. Glotzer, M., A.W. Murray, and M.W. Kirschner, *Cyclin is degraded by the ubiquitin pathway [see comments].* Nature, 1991. **349**(6305): p. 132-8.

15. Sigrist, S., et al., *Exit from mitosis is regulated by Drosophila fizzy and the sequential destruction of cyclins A, B and B3.* Embo Journal, 1995. **14**(19): p. 4827-38.

16. Clute, P. and J. Pines, *Temporal and spatial control of cyclin B1 destruction in metaphase.* Nature Cell Biology, 1999. **1**(2): p. 82-7.

17. Maldonado-Codina, G. and D.M. Glover, *Cyclins A and B associate with chromatin and the polar regions of spindles, respectively, and do not undergo complete degradation at anaphase in syncytial Drosophila embryos.* Journal of Cell Biology, 1992. **116**(4): p. 967-76.

18. Huang, J. and J.W. Raff, *The disappearance of cyclin B at the end of mitosis is regulated spatially in Drosophila cells.* Embo Journal, 1999. **18**(8): p. 2184-95.

19. Holloway, S.L., et al., *Anaphase is initiated by proteolysis rather than by the inactivation of maturation-promoting factor.* Cell, 1993. **73**(7): p. 1393-402.

20. Shirayama, M., et al., *APC(Cdc20) promotes exit from mitosis by destroying the anaphase inhibitor Pds1 and cyclin Clb5 [see comments].* Nature, 1999. **402**(6758): p. 203-7.

21. Morgan, D.O., *Regulation of the APC and the exit from mitosis.* Nature Cell Biology, 1999. **1**(2): p. E47-53.

22. Cohen-Fix, O., et al., *Anaphase initiation in Saccharomyces cerevisiae is controlled by the APC-dependent degradation of the anaphase inhibitor Pds1p.* Genes and Development, 1996. **10**(24): p. 3081-93.

23. Ciosk, R., et al., *An ESP1/PDS1 complex regulates loss of sister chromatid cohesion at the metaphase to anaphase transition in yeast.* Cell, 1998. **93**(6): p. 1067-76.

24. Yamamoto, A., V. Guacci, and D. Koshland, *Pds1p, an inhibitor of anaphase in budding yeast, plays a critical role in the APC and checkpoint pathway(s).* Journal of Cell Biology, 1996. **133**(1): p. 99-110.

25. Funabiki, H., et al., *Fission yeast Cut2 required for anaphase has two destruction boxes.* Embo Journal, 1997. **16**(19): p. 5977-87.

26. D'Andrea, R.J., et al., *The three rows gene of Drosophila melanogaster encodes a novel protein that is required for chromosome disjunction during mitosis.* Molecular Biology of the Cell, 1993. **4**(11): p. 1161-74.

27. Leismann, O., et al., *Degradation of Drosophila PIM regulates sister chromatid separation during mitosis.* Genes and Development, 2000. **14**(17): p. 2192-205.

28. Juang, Y.L., et al., *APC-mediated proteolysis of Ase1 and the morphogenesis of the mitotic spindle.* Science, 1997. **275**(5304): p. 1311-4.

29. Pfleger, C.M. and M.W. Kirschner, *The KEN box: an APC recognition signal distinct from the D box targeted by Cdh1.* Genes and Development, 2000. **14**(6): p. 655-65.

30. McGarry, T.J. and M.W. Kirschner, *Geminin, an inhibitor of DNA replication, is degraded during mitosis.* Cell, 1998. **93**(6): p. 1043-53.

31. Funabiki, H. and A.W. Murray, *The Xenopus chromokinesin Xkid is essential for metaphase chromosome alignment and must be degraded to allow anaphase chromosome movement [see comments].* Cell, 2000. **102**(4): p. 411-24.

32. Haas, A.L. and T.J. Siepmann, *Pathways of ubiquitin conjugation.* Faseb Journal, 1997. **11**(14): p. 1257-68.

33. Hochstrasser, M., *Ubiquitin, proteasomes, and the regulation of intracellular protein degradation.* Current Opinion in Cell Biology, 1995. **7**(2): p. 215-23.

34. Wilkinson, K.D., *Regulation of ubiquitin-dependent processes by deubiquitinating enzymes.* Faseb Journal, 1997. **11**(14): p. 1245-56.

35. King, R.W., et al., *A 20S complex containing CDC27 and CDC16 catalyzes the mitosis-specific conjugation of ubiquitin to cyclin B.* Cell, 1995. **81**(2): p. 279-88.

36. Sudakin, V., et al., *The cyclosome, a large complex containing cyclin-selective ubiquitin ligase activity, targets cyclins for destruction at the end of mitosis.* Molecular Biology of the Cell, 1995. **6**(2): p. 185-97.

37. Irniger, S., et al., *Genes involved in sister chromatid separation are needed for B-type cyclin proteolysis in budding yeast [published erratum appears in Cell 1998 May 1;93(3):487].* Cell, 1995. **81**(2): p. 269-78.

38. Visintin, R., S. Prinz, and A. Amon, *CDC20 and CDH1: a family of substrate-specific activators of APC-dependent proteolysis.* Science, 1997. **278**(5337): p. 460-3.

39. Zachariae, W., et al., *Identification of subunits of the anaphase-promoting complex of Saccharomyces cerevisiae.* Science, 1996. **274**(5290): p. 1201-4.

40. Zachariae, W., et al., *Mass spectrometric analysis of the anaphase-promoting complex from yeast: identification of a subunit related to cullins.* Science, 1998. **279**(5354): p. 1216-9.

41. Peters, J.M., et al., *Identification of BIME as a subunit of the anaphase-promoting complex.* Science, 1996. **274**(5290): p. 1199-201.

42. Lamb, J.R., et al., *Cdc16p, Cdc23p and Cdc27p form a complex essential for mitosis.* Embo Journal, 1994. **13**(18): p. 4321-8.

43. Lamb, J.R., S. Tugendreich, and P. Hieter, *Tetratrico peptide repeat interactions: to TPR or not to TPR?* Trends in Biochemical Sciences, 1995. **20**(7): p. 257-9.

44. Deshaies, R.J., *SCF and Cullin/Ring H2-based ubiquitin ligases.* Annual Review of Cell and Developmental Biology, 1999. **15**(4): p. 435-67.

45. Visintin, R., et al., *The phosphatase Cdc14 triggers mitotic exit by reversal of Cdk-dependent phosphorylation.* Molecular Cell, 1998. **2**(6): p. 709-18.

46. Foe, V.E., G.M. Odell, and B.A. Edgar, *Mitosis and morphogenesis in the Drosophila embryo: Point and counterpoint*, in *The development of Drosophila melanogaster*, M. Bate and A.M. Arias, Editors. 1993, Cold Spring Harbor Press. p. 149-300.

47. Edgar, B.A. and P.H. O'Farrell, *The three postblastoderm cell cycles of Drosophila embryogenesis are regulated in G2 by string*. Cell, 1990. **62**(3): p. 469-80.

48. Foe, V.E., *Mitotic domains reveal early commitment of cells in Drosophila embryos*. Development, 1989. **107**(1): p. 1-22.

49. Lane, M.E., et al., *Dacapo, a cyclin-dependent kinase inhibitor, stops cell proliferation during Drosophila development*. Cell, 1996. **87**(7): p. 1225-35.

50. de Nooij, J.C., M.A. Letendre, and I.K. Hariharan, *A cyclin-dependent kinase inhibitor, Dacapo, is necessary for timely exit from the cell cycle during Drosophila embryogenesis*. Cell, 1996. **87**(7): p. 1237-47.

51. Sigrist, S.J. and C.F. Lehner, *Drosophila fizzy-related down-regulates mitotic cyclins and is required for cell proliferation arrest and entry into endocycles*. Cell, 1997. **90**(4): p. 671-81.

52. Su, T.T., S.D. Campbell, and P.H. O'Farrell, *The cell cycle program in germ cells of the Drosophila embryo*. Developmental Biology, 1998. **196**(2): p. 160-70.

53. Bate, M. and A. Martinez Arias, eds. *The Development of Drosophila Melanogaster*. 1 ed. Vol. 1. 1993, Cold Spring Harbor Laboratory Press. 1523.

54. Minshull, J., et al., *Protein phosphatase 2A regulates MPF activity and sister chromatid cohesion in budding yeast.* Current Biology, 1996. **6**(12): p. 1609-20.

55. Su, T.T., et al., *Exit from mitosis in Drosophila syncytial embryos requires proteolysis and cyclin degradation, and is associated with localized dephosphorylation.* Genes and Development, 1998. **12**(10): p. 1495-503.

56. Rimmington, G., B. Dalby, and D.M. Glover, *Expression of N-terminally truncated cyclin B in the Drosophila larval brain leads to mitotic delay at late anaphase.* Journal of Cell Science, 1994. **107**(Pt 10)(2): p. 2729-38.

57. Schägger, H. and G. von Jagow, *Tricine-sodium dodecyl sulfate-polyacrylamide gel electrophoresis for the separation of proteins in the range from 1 to 100 kDa.* Analytical Biochemistry, 1987. **166**(2): p. 368-79.

58. Su, T.T., N. Yakubovich, and P.H. O'Farrell, *Cloning of Drosophila MCM homologs and analysis of their requirement during embryogenesis.* Gene, 1997. **192**(2): p. 283-9.

59. Tugendreich, S., et al., *CDC27Hs colocalizes with CDC16Hs to the centrosome and mitotic spindle and is essential for the metaphase to anaphase transition.* Cell, 1995. **81**(2): p. 261-8.

60. Fang, G., H. Yu, and M.W. Kirschner, *Direct binding of CDC20 protein family members activates the anaphase-promoting complex in mitosis and G1.* Molecular Cell, 1998. **2**(2): p. 163-71.

61. Ashburner, M., ed. *Drosophila A Laboratory Manual.* 1 ed. Vol. 2. 1989, Cold Spring Harbor Laboratory Press. 434.

62. Knoblich, J.A., et al., *Cyclin E controls S phase progression and its down-regulation during Drosophila embryogenesis is required for the arrest of cell proliferation.* Cell, 1994. **77**(1): p. 107-20.

63. Casso, D., F.A. Ramírez-Weber, and T.B. Kornberg, *GFP-tagged balancer chromosomes for Drosophila melanogaster.* Mechanisms of Development, 1999. **88**(2): p. 229-32.

64. DiGregorio, P.J., J.A. Ubersax, and P.H. O'Farrell, *Hypoxia and Nitric Oxide Induce a Rapid, Reversible Cell Cycle Arrest of the Drosophila Syncytial Divisions.* Journal of Biological Chemistry, 2001. **276**(3): p. 1930-`937.

65. Charles, J.F., et al., *The Polo-related kinase Cdc5 activates and is destroyed by the mitotic cyclin destruction machinery in S. cerevisiae.* Current Biology, 1998. **8**(9): p. 497-507.

66. Stratmann, R. and C.F. Lehner, *Separation of sister chromatids in mitosis requires the Drosophila pimples product, a protein degraded after the metaphase/anaphase transition.* Cell, 1996. **84**(1): p. 25-35.

67. Hwang, L.H., *The Regulation of the Exit from Mitosis in Saccharomyces cerevisiae*, in *Biochemistry*. 1998, University of California, San Francisco: San Francisco. p. 170.

68. Dawson, I.A., S. Roth, and S. Artavanis-Tsakonas, *The Drosophila cell cycle gene fizzy is required for normal degradation of cyclins A and B during mitosis and has homology to the CDC20 gene of Saccharomyces cerevisiae.* Journal of Cell Biology, 1995. **129**(3): p. 725-37.

69. Shirayama, M., et al., *The Polo-like kinase Cdc5p and the WD-repeat protein Cdc20p/fizzy are regulators and substrates of the anaphase promoting complex in Saccharomyces cerevisiae.* Embo Journal, 1998. **17**(5): p. 1336-49.

70. Schwab, M., A.S. Lutum, and W. Seufert, *Yeast Hct1 is a regulator of Clb2 cyclin proteolysis.* Cell, 1997. **90**(4): p. 683-93.

71. Kotani, S., et al., *Regulation of APC activity by phosphorylation and regulatory factors.* Journal of Cell Biology, 1999. **146**(4): p. 791-800.

72. Ohtoshi, A., et al., *Human p55(CDC)/Cdc20 associates with cyclin A and is phosphorylated by the cyclin A-Cdk2 complex.* Biochemical and Biophysical Research Communications, 2000. **268**(2): p. 530-4.

73. Yudkovsky, Y., et al., *Phosphorylation of Cdc20/fizzy negatively regulates the mammalian cyclosome/APC in the mitotic checkpoint.* Biochemical and Biophysical Research Communications, 2000. **271**(2): p. 299-304.

74. Hwang, L.H., et al., *Budding yeast Cdc20: a target of the spindle checkpoint [see comments] [published erratum appears in Science 1998 May 29;280(5368):1331].* Science, 1998. **279**(5353): p. 1041-4.

75. Kim, S.H., et al., *Fission yeast Slp1: an effector of the Mad2-dependent spindle checkpoint [see comments].* Science, 1998. **279**(5353): p. 1045-7.

76. Fang, G., H. Yu, and M.W. Kirschner, *The checkpoint protein MAD2 and the mitotic regulator CDC20 form a ternary complex with the anaphase-promoting complex to control anaphase initiation.* Genes and Development, 1998. **12**(12): p. 1871-83.

77. Jaspersen, S.L., J.F. Charles, and D.O. Morgan, *Inhibitory phosphorylation of the APC regulator Hct1 is controlled by the kinase Cdc28 and the phosphatase Cdc14.* Current Biology, 1999. **9**(5): p. 227-36.

78. Zachariae, W., et al., *Control of cyclin ubiquitination by CDK-regulated binding of Hct1 to the anaphase promoting complex.* Science, 1998. **282**(5394): p. 1721-4.

79. Listovsky, T., et al., *Cdk1 is essential for mammalian cyclosome/APC regulation.* Experimental Cell Research, 2000. **255**(2): p. 184-91.

80. Amon, A., *Regulation of B-type cyclin proteolysis by Cdc28-associated kinases in budding yeast.* Embo Journal, 1997. **16**(10): p. 2693-702.

81. Félix, M.A., et al., *Triggering of cyclin degradation in interphase extracts of amphibian eggs by cdc2 kinase.* Nature, 1990. **346**(6282): p. 379-82.

82. Lahav-Baratz, S., et al., *Reversible phosphorylation controls the activity of cyclosome-associated cyclin-ubiquitin ligase.* Proceedings of the National Academy of Sciences of the United States of America, 1995. **92**(20): p. 9303-7.

83. Lorca, T., et al., *Fizzy is required for activation of the APC/cyclosome in Xenopus egg extracts.* Embo Journal, 1998. **17**(13): p. 3565-75.

84. Rudner, A.D. and A.W. Murray, *Phosphorylation by Cdc28 activates the Cdc20-dependent activity of the anaphase-promoting complex.* Journal of Cell Biology, 2000. **149**(7): p. 1377-90.

85. Shteinberg, M., et al., *Phosphorylation of the cyclosome is required for its stimulation by Fizzy/cdc20.* Biochemical and Biophysical Research Communications, 1999. **260**(1): p. 193-8.

86. Descombes, P. and E.A. Nigg, *The polo-like kinase Plx1 is required for M phase exit and destruction of mitotic regulators in Xenopus egg extracts.* Embo Journal, 1998. **17**(5): p. 1328-35.

87. Kotani, S., et al., *PKA and MPF-activated polo-like kinase regulate anaphase-promoting complex activity and mitosis progression.* Molecular Cell, 1998. **1**(3): p. 371-80.

88. Thomas, B.J., et al., *roughex down-regulates G2 cyclins in G1.* Genes and Development, 1997. **11**(10): p. 1289-98.

89. Dong, X., et al., *Control of G1 in the developing Drosophila eye: rca1 regulates Cyclin A.* Genes and Development, 1997. **11**(1): p. 94-105.

90. Follette, P.J. and P.H. O'Farrell, *Cdks and the Drosophila cell cycle.* Current Opinion in Genetics and Development, 1997. **7**(1): p. 17-22.

91. Lehner, C.F. and P.H. O'Farrell, *Expression and function of Drosophila cyclin A during embryonic cell cycle progression.* Cell, 1989. **56**(6): p. 957-68.

92. Lehner, C.F. and P.H. O'Farrell, *The roles of Drosophila cyclins A and B in mitotic control.* Cell, 1990. **61**(3): p. 535-47.

93. Lukas, C., et al., *Accumulation of cyclin B1 requires E2F and cyclin-A-dependent rearrangement of the anaphase-promoting complex.* Nature, 1999. **401**(6755): p. 815-8.

94. Hayashi, S. and M. Yamaguchi, *Kinase-independent activity of Cdc2/cyclin A prevents the S phase in the Drosophila cell cycle.* Genes To Cells, 1999. **4**(2): p. 111-22.

95. Wilson, J.D., et al., eds. *Harrison's Principle of Internal Medicine.* 12 ed. 1991, McGraw-Hill Book Co.: New York. 2568.

96. Green, S.L. and A.J. Giaccia, *Tumor hypoxia and the cell cycle: implications for malignant progression and response to therapy.* Cancer Journal from Scientific American, 1998. **4**(4): p. 218-23.

97. Hochachka, P.W., et al., *Unifying theory of hypoxia tolerance: molecular/metabolic defense and rescue mechanisms for surviving oxygen lack.* Proceedings of the National Academy of Sciences of the United States of America, 1996. **93**(18): p. 9493-8.

98. Guillemin, K. and M.A. Krasnow, *The hypoxic response: huffing and HIFing.* Cell, 1997. **89**(1): p. 9-12.

99. Wingrove, J.A. and P.H. O'Farrell, *Nitric oxide contributes to behavioral, cellular, and developmental responses to low oxygen in Drosophila.* Cell, 1999. **98**(1): p. 105-14.

100. Foe, V.E. and B.M. Alberts, *Reversible chromosome condensation induced in Drosophila embryos by anoxia: visualization of interphase nuclear organization.* Journal of Cell Biology, 1985. **100**(5): p. 1623-36.

101. Zalokar, M. and I. Erk, *Division and Migration of Nuclei during Early Embryogenesis of Drosophila melanogaster.* Journal de Microscopie et de Biologie Cellulaire, 1976. **25**: p. 97-107.

102. Truman, J.W., J. De Vente, and E.E. Ball, *Nitric oxide-sensitive guanylate cyclase activity is associated with the maturational phase of neuronal development in insects.* Development, 1996. **122**(12): p. 3949-58.

103. Kuzin, B., et al., *Nitric oxide regulates cell proliferation during Drosophila development.* Cell, 1996. **87**(4): p. 639-49.

104. Bredt, D.S. and S.H. Snyder, *Nitric oxide: a physiologic messenger molecule.* Annual Review of Biochemistry, 1994. **63**(2): p. 175-95.

105. Clarkson, M. and R. Saint, *A His2AvDGFP fusion gene complements a lethal His2AvD mutant allele and provides an in vivo marker for Drosophila chromosome behavior.* Dna and Cell Biology, 1999. **18**(6): p. 457-62.

106. Elledge, S.J., *Cell cycle checkpoints: preventing an identity crisis.* Science, 1996. **274**(5293): p. 1664-72.

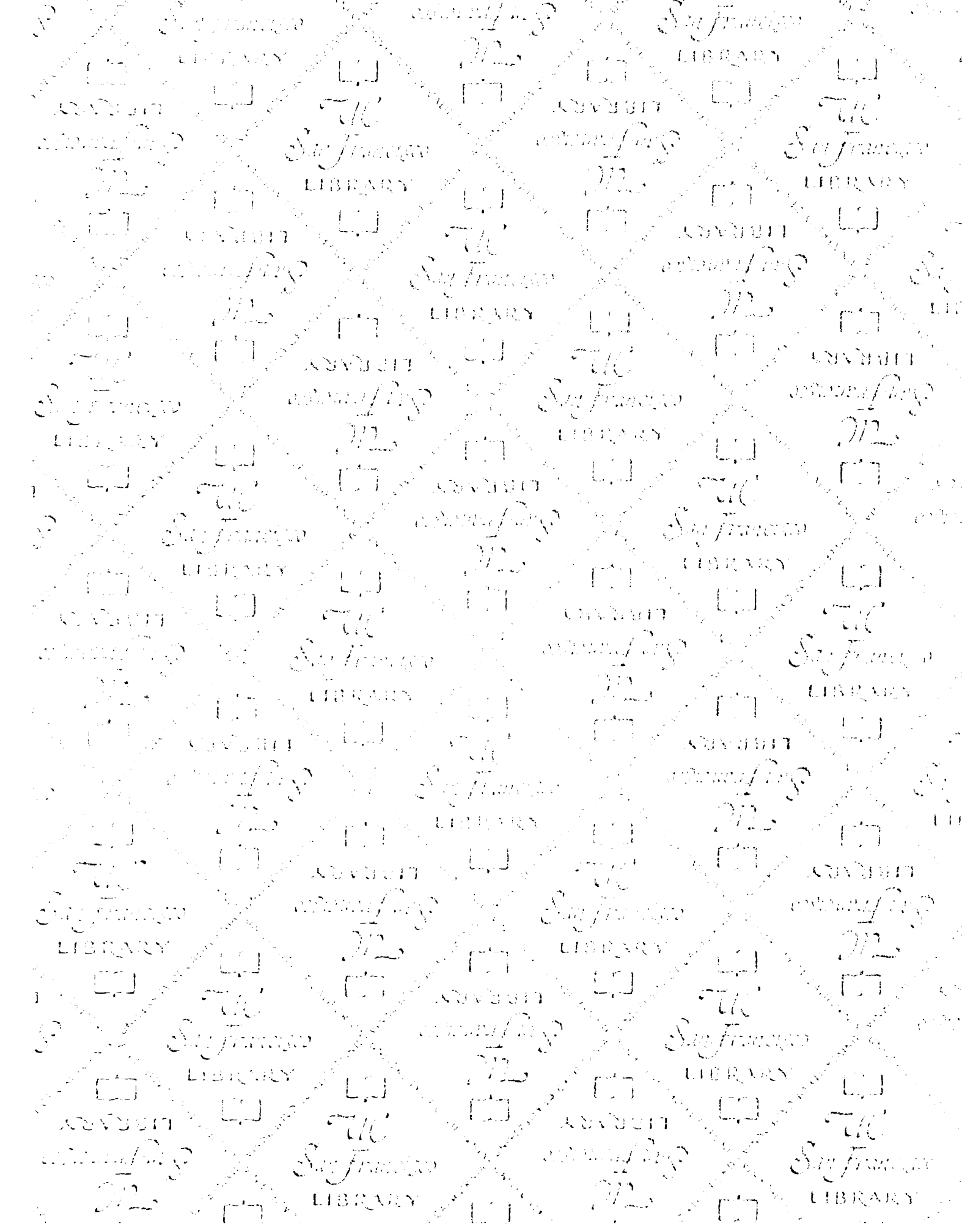
San Francisco
LIBRARY